RADIATION ABSORPTION CORRECTION IN THE MEASUREMENT OF TEMPERATURE IN A 30 ATMOSPHERE AIR ARC

A THESIS

Presented to

The Faculty of the Division

of Graduate Studies

By

Joseph T. Salmon, Jr.

In Partial Fulfillment

of the Requirements for the Degree

Master of Science in the School

of Mechanical Engineering

Georgia Institute of Technology

March, 1978

RADIATION ABSORPTION CORRECTION IN THE MEASUREMENT OF TEMPERATURE IN A 30 ATMOSPHERE AIR ARC

Approved:

A. V. Larson, Chairman

M. R. Corley

P. Durbetaki

Date approved by Chairman: 3/11/78

ACKNOWLEDGMENTS

During the course of my graduate research, Dr. A. V. Larson, my thesis advisor, provided invaluable insights and suggestions, and I am deeply indebted to him for this help. I am also grateful to Mr. R. T. Murray for his instruction and assistance with the laboratory apparatus. Dr. M. R. Corley and Dr. P. Durbetaki, my thesis reading committee members, also provided their time and professional support during the preparation of this paper.

Special thanks go to Mr. D. P. Dodson for his help in the preliminary and experimental phases of this research and Mr. W. L. Christy for his assistance during the experiments. Mrs. Sharon Butler deserves my appreciation for her typing and editing assistance on the thesis manuscript.

I am very grateful to my parents for their guidance and support throughout my educational career, and to my wife for her support during the preparation of this paper.

TABLE OF CONTENTS

LIST OF TABLES

LIST OF ILLUSTRATIONS

Figure Page

LIST OF SYMBOLS

$A_{u\ell}$	electron transition probability
E_i	electron energy of the i^{th} bound state
I	radiant intensity
I_λ	monochromatic radiant intensity
M	atomic mass [kg]
N_i	ion number density
p	pressure
p_λ	monochromatic profile
R	arc radius
T	temperature
U	atomic partition function
X_c	mole fraction of component c
c	speed of light in vacuum
d	electron Stark shift of spectral line peak from line center
d_t	total Stark shift of spectral line peak from line center
e	charge of an electron
g_i	statistical weight for i^{th} electron energy state
h	Planck constant
k	Boltzmann constant
r	radial position within arc
w	Stark broadening electron (half) half-width
w_D	Doppler broadening (half) half-width

w_s	total Stark broadening (half) half-width
w_v	Voight profile (half) half-width
α	Stark broadening ion impact parameter
$\Delta\lambda_D$	Doppler width
ε	emission coefficient
ε_c	continuum emission coefficient
$\varepsilon_{c\lambda}$	monochromatic continuum emission coefficient
ε_L	spectral line emission coefficient
ε_λ	monochromatic spectral line emission coefficient
$\varepsilon_{\lambda p}$	peak monochromatic spectral line emission coefficient
ε_o	permittivity of vacuum
κ	absorption coefficient
κ_λ	monochromatic absorption coefficient
λ	wavelength
λ_o	center of spectral emission line
μ	atomic weight
ν	electromagnetic radiation frequency

SUMMARY

When attempting to determine optically the temperature within a plasma at pressures significantly higher than one atmosphere, it must be determined if there is an appreciable amount of reabsorption of the radiation emitted within that plasma. If there is significant reabsorption the experimenter must account for it to accurately describe the environment within the plasma.

Two computer programs were developed to analyze experimental data taken from side-on optical observations of an axisymmetric electric arc operated at high pressures. One program was designed to determine the radial temperature distribution with the arc assumed optically thin. The other program was designed to take the output from the first program and adjust these temperatures to account for any reabsorption within the arc. The two programs were found to be accurate and mutually consistent when tested during program development.

An 11.9 ampere air arc was operated at a pressure of 30 atmospheres and the intensities of two spectral emission lines were measured across the side of the arc. Absorption of arc radiation by air byproducts immediately surrounding the arc was determined from backlight measurements through the medium containing these byproducts. Final temperature

profiles obtained from the two spectral line intensity measurements, corrected for medium absorption, agreed within three percent of each other. Reabsorption of radiation within the arc was found to be significant and was accounted for in the determination of these final temperature profiles.

CHAPTER I

INTRODUCTION

Before transport properties of a hot gas can be determined, the local thermodynamic state of that gas throughout the system must be found. When the gas is in local thermodynamic equilibrium (LTE) there is a distinct relationship between the radiated power of an isolated spectral line emitted by a volume element of a plasma and the temperature of that element. If the amount of radiant intensity is not significantly absorbed before it is detected, finding that volume element's emission coefficient is only a problem involving the total source geometry and the spatial radiant intensity distribution. For example, if the plasma has cylindrical symmetry and is viewed edge-on, the Abel transformation [2] may be used. However, this model is not sufficient if there is significant absorption of radiation at that wavelength within the plasma. In this case the actual radiation transport through the plasma must be studied on a monochromatic basis.

Preliminary investigation of an air arc [1] indicated that at a pressure of 30 atmospheres there was a significant amount of absorption in the optical path for the green to near ultraviolet region of the spectrum. Subsequent

measurements indicated that significant absorption also took place in the red and near infrared region; however, this absorption was not nearly as great as that absorption found at the shorter wavelengths. This attenuation appeared to occur in the region immediately outside the arc and was weakly dependent upon wavelength.

Since a spectral emission line was to be used to determine internal temperature distributions the possibility of self absorption of radiation at the wavelength of that line was explored. Preliminary rough calculations made manually indicated that self absorption within the arc may need to be accounted for in the temperature determination process.

The purpose of this research was to determine the actual absorption effects within the air arc and in the optical path immediately outside the arc. These effects were then taken into consideration in the determination of the radial temperature profile of the arc. No known prior research has produced publications mentioning the use of spectral line absorption profiles to make temperature corrections in cylindrical arcs observed from the side, and one paper [1] has mentioned the presence of significant absorption in the medium immediately surrounding a steady state air arc operated at high pressures.

In this paper two computer programs will be introduced along with the theory used by the programs. They provide a

consistent approach and offer insights into the behavior of the observations of arc phenomena at high pressures.

CHAPTER II

THEORY

The method used in this experiment for examining electric arcs with cylindrical symmetry was to optically measure the intensity of the arc from the side as shown in Figure 2-1. From these measurements an attempt was made to use the geometrical symmetries to obtain insights about the nature of the plasma inside the arc. This process required a knowledge of the characteristics of a hot radiating gas in addition to the arc geometry.

For any particular volume element within a plasma, radiation is emitted and absorbed by several mechanisms. These mechanisms, shown in Figure 2-2, lead to an emission spectrum with properties shown in Figure 2-3. The wavelength, λ, of the emitted or absorbed radiation is determined by

$$E_1 - E_2 = \frac{hc}{\lambda} \qquad (2\text{-}1)$$

where E_1 and E_2 are the electron energies before and after the event, h is Planck's Constant, and c is the speed of light through a vacuum. The continuum emission is caused by interactions between free electrons and neighboring ions while

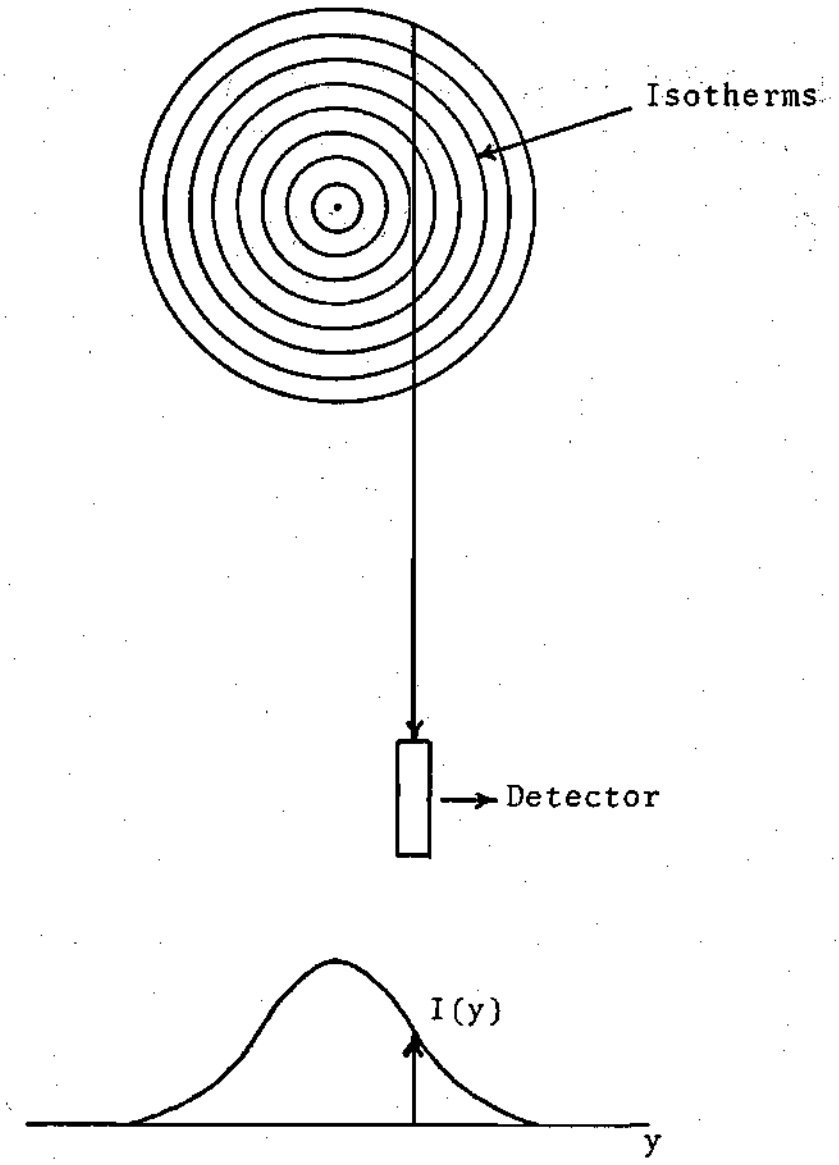

Figure 2-1. Side-on Optical Measurements Used to Find the Internal Temperature Distribution of the Arc

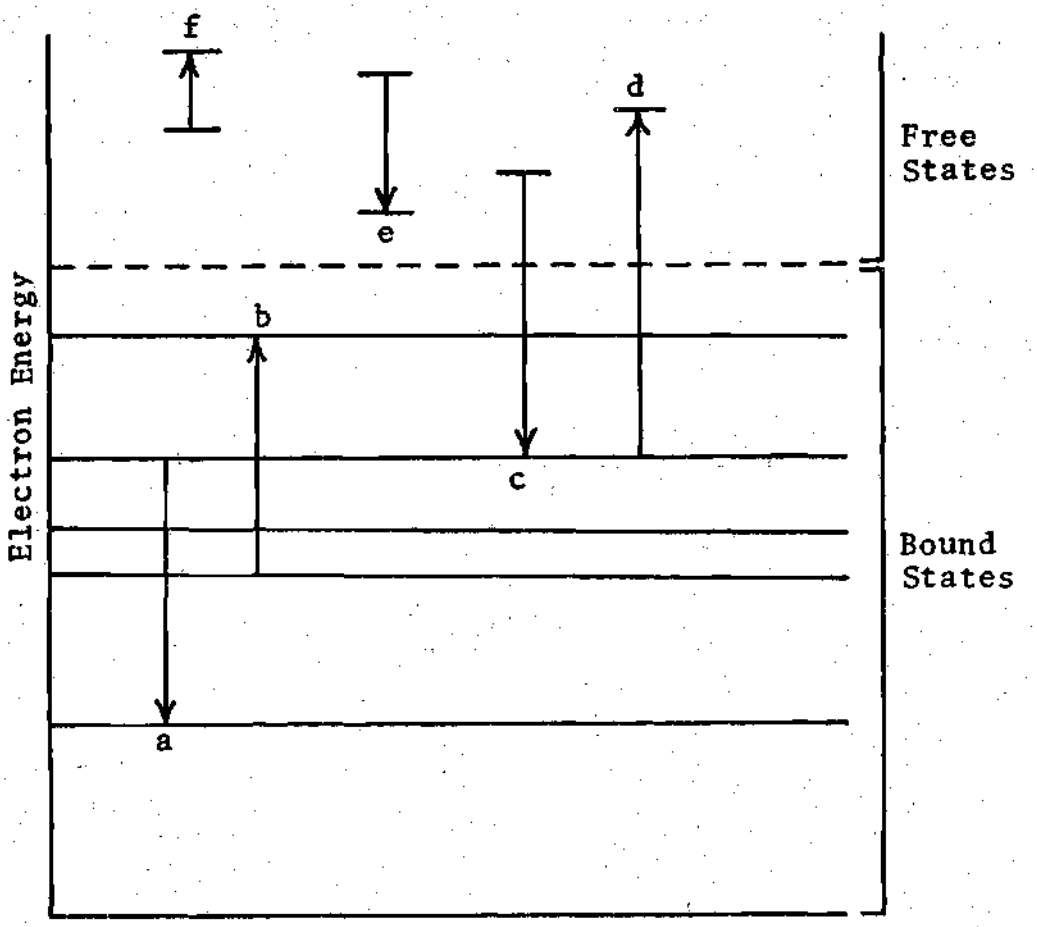

Figure 2-2. Mechanisms of Atomic Emission and Absorption

(a) bound-bound emission
(b) bound-bound absorption
(c) free-bound emission
(d) bound-free absorption
(e) free-free emission
(f) free-free absorption
[From Siegel and Howell, Thermal Radiation Heat Transfer, McGraw-Hill, New York, 1972]

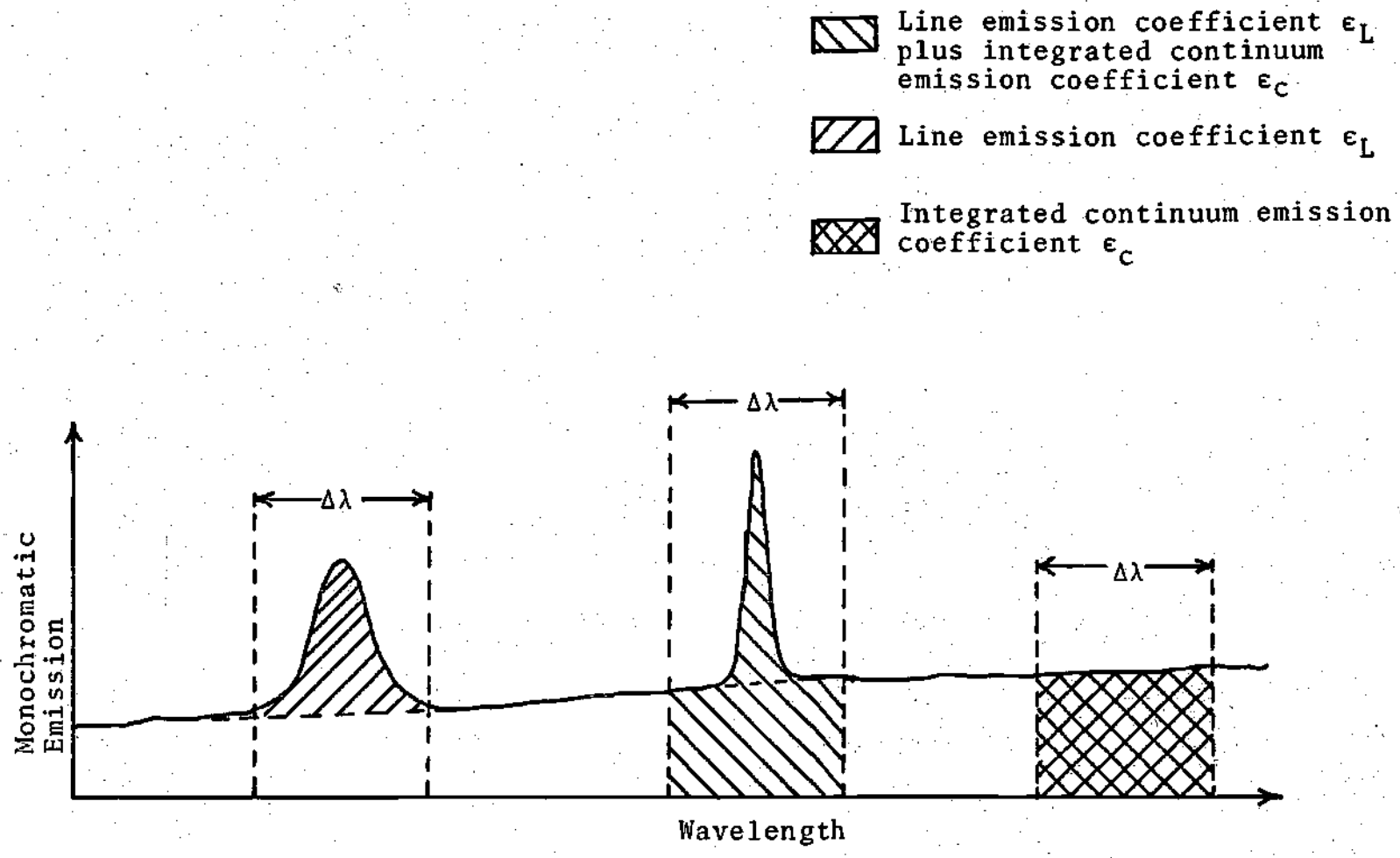

Figure 2-3. Schematic of Spectral Distribution of Radiation from a Plasma Volume Element Where Δλ is the Spectrometer Spectral Bandpass

line emissions are caused by changes in energy states by electrons bound to an atom. The energies of the bound states are discrete as opposed to energies of free electrons and, hence, emit radiation at discrete wavelengths. The line emission coefficient ε_L is the line radiant power emitted per unit volume of gas per unit solid angle. It is produced by the loss of energy by an electron in the transition from a higher energy bound state to a lower energy bound state. The monochromatic continuum emission coefficient $\varepsilon_{c\lambda}$ is the radiant power emitted per unit volume of gas per unit solid angle per unit wavelength. The continuum emission ε_c is the integrated monochromatic continuum emission coefficient over the finite wavelength interval measured by the spectrometer.

The detected radiant intensity from a plasma is a consequence of emitted radiation from volume elements within the plasma which lie in a straight line coincident with the optical path to the detector, as shown in Figure 2-4. If the plasma does not significantly absorb radiation, the intensity is the sum of the emitted radiation from each volume element over the length of the optical path inside the plasma. One can apply this statement to the monochromatic intensity, the spectral line intensity, or the total radiant intensity. This summation

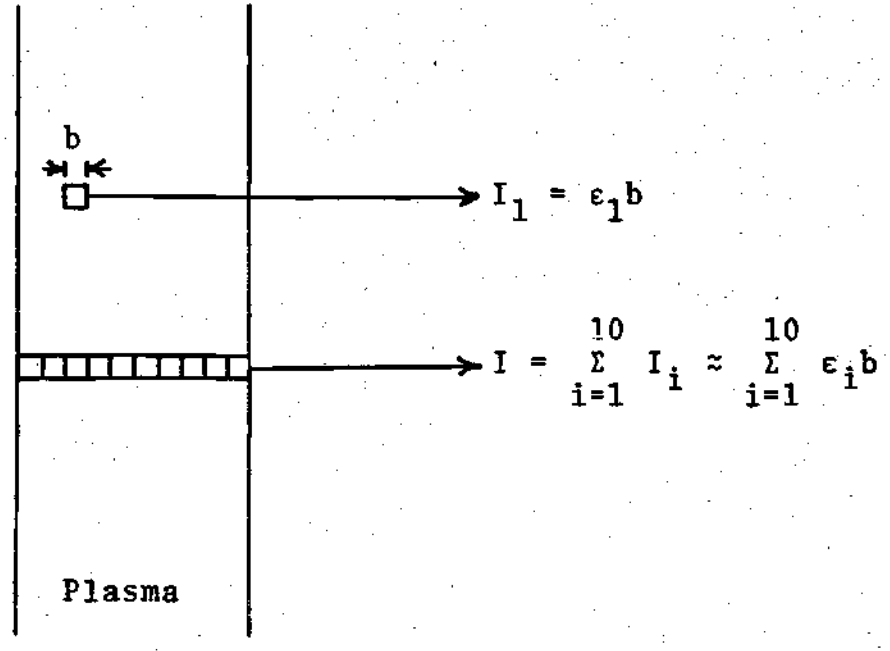

Figure 2-4. Relationship Between the Intensity and the Local Emission Coefficients Along an Optical Path for a Nonabsorbing Plasma (Optically Thin)

$$I = \int_{x_1}^{x_2} \varepsilon \, dx \qquad (2\text{-}2)$$

is illustrated in Figure 2-5 for a cylindrically symmetric plasma observed from the side. In this case equation (2-2) reduces to

$$I(y) = 2\int_{y}^{R} \frac{r\varepsilon(r)}{\sqrt{r^2-y^2}} \, dr \qquad (2\text{-}3)$$

and, knowing the radial distribution of the emission coefficient, one can determine the lateral intensity distribution. Equation (2-3) can be inverted to yield

$$\varepsilon(r) = -\frac{1}{\pi}\int_{r}^{R} \frac{\frac{dI}{dy}}{\sqrt{y^2-r^2}} \, dy \qquad (2\text{-}4)$$

which is known as the Abel transformation [2].

When a plasma is in LTE, a number of tools may be used to determine the thermodynamic state of the system. Number densities of the different components are definite functions of the temperature and pressure and can be found by using the ideal gas law and minimizing the Gibbs free energy of the system. The populations of electrons in excited energy states follow a Boltzmann distribution. These consequences of the LTE assumption lead to [2]

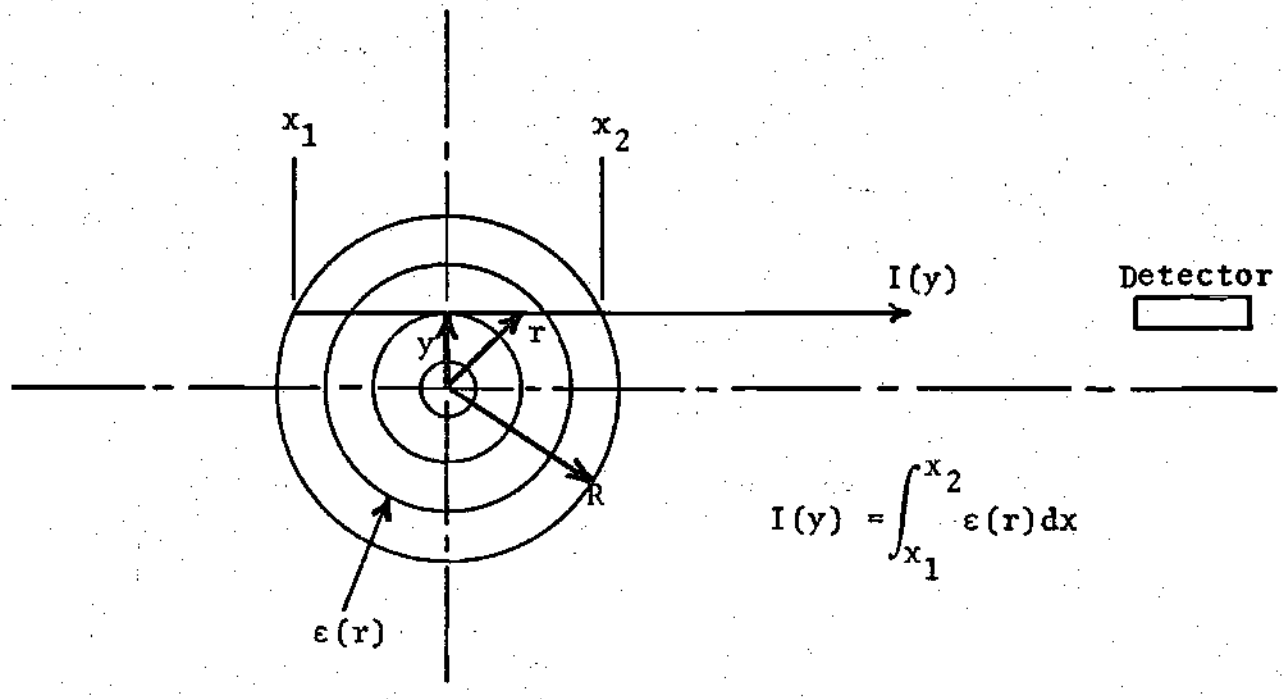

Figure 2-5. Emission Coefficient Contributions to the Lateral Intensity Distribution

$$\varepsilon_L = \frac{h\nu}{4\pi} g_u A_{u\ell} \frac{p}{kT} \frac{X_c(T)}{U(t)} \exp\left(-\frac{E_u}{kT}\right) \qquad (2\text{-}5)$$

for any spectral emission line. In this equation ν is the spectral line frequency, P is the pressure, T is the temperature, E_u is the energy of the upper bound electron state, $A_{u\ell}$ is the atomic transition probability, g_u is the upper bound state statistical weight, and k is Boltzmann's constant. The atomic partition function U is a function of temperature, and the mole fraction of the radiating component X_c is a function of temperature and pressure. Values for U were found in Drawin and Felenbok [3], values for $A_{u\ell}$ and E_u were found in NBS Atomic Transition Data [4], and values for X_c were found in Predvoditelev [5,6]. For a specific pressure knowledge of these values as a function of temperature enables one to obtain a definite relationship between the temperature of that species and the emission coefficient ε_L. This specific relationship is unique for each emission line and once determined one can obtain the temperature of a particular volume element by finding its emission coefficient from intensity measurements.

When self-absorption is negligible one can use equation (2-4) to find ε_L as a function of arc radius. When absorption by the plasma is significant at the emission line used in temperature determination, one must study the transport of monochromatic radiation across each chord in the arc. The

governing equation

$$\frac{dI_\lambda}{dx} = \epsilon_\lambda - \kappa_\lambda I_\lambda \tag{2-6}$$

where κ_λ is the reduced monochromatic absorption coefficient, is an attempt to describe the actual mechanism of radiation transport in a hot radiating gas. If a backlight source were placed behind the plasma and the absorption of backlight radiation were independent of wavelength, the governing equation would be

$$\frac{dI}{dx} = -\kappa I \tag{2-7}$$

over the wavelength interval to be studied. This equation has the solution

$$I = I_o \exp\left(-\int_{-x_1}^{x_1} \kappa dx\right) \tag{2-8}$$

and for a cylindrical arc as described in Figure 2-5

$$I = I_o \exp\left(-2\int_{o}^{x_1} \kappa dx\right) \tag{2-9}$$

since κ is symmetric with the arc axis. If the source were moved to this axis one can find the relation

$$\frac{I'}{I_o} = \sqrt{\frac{I}{I_o}} \qquad (2\text{-}10)$$

where I' is the intensity observed for the source located at the arc axis.

Since the absorption coefficient may be a function of wavelength (see Appendix A), there is no way to convert equation (2-6) to describe the transport of a whole emission line across the arc. Therefore, one must understand and use the spectral distribution of that emission line and solve equation (2-6) on a monochromatic scale. This spectral distribution of the line emission coefficient could be analyzed by subtracting the monochromatic continuum values from the monochromatic emission coefficients and normalizing the total area under the resultant curve. The final profile, similar to Figure 2-6, can be multiplied by the line emission coefficient to yield the distribution of the monochromatic emission coefficients ϵ_λ.

Although there are many mechanisms in a plasma which broaden emission lines, this paper will focus on only two of them: Doppler and Stark broadening. At temperatures around 10,000°K the presence of coulomb forces from ions and free electrons insures the dominance of Stark broadening. At lower temperatures Doppler broadening may have a significant effect upon the total broadening since the local percentage of charged particles is much smaller than those percentages at higher temperatures.

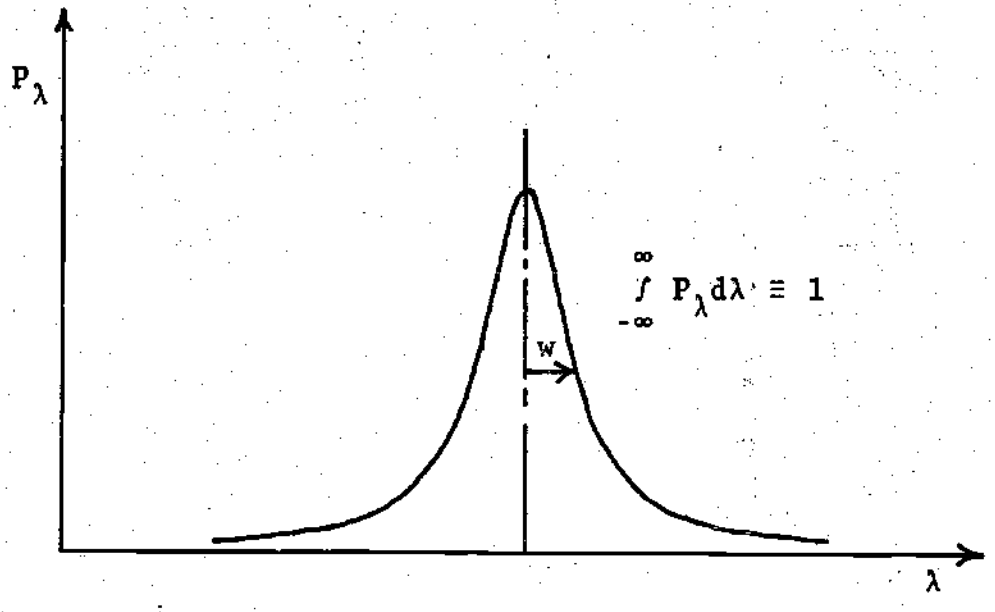

Figure 2-6. Line Emission Coefficient Profile

Doppler broadening is a consequence of the velocity distribution of the radiating components. If the plasma is in LTE the velocity conforms to a Maxwell-Boltzmann distribution, which is Gaussian in character. The resultant monochromatic spectral distribution of such an emission line becomes

$$\varepsilon_\lambda = \frac{\varepsilon_L}{(\Delta\lambda_D)\sqrt{\pi}} \exp\left[-\left(\frac{\lambda-\lambda_o}{\Delta\lambda_D}\right)^2\right] \qquad (2\text{-}11)$$

where $\Delta\lambda_D$ is the distance from the line peak where

$$\varepsilon_\lambda = \varepsilon_{\lambda p} \exp(-1) \qquad (2\text{-}12)$$

and the integral of equation (2-11) over all wavelengths is the line emission coefficient. This distribution is shown in Figure 2-7. The relationship [8]

$$\Delta\lambda_D = \left(\frac{2kT\lambda_o^2}{Mc^2}\right)^{1/2} = 4.30\times10^{-7}\ \lambda_o\sqrt{\frac{T}{\mu}} \qquad (2\text{-}13)$$

indicates that the Doppler broadening mechanism for each spectral line is independent of pressure. The Doppler (half) half-width w_D, half the distance between the two points with values equal to half the profile peak value, is shown in Figure 2-7 and can be found by

$$w_D = (\Delta\lambda_D)\sqrt{\ell n\ 2} \tag{2-14}$$

as a consequence of the definition of $\Delta\lambda_D$.

Stark broadening is not such an easily understood mechanism. It is one of a number of mechanisms which are grouped together as pressure broadening mechanisms and is a consequence of coulomb interactions between charged particles and neutral radiators. The influence of Stark broadening is primarily dependent upon the electron number density and is dispersive in character [7]. If the ion broadening contribution is small when compared to the electron impact contribution, the profile is Lorentzian and is described by

$$\varepsilon_\lambda = \frac{\varepsilon_L}{\pi w_s\left[1+\left(\frac{\lambda-\lambda_o-d}{w_s}\right)^2\right]} \tag{2-15}$$

where w_s is the Stark (half) half-width. In addition to broadening the spectral line Stark broadening shifts the peak by a distance "d_t" from the original line center, as shown in Figure 2-8. The values for w_s and d_t can be obtained from

$$\begin{aligned} w_s &\simeq w + 1.75\alpha\ (1-0.75r)w \\ d_t &\simeq d \pm 2.0\alpha\ (1-0.75r)w \end{aligned} \tag{2-16}$$

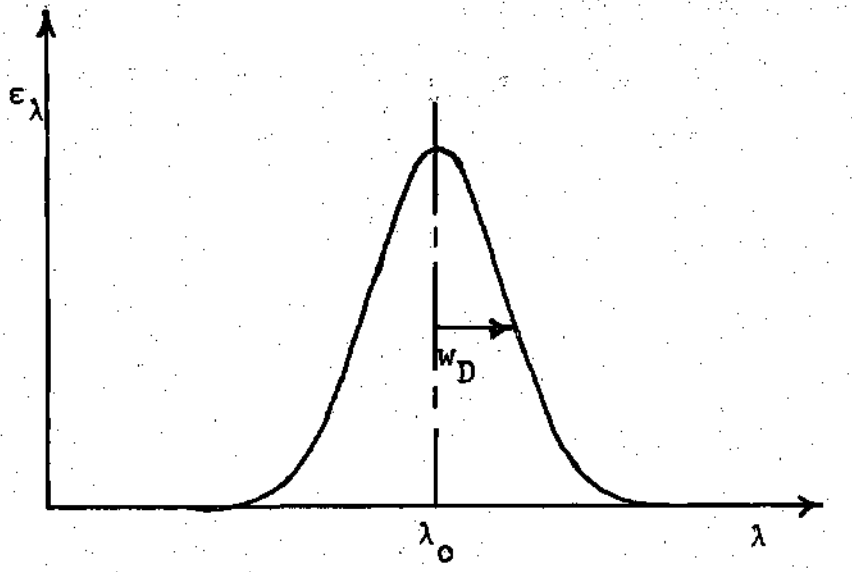

Figure 2-7. Spectral Distribution of Doppler Broadened Emission Line about Line Center λ_o

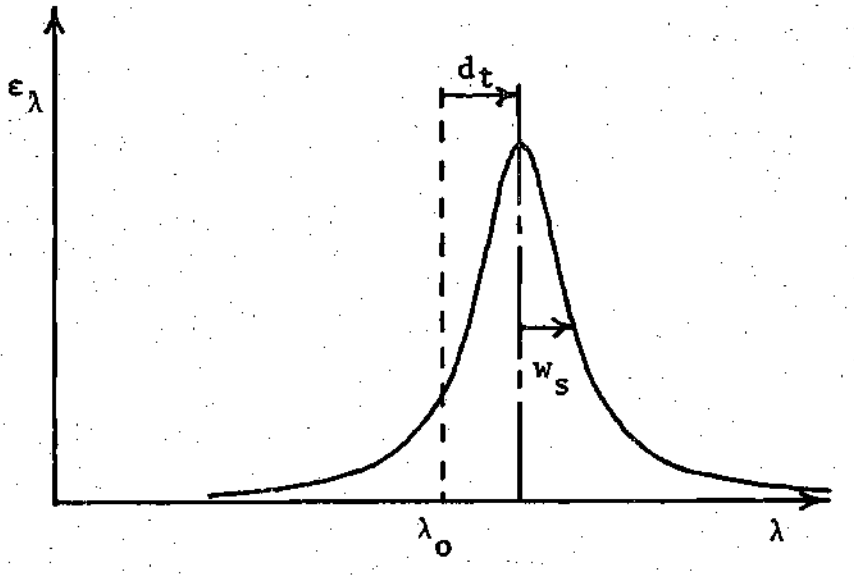

Figure 2-8. Spectral Distribution of Stark Broadened Emission Line about Line Center λ_o. Ion Broadening Assumed to be Insignificant.

where w, d, and α are tabulated for many of the spectral lines by Griem [9]. In these tables the percentage of the ion contribution is also tabulated. These theoretical values have been experimentally checked by Helbig, et al. [10] for many nitrogen emission lines. Helbig stated that when the ion impact parameter α is set equal to zero, the experimental data has better agreement with theory. One can determine r from

$$r = 6^{1/2}\ \pi^{1/6}\ \left(\frac{e^2}{4\pi\varepsilon_o kT}\right)^{1/2}\ N_i^{1/6} \qquad (2\text{-}17)$$

where r is the dimensionless ratio between the mean distance between ions and the Debye radius. In the equation for d_t one must use the sign of the low temperature limit for d found in the tables.

When the Stark (half) Half-width w_s is significantly larger than the Doppler (half) half-width w_D, one may neglect the effect of Doppler broadening when studying such line profiles [8,11]. When w_D is significantly larger than w_s, the central region has a dominant Doppler shape, but the wings are still primarily Lorentz in shape. This consequence is caused by a much faster drop in the wings for the Doppler profile, as shown in Figure 2-9. When the two (half) half-widths are comparable, one must convolve the two profiles resulting in

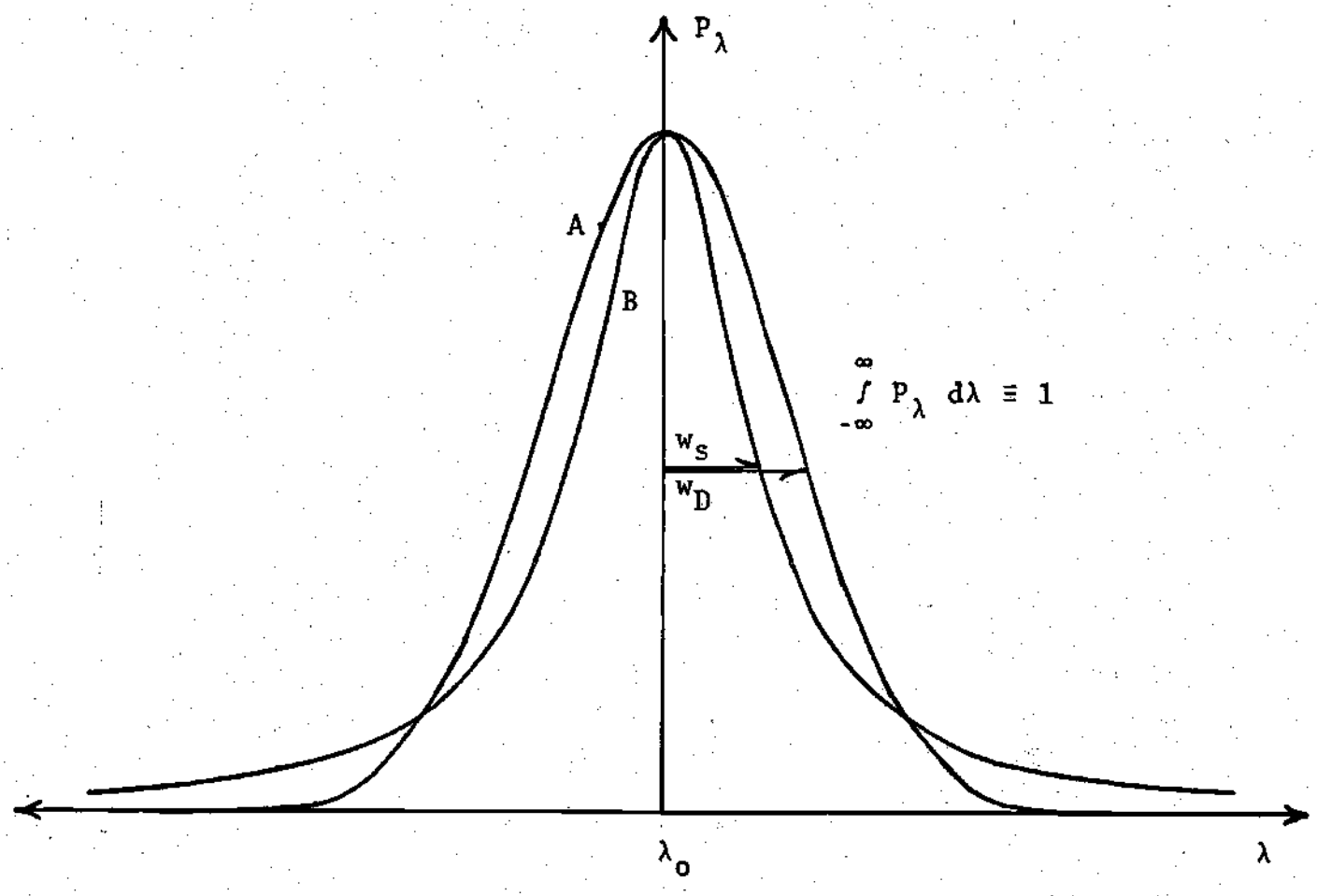

Figure 2-9. Doppler (A) and Stark (B) Profiles where $w_D > w_S$

$$\varepsilon_\lambda = \frac{\varepsilon_L}{\pi\sqrt{\pi}\, w_s}\int_{-\infty}^{\infty} \frac{e^{-x^2}}{1 + \left(\frac{\lambda-\lambda_o-d-(\Delta\lambda_D)x}{w_s}\right)^2}\, dx \qquad (2\text{-}18)$$

which is a Voigt profile, shown in Figure 2-10. For a particular spectral emission line the influence of Doppler broadening decreases for an increase in pressure.

Once the spectral distribution for an emission line is known as a function of temperature, one can apply this knowledge to investigate the actual radiation transport across the arc. Since the arc is in LTE, one may use Kirchoff's Law (see Appendix A)

$$\kappa_\lambda = \frac{\varepsilon_\lambda}{B_\lambda} \qquad (2\text{-}19)$$

to relate the monochromatic emission coefficient ε_λ and the monochromatic absorption coefficient κ_λ for any temperature. In this equation B_λ is the monochromatic blackbody intensity. This relationship can be used with equation (2-6) to obtain

$$\frac{dI_\lambda}{dx} = \varepsilon_\lambda\left(1 - \frac{I_\lambda}{B_\lambda}\right) \qquad (2\text{-}20)$$

where ε_λ and B_λ can be found for any temperature distribution at any specific pressure. Equation (2-20) describes the actual monochromatic radiation transport in any straight line

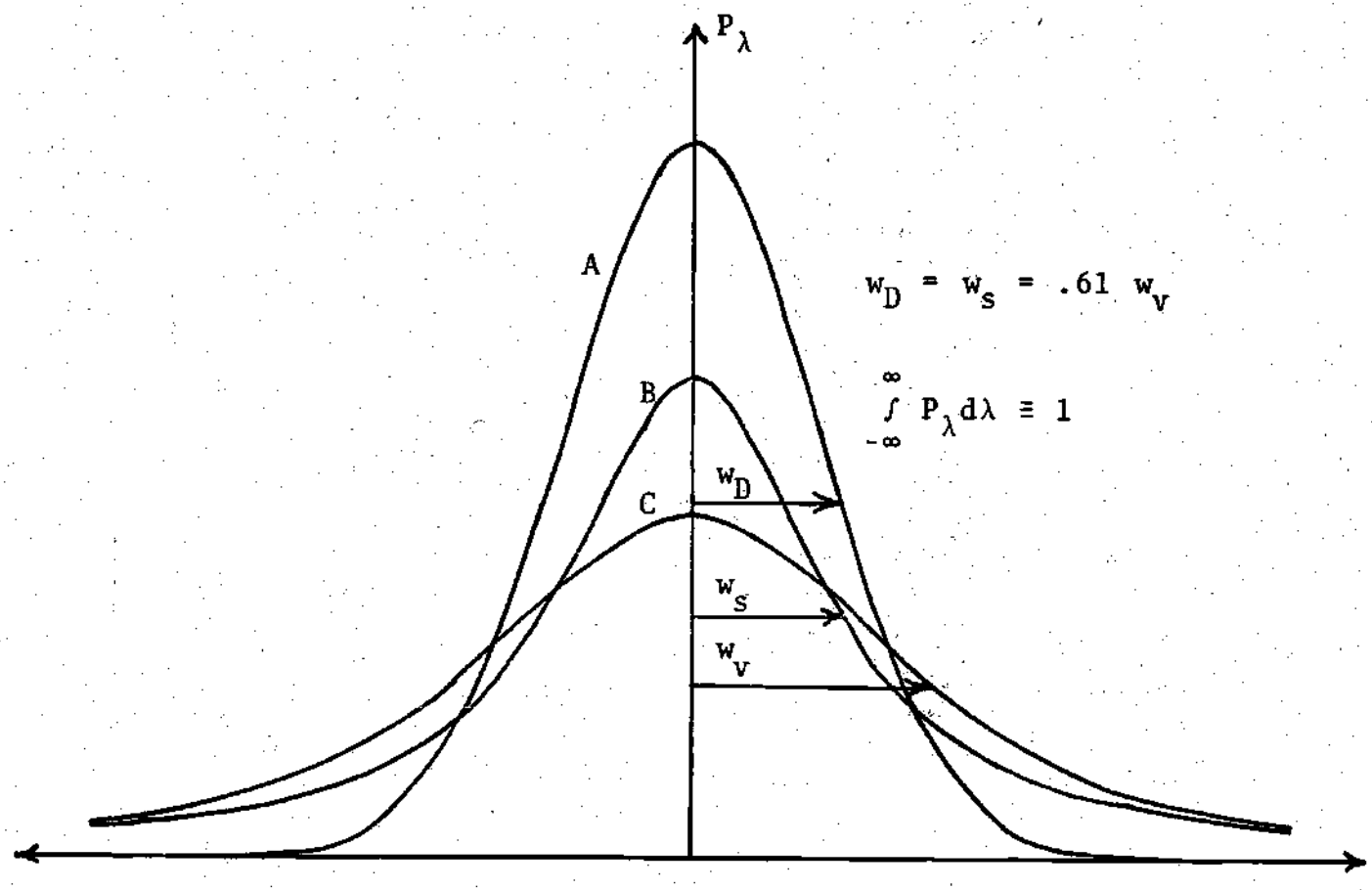

Figure 2-10. Doppler (A) and Stark (B) Profiles with Their Resultant Voight Profile (C)

through an arc in LTE. Once the spectral intensity distribution leaving the arc at some spatial position is integrated across the spectral line, one can determine the actual observed total line intensity leaving the arc at that spatial position. Finding these intensities at different spatial positions enables one to predict the observed spatial intensity distribution for that line for any temperature distribution within an absorbing arc.

CHAPTER III

APPARATUS

Much of the equipment used in this research came to this facility from Wright Patterson AFB in Ohio, and the remaining equipment was furnished by the School of Mechanical Engineering at the Georgia Institute of Technology. Refinements of the actual cascade device enabling steady state air arc operation up to 100 atmospheres were largely performed by Murray [12] with the help of others [1] at this facility. A schematic of the complete instrumentation is shown in Figure 3-1.

The cascade assembly consisted of a thoriated tungsten cathode, a tungsten anode, and a segmented containment wall formed by a stack of copper plates. These plates, made of oxygen-free high conductivity copper, were insulated from each other by thin sheets of lexan. Each plate consisted of two sheets, the thicker one having machined water channels to provide adequate cooling during operation of the arc, as shown in Figure 3-2. The holes at the four corners provided common water entrances and exits for each plate. High temperature silicone rubber washers formed water seals around these holes and larger washers were placed around the center holes to provide a closed arc channel. These larger washers

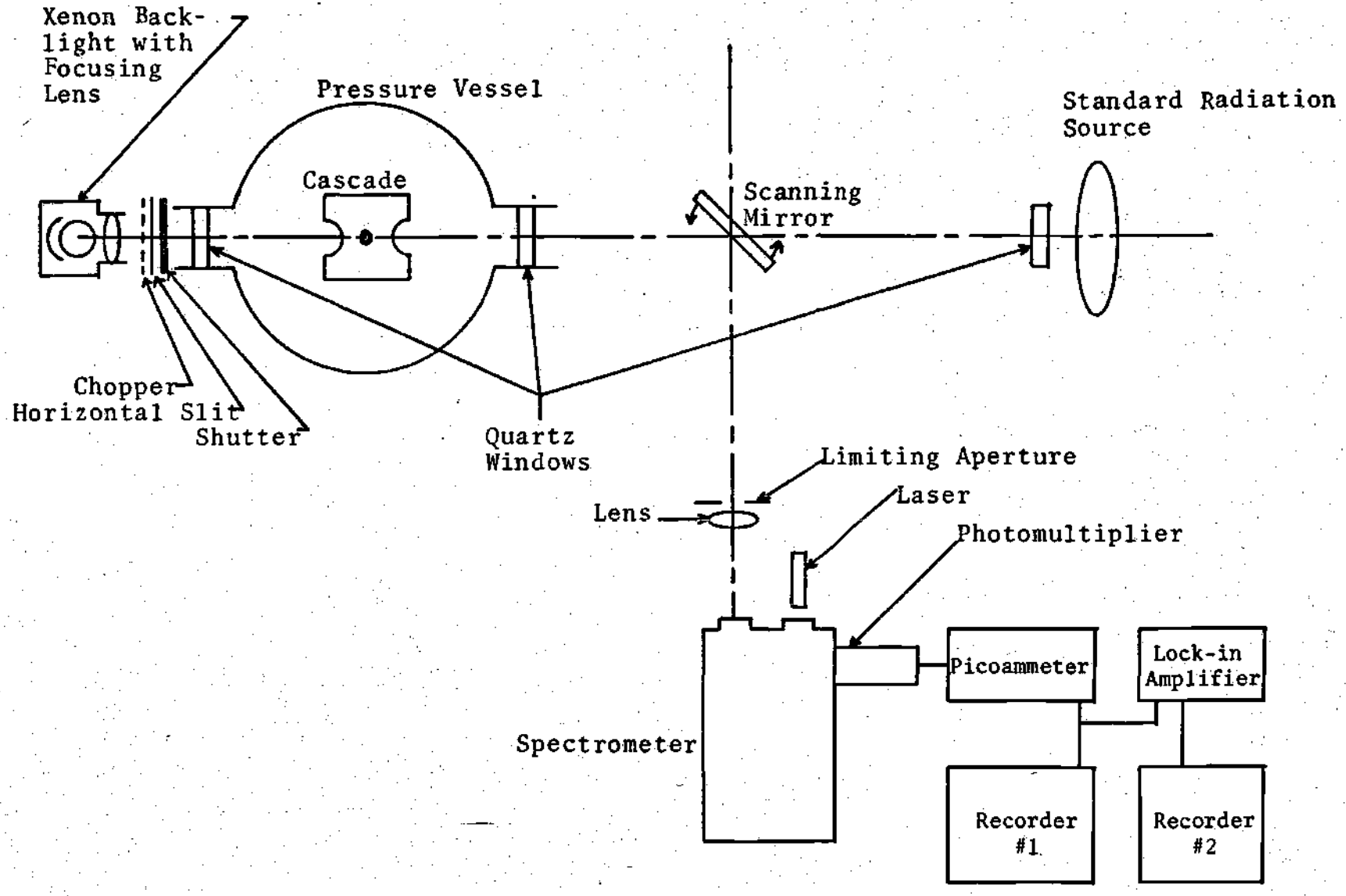

Figure 3-1. Schematic of Apparatus

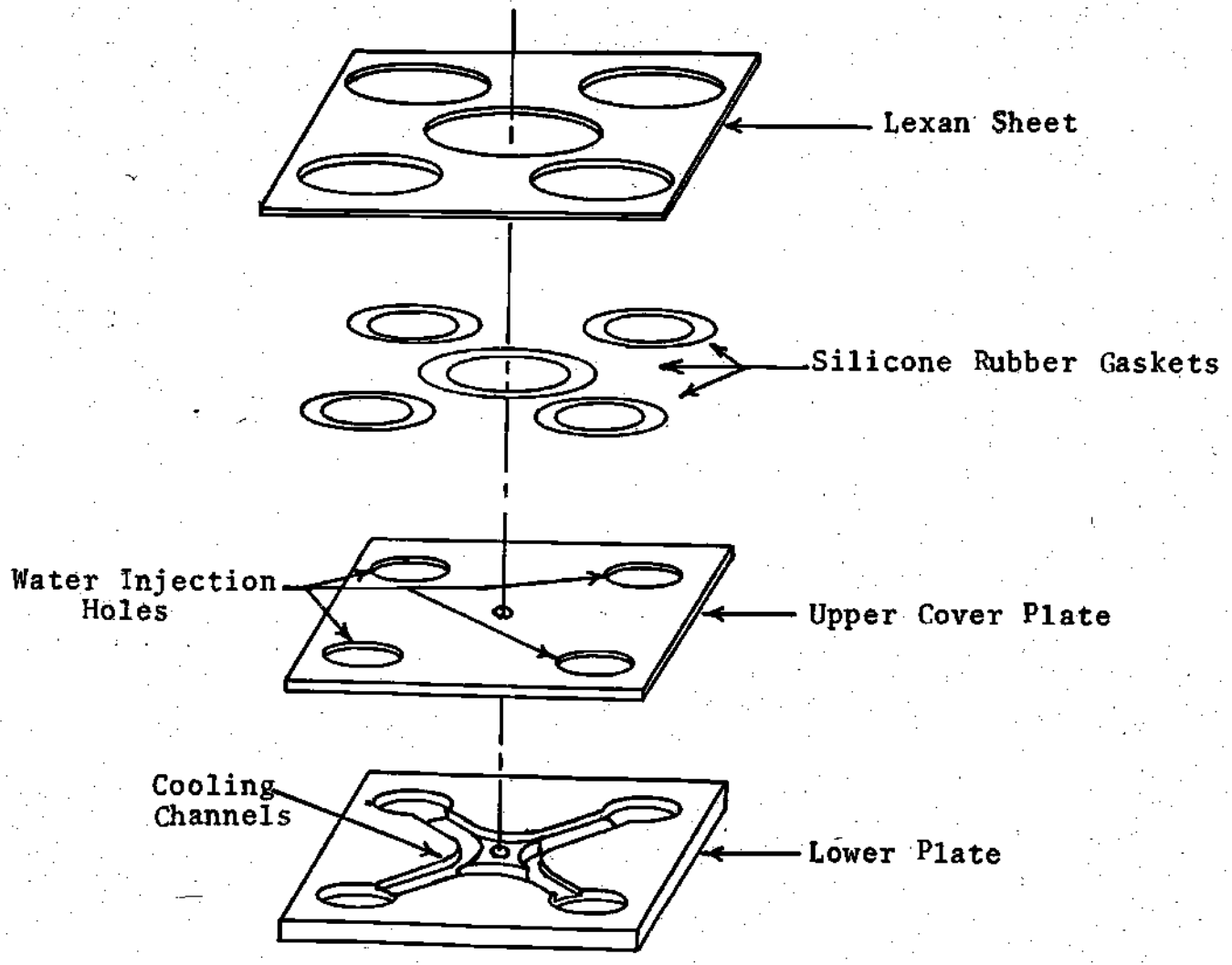

Figure 3-2. Cascade Plate Construction and Accessories from Dodson [1]

also protected the lexan insulators from heat damage caused by the arc. The only places these larger washers were not used were in the window gap and in several breather ports facilitating the removal of gases from the arc column. The central hole was rounded, as shown in Figure 3-3, to inhibit any hot spots in the containment wall where the arc could affix itself. The entire assembly of the cascade is shown in Figure 3-4.

Since the copper plates were electrically insulated from each other and from ground, they floated at the local average arc voltage during operation of the arc. Therefore, these plates were electrically connected to a scanning unit, a digital voltmeter, and a plotter to provide voltage and electric field measurements of the arc. The electric field was determined by assuming that for an arc length with constant chemical properties along its axial length the voltage drop per unit length, the electric field, was also constant. This property was determined by measuring the voltage drop between two nonadjacent plates located on opposite sides of the window gap. This potential difference was run through a differential amplifier. The amplifier was used as an analog to the distance between the plates, along with a scale factor bringing the displayed voltage reading to less than ten volts.

The arc current was determined by measuring from a calibrated shunt off the main power line to the cathode.

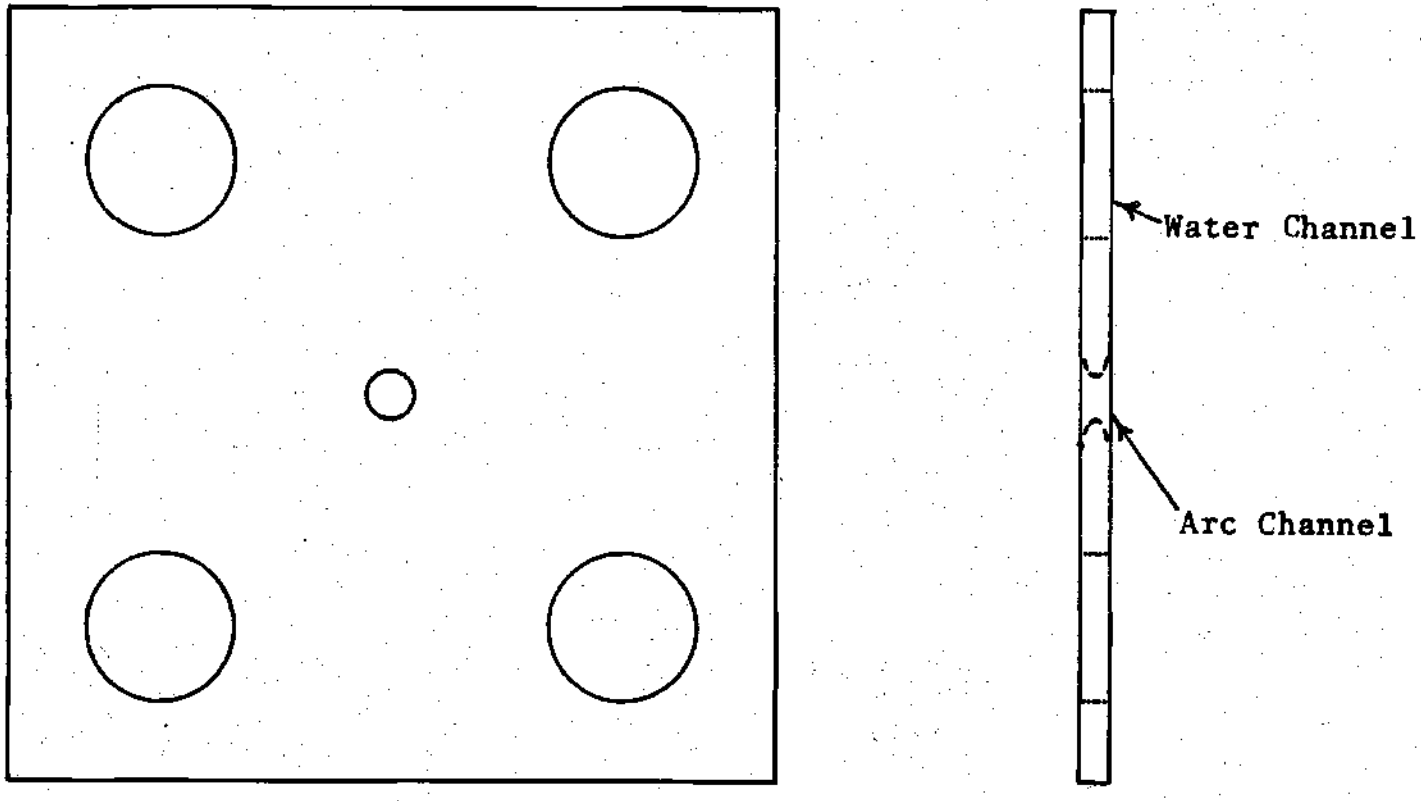

Figure 3-3. Schematic of Plate Showing the Curved Side of the Arc Channel Hole

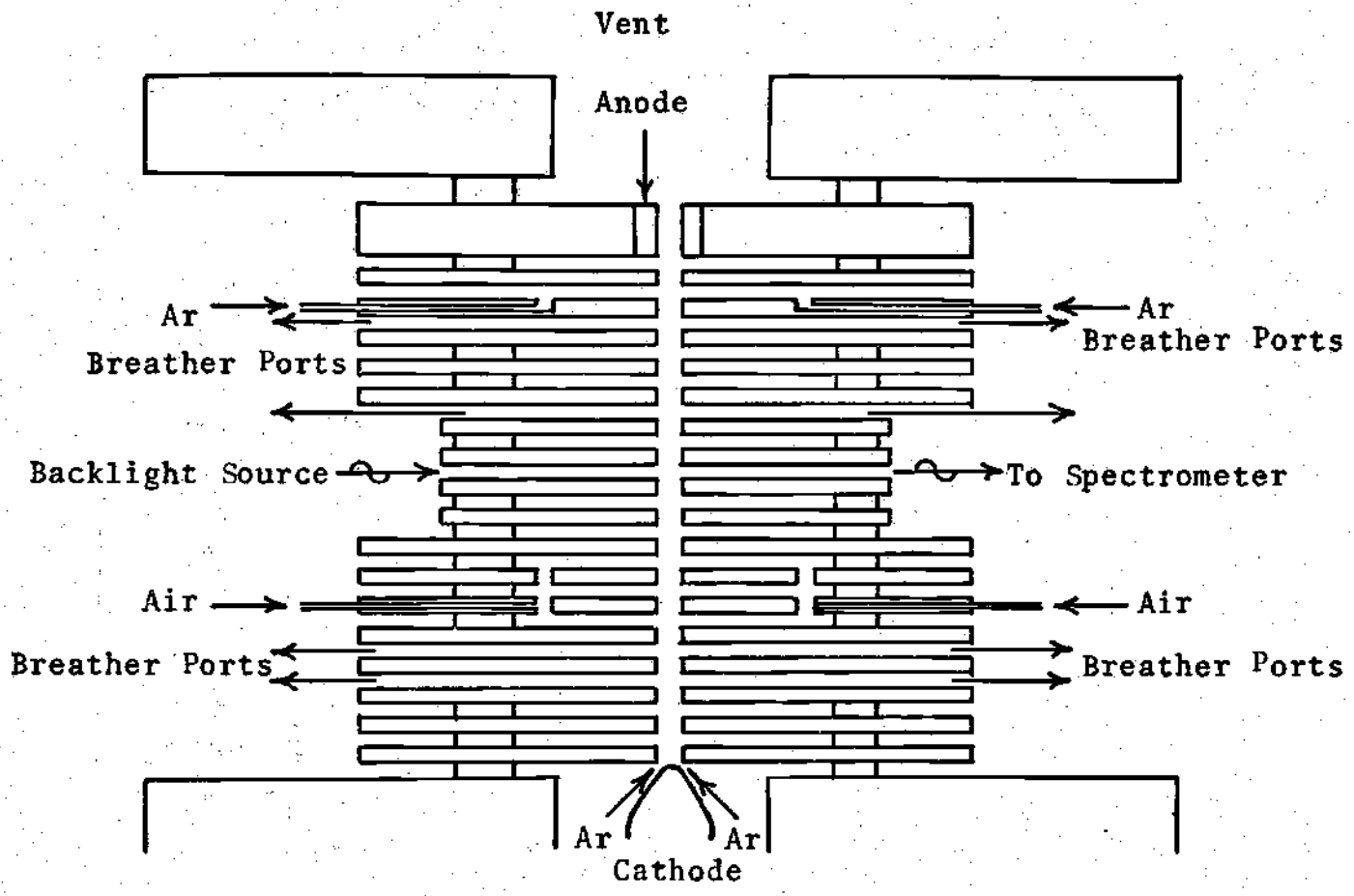

Figure 3-4. Schematic of Cascade System

This measurement was also made through a differential amplifier with the gain adjusted to scale the readings to less than ten volts. The total voltage drop across the arc was measured by using a similar technique.

The cascade was placed inside a pressure vessel, rated at 250 atmospheres, in such a way that the cascade window section was aligned with the chamber windows providing a straight optical path through the pressure vessel.

A McPherson model 2051 spectrometer was used to spectrally isolate the arc radiation, and a S-20 photomultiplier tube was used to detect the spectrally isolated optical signal and convert the signal to an electric current. A Keithley model 416 high speed picoammeter converted this small current to a three volt maximum output signal. This signal was measured and plotted by a Gould "Clevite model 250" brush recorder.

A front surfaced mirror was used to reflect the arc signal approximately 90° and provide scanning capability by rotating. The axis of rotation for the mirror coincided with the middle of the front surface preventing any change in the optical distance from the arc to the spectrometer while the mirror rotated. A lens was also placed in the optical path focusing the arc image onto the spectrometer entrance slits.

An Oriel 1000 watt xenon arc lamp with a focusing lens was placed in the optical path behind the pressure vessel, and this lens was set to focus the lamp upon the arc column.

This setting gave maximum intensity along the optical path and a very uniform intensity distribution across the window section. A chopper wheel and a limiting aperture slit were placed between the backlight and the pressure vessel to provide a chopped backlight signal to be differentiated from the steady state arc signal. This chopped signal was separated from the arc signal by a PAR model JB-5 lock-in amplifier connected to the output of the picoammeter. This separated signal was then plotted by a second brush recorder.

A shutter was placed between the chopper wheel and the pressure vessel. This shutter enabled one to obtain absolute intensity measurements of the arc itself for determination of temperature distributions. A helium-neon laser was used to provide an optical path aligning all the optical instrumentation along this path. Once all the optics were aligned the system was ready to use.

Radiation standard sources were placed on the opposite side of the scanning mirror from the pressure vessel. These sources were placed so that the image of the sources upon the spectrometer was in focus. Having the sources in focus insured that the optical distance between the standard source and the focusing lens was equal to the distance between the arc and the lens. The sources used were a Molarc 2803°K carbon arc with power supply and a tungsten ribbon lamp with power supply.

CHAPTER IV

PROCEDURE

The proposed cross-section of the arc region in the window area of the cascade, shown in Figure 4-1, had the arc in the center surrounded by a medium which severely attenuates backlight radiation. The purpose of this experiment was to measure the effective transmittance across the arc, determine the wavelength dependence of the transmittance, and use this information to obtain a consistent temperature profile from absolute intensity measurements using at least two spectral emission lines from different air components.

Once the cascade was placed in the pressure vessel and the optics were aligned, final preparations were made for the experiment. The spectrometer exit slits were opened to 2 mm, which would pass most of the spectral line intensity to the photomultiplier tube. The electronic instruments were allowed to warm up for more than one hour before the experiment started.

Once everything was ready, the pressure vessel was sealed and pressurized with argon, and the backlight was started. With the chamber pressure at 30 atmospheres and the shutter open, the entire window gap was laterally scanned. These scans, taken at 862.9 nm, 856.8 nm, 850 nm, and

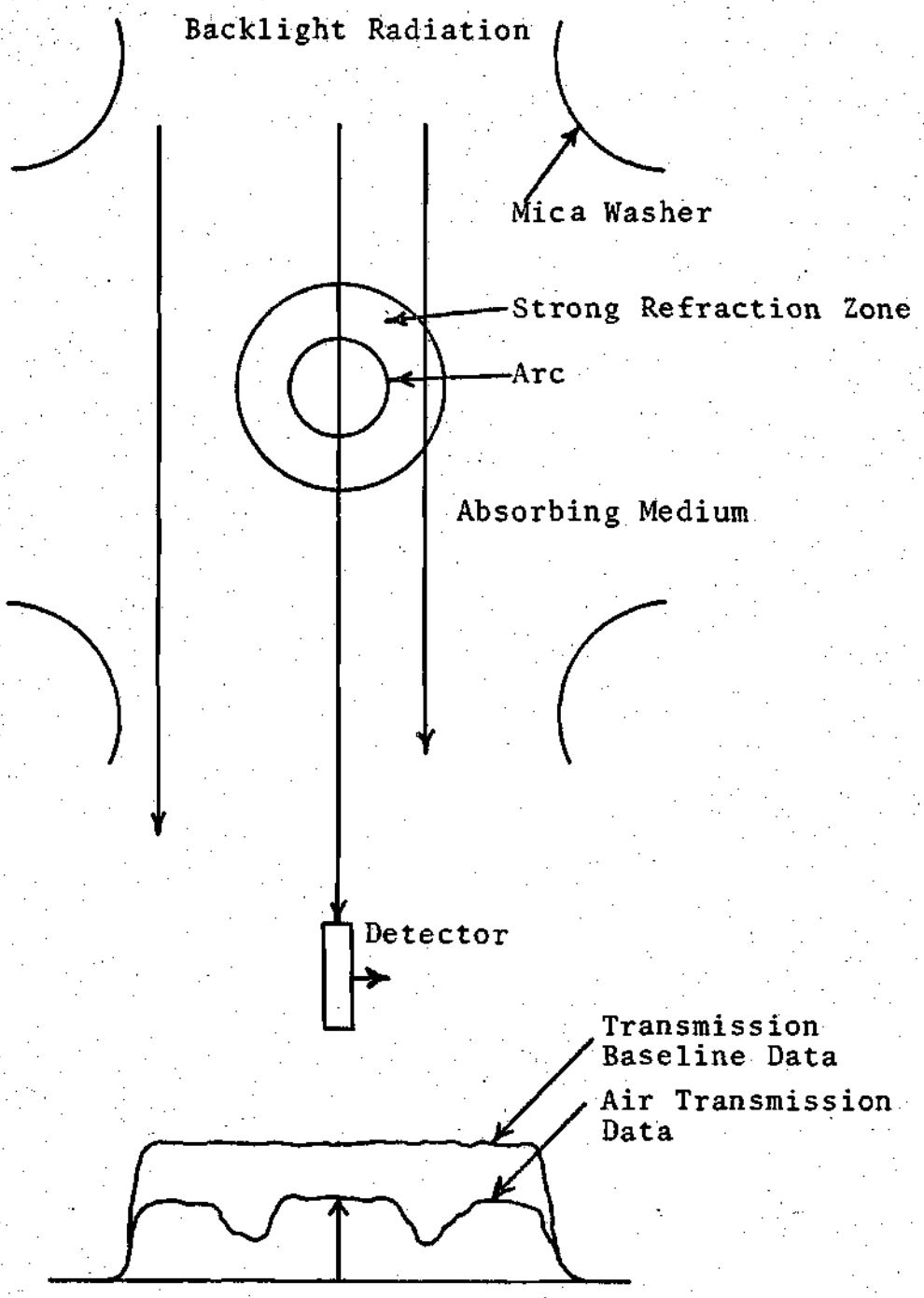

Figure 4-1. Schematic of Arc Region and Transmission Measurement Setup

844.65 nm, provided baseline transmission data for three spectral air emission lines and a convenient baseline continuum transmission measurement. Next a spectral scan from 865 nm to 840 nm was taken of the backlight image over the water channel to the side of the arc channel, as shown in Figure 4-2. This scan provided additional absorption baseline information. The chamber was then depressurized to one atmosphere.

With the chamber at one atmosphere it was reopened, and a starting stick with a known diameter was placed in the arc channel. With the starting stick in place a lateral (spatial) scan was made to provide a calibrated scale factor to be used to measure the arc radius. The lateral scan was repeated with the stick out to determine the backlight intensity distribution directly behind the arc channel. The arc was started, the chamber was sealed, and it was repressurized with argon. When the arc was operating at 30 atmospheres of argon, a complex refraction pattern of the backlighted arc was seen focused upon the spectrometer entrance slits, as shown schematically in Figure 4-3. The backlight intensity distribution measurements in the arc region did not appear to be affected as long as the horizontal entrance slit on the spectrometer did not accept radiation from the upper or lower refraction zones. This condition was accomplished by narrowing the horizontal entrance slit, making the gap smaller than the focused image of the unaffected region prior

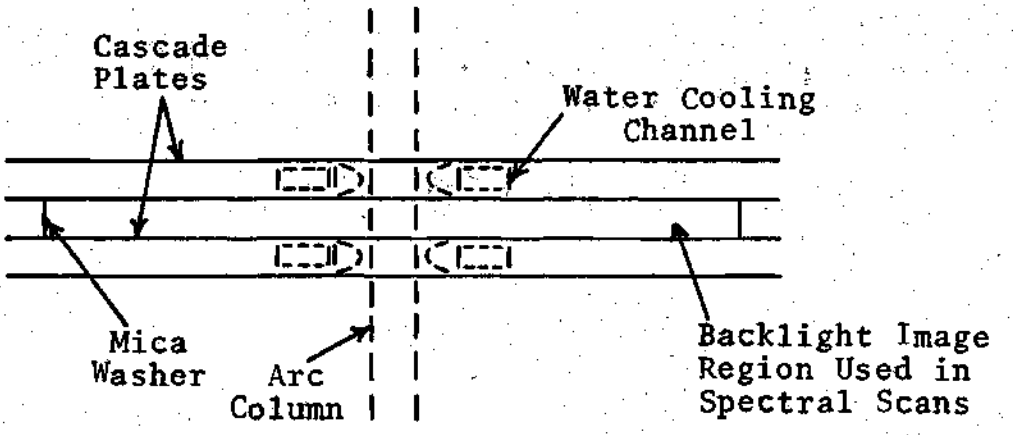

Figure 4-2. Schematic of Window Section in Arc Assembly as Seen from Spectrometer

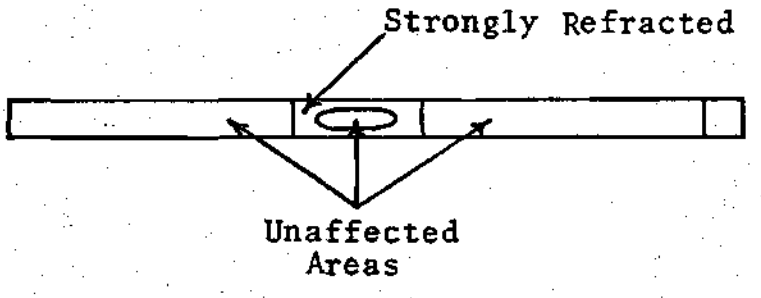

Figure 4-3. Schematic Showing Refraction Zones in Backlight Image Upon the Spectrometer. Vertical Refraction Zones Correspond to Water Channels

to the experiment. The spectrometer was aligned so that this slit was in the center of the unaffected region. Before air was introduced into the test section the same lateral and spectral scans were repeated, and preparations for air operation were made. Such preparations included closing the spectrometer exit slit to increase the resolution to less than .1 nm.

The spectrum of an air-argon mixture has an argon emission line at 842.2 nm and an oxygen line at 844.65 nm. When air was introduced into the test section these line intensities were compared to check for air purity. Purity was considered accomplished when the argon emission line was not detected and the height of the oxygen no longer increased. Once this purity was established the exit slit was reopened to its original position, and the spectrometer was set at a wavelength of 844.65 nm. Two lateral scans were taken with the backlight shutter open for transmission measurements, and six lateral scans were taken with the shutter closed to get absolute intensity distributions across the arc. The spectrometer was then set at a wavelength of 850 nm, with four lateral scans taken with an open shutter and four scans taken with the shutter closed.

After the 850 nm continuum scans were completed, the spectrometer exit slit was narrowed and the test section was reexamined for pure air. The slits were then reopened to 2 mm and the spectrometer was set at a wavelength of 856.8 nm.

At this wavelength lateral scans were taken with the shutter opened and closed, and the procedure was repeated at 862.9 nm.

Once the 862.9 nm data were acquired, the backlight image outside of the side water channel was focused upon the spectrometer entrance slits, and a spectral scan was taken over the wavelength interval of 865 nm to 840 nm. Once this scan was completed lateral scans across the arc were repeated, with and without the backlight, at the 844.65 nm wavelength. These scans checked the repeatability of the data and checked the deterioration of the optical path transmittance over the time span of the air experiment. Once these scans were completed, the air was turned off and the experiment was terminated.

Once the chamber was depressurized standard radiation sources were set in place as described in the apparatus section. Measurements from these sources were taken at all four wavelengths to calibrate the absolute intensity measurements and enabled one to find the temperature distribution within the arc.

CHAPTER V

COMPUTER PROGRAMS

In order to determine the temperature distribution within the arc two computer programs were developed. The preliminary program TPAD (Transparent Polynomial Abel Diagnostics) was developed to acquire a good first estimate of the temperature distribution. The primary program LOCAD (Line Opacity Corrections for Arc Diagnostics) was developed to determine, from a given temperature profile, how much radiant intensity is observed and how much is absorbed. The program was also given the capability to adjust the temperature distribution within the arc correcting for any absorbed radiation and producing a new temperature profile more representative of the actual conditions within the arc.

When one works with arcs operated at or below pressures of one atmosphere, the spectrometer exit slit may be opened increasing the wavelength handpass to the photomultiplier tube. In many cases it is possible to allow the entire line intensity to be read at once. When the pressure is increased the spectral lines are pressure broadened enough to cause a significant percentage of the spectral line intensity to lie outside this bandpass. Knowing the temperature dependence of the line emission coefficient and

assuming a Lorentz spectral distribution around line center, one may use the known spectrometer spectral resolution to predict the percentage of the line emission coefficient which is cut off by the finite spectral resolution.

The TPAD program reads a line emission coefficient library starting at 6000°K and incrementing by 200°K up to 16000°K. It reads in Stark broadening parameters and adjusts the emission coefficient library to compensate for the finite exit slit width in the observations. This compensation is achieved by finding the percentage of the line emission coefficient which falls within the spectral bandpass at each temperature, multiplying that emission coefficient by that percentage, and obtaining a new emission coefficient corresponding to that temperature. This process is depicted in Figure 5-1.

After the new emission coefficient library is set up, the program reads the observed non-zero spectral line intensities at a number of equally spaced base points and calculates third degree least square coefficients [13] for each point using that point and three points on each side of that point. These polynomials are then differentiated to obtain the approximate slope of the intensity with respect to the y-direction at each data point. This process is demonstrated in Figure 5-2. These slopes are then fit with a third degree polynomial for each interval between two adjacent base points. One point on each side of these two

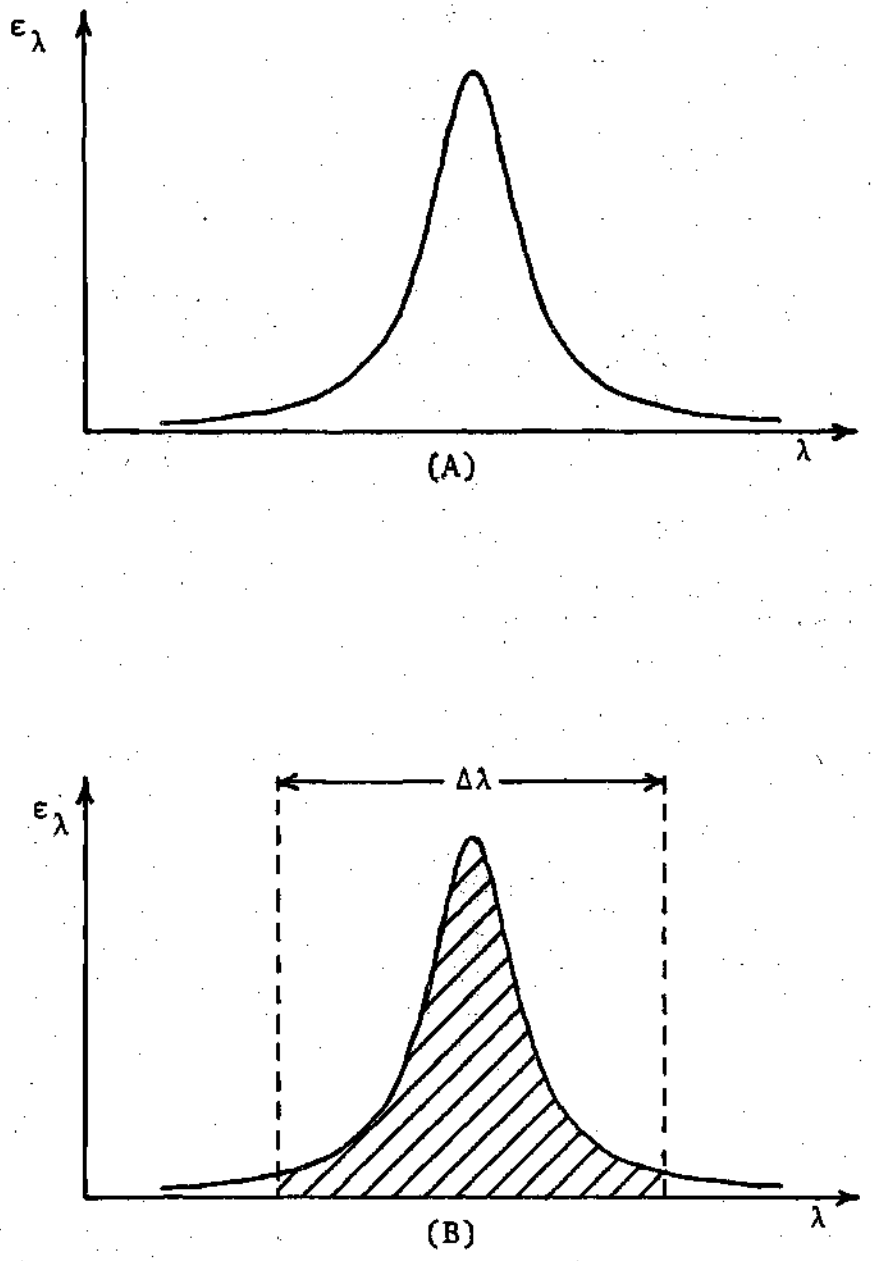

Figure 5-1. Method Used for Finding the Reference Emission Coefficient, Hatched Area in (B), Accounting for Finite Spectral Bandpass of Spectrometer from the Actual Emission Coefficient, Area Under Curve in (A), for a Fixed Temperature

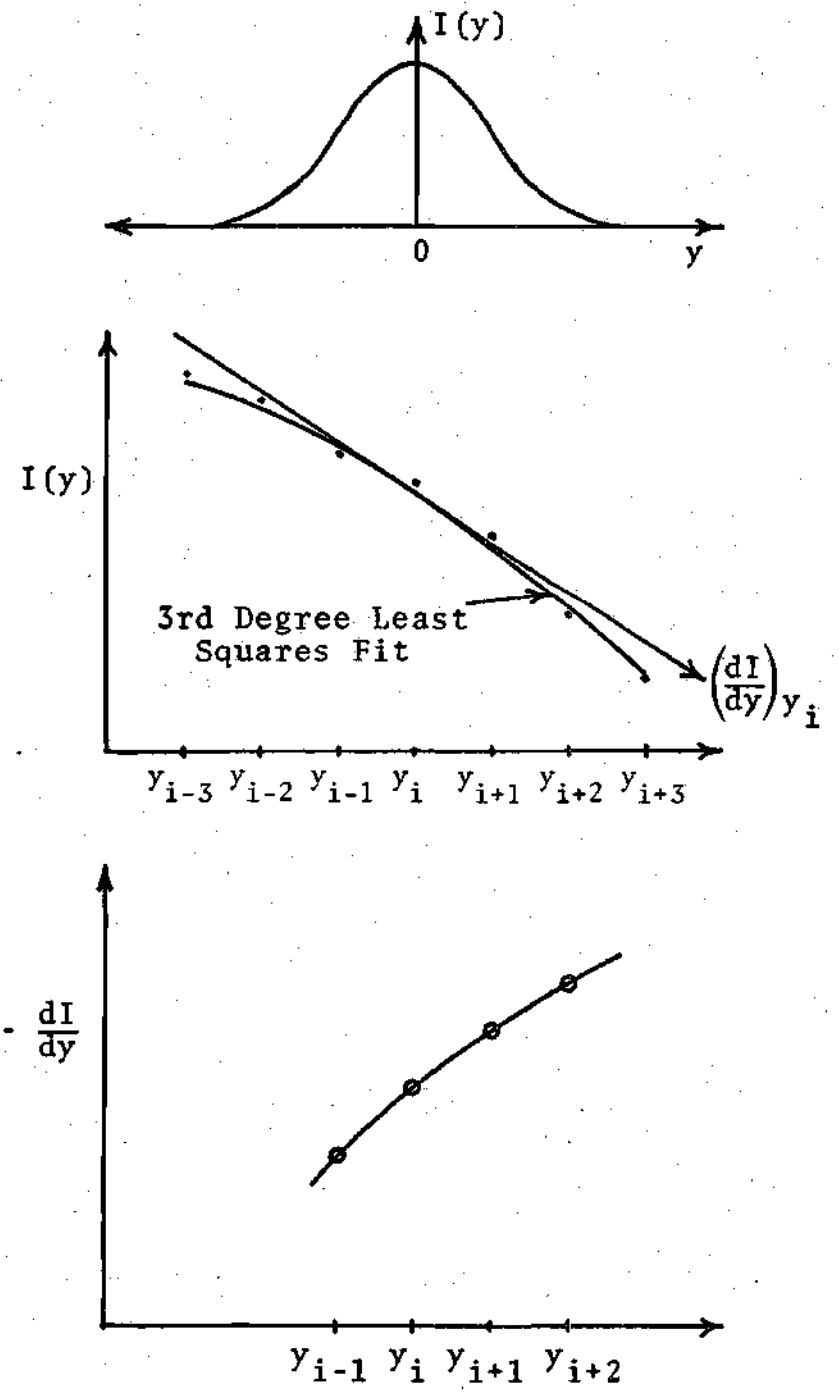

Figure 5-2. Method of Determining $I'_i(y) = a_{0,i} + a_{1,i}y + a_{2,i}y^2 + a_{3,i}y^3$ Over the Closed Interval $[y_i, y_{i+1}]$

base points is used to obtain the four required base points for each polynomial. These polynomials are used to calculate a closed form solution

$$\epsilon_i(r_j) = -\frac{1}{\pi}\int_{r_i}^{r_{i+1}} \frac{\left(\frac{dI}{dy}\right)_i}{\sqrt{y^2-r_j^2}}\,dy \qquad (5\text{-}1)$$

$$\frac{dI}{dy}_i = a_{0i} + a_{1i}y + a_{2i}y^2 + a_{3i}y^3: \quad y_i \le y \le y_{i+1}$$

for each interval. These intervals are then summed to yield the Abel transformation

$$\epsilon(r_j) = \sum_{i=j}^{ND} \epsilon_i(r_j) = -\frac{1}{\pi}\sum_{i=j}^{ND}\int_{r_i}^{r_{i+1}} \frac{\left(\frac{dI}{dy}\right)_i}{\sqrt{y^2-r_j^2}}\,dy \qquad (5\text{-}2)$$

where ND is the number of intensity values read. The solution to this transformation is the radial emission coefficient profile which is parabolically fit to the emission coefficient library to obtain the radial temperature distribution.

Since these emission coefficients were determined using intensities observed with a finite spectral bandpass, the program adjusts the determined emission coefficients by reversing the procedure used at the beginning of the program and shown in Figure 5-1. This process, shown in Figure 5-3,

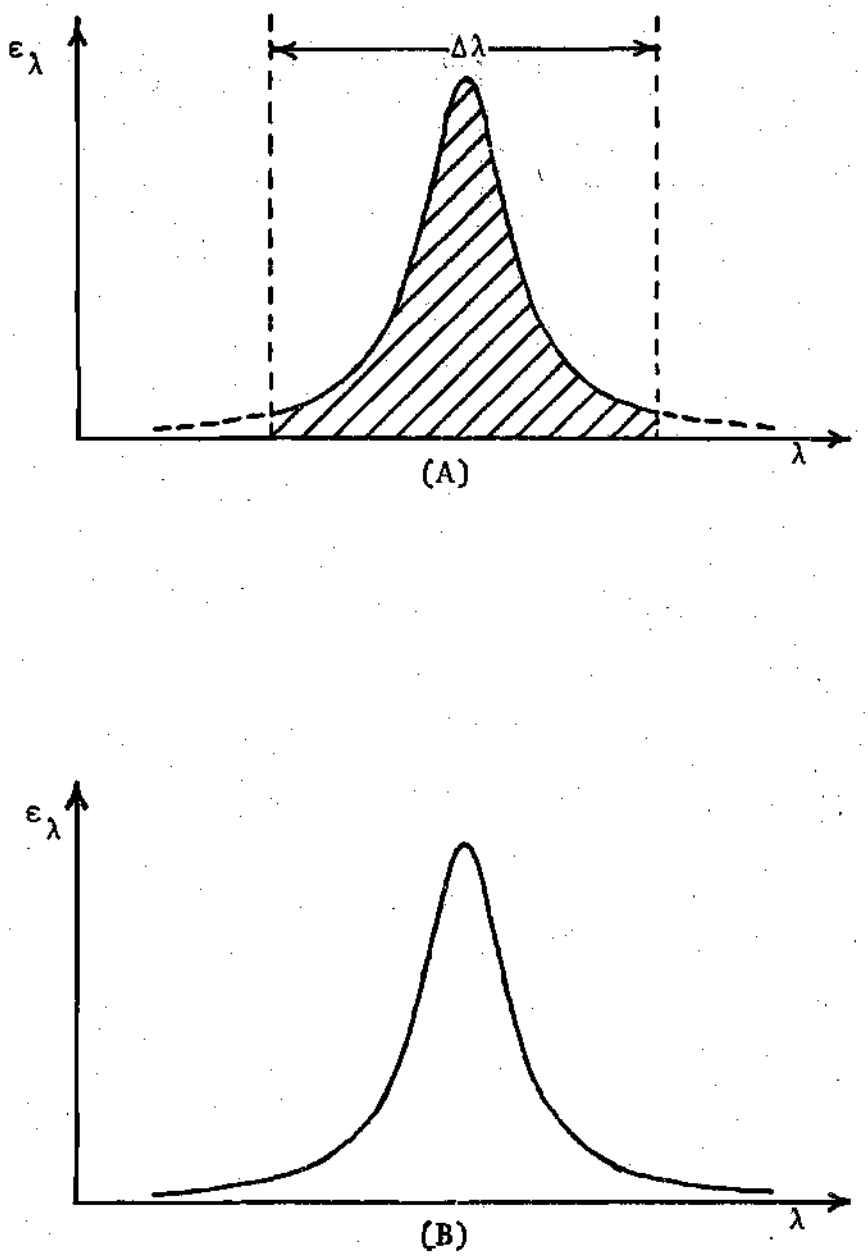

Figure 5-3. Method Used for Recovering that Percentage of the Spectral Line Emission Coefficient not Detected by the Spectrometer, Nonhatched Area in (A), to Obtain Total Line Emission Coefficient (B). (Reversal of Process Shown in Figure 5-1.)

yields a better approximation of the actual emission coefficient profile. The program now prints the actual emission coefficient and the temperature for each radial position in the arc. The emission coefficients and other information are also dumped into a data file for subsequent use by the next program discussed here.

In TPAD, great care must be taken in determining the spatial intensity distribution from the data. Small errors in the data can lead to large errors in the calculation of the spatial derivative $\frac{dI}{dy}$. The derivative value at each base point is printed enabling the user to check the accuracy of his data points. The least square method used in finding these derivatives tends to smooth small errors, but it cannot correct a trend of inaccuracies in one direction. In general, this program is quite stable and gives the user a good first approximation for small optical opacities for the spectral line being used.

The emission coefficient and temperature profiles generated by TPAD were obtained by assuming that self absorption within the arc was negligible. When absorption cannot be ignored the radiation transport equation in one direction becomes

$$\frac{dI_\lambda}{dx} = \varepsilon_\lambda \left(1 - \frac{I_\lambda}{B_\lambda}\right) \qquad (5\text{-}3)$$

where I_λ and ε_λ are strong functions of wavelength and arc position. The monochromatic blackbody function B_λ is also a strong function of temperature but is almost constant over the small wavelength interval of 1.3 nm used as the spectral bandpass for the spectrometer. The LOCAD program takes the line emission profile generated by TPAD and generates a spectral emission coefficient distribution fitting a Lorentz profile to each line emission coefficient. LOCAD then solves equation (5-3) using Gill's Runge-Kutta method [13,14] at discrete wavelengths to obtain a discrete spectral intensity distribution at each y position corresponding to each radial position output from TPAD, as seen in Figure 5-4. Gill's method was chosen, since it is a one-step method and the distance between equidistant radial circles are not equidistant along chords which do not pass through the central axis. With Gill's method information is needed at the midpoint between each two adjacent base points. This information was gathered by finding the radius of each midpoint and using radial parabolic interpolation as shown in Figure 5-5.

The transport of I_λ is followed at 79 discrete wavelengths about line center and can be initially set to zero or to any value simulating a backlight source. Once I_λ leaving the arc is obtained for any or all spatial positions, they are integrated across the spectral bandpass by using Simpson's one-third rule. The program then prints the

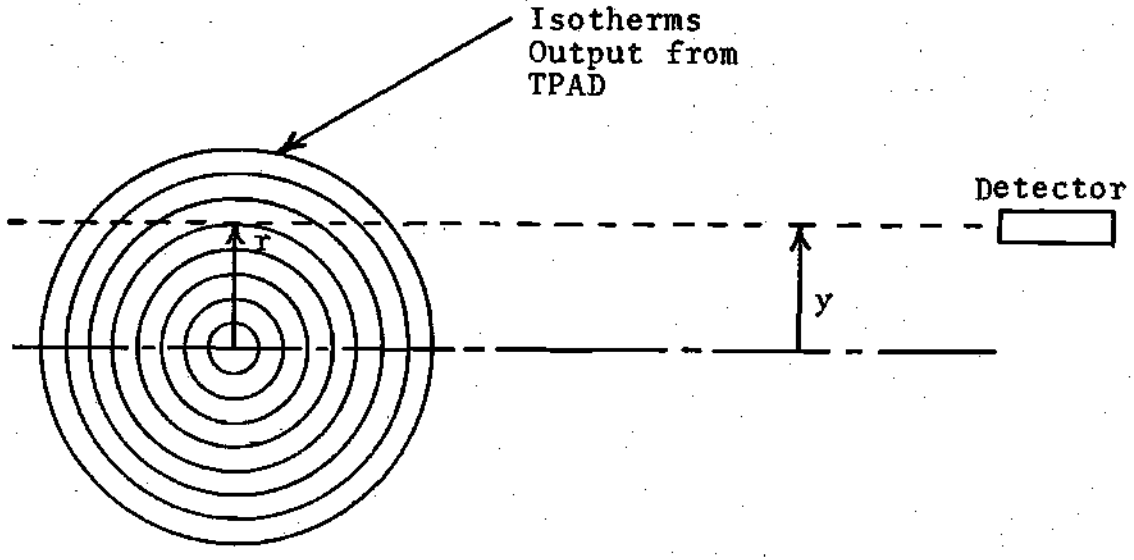

Figure 5-4. Correlation Between y-Values Used in LOCAD and r-Values Output from TPAD

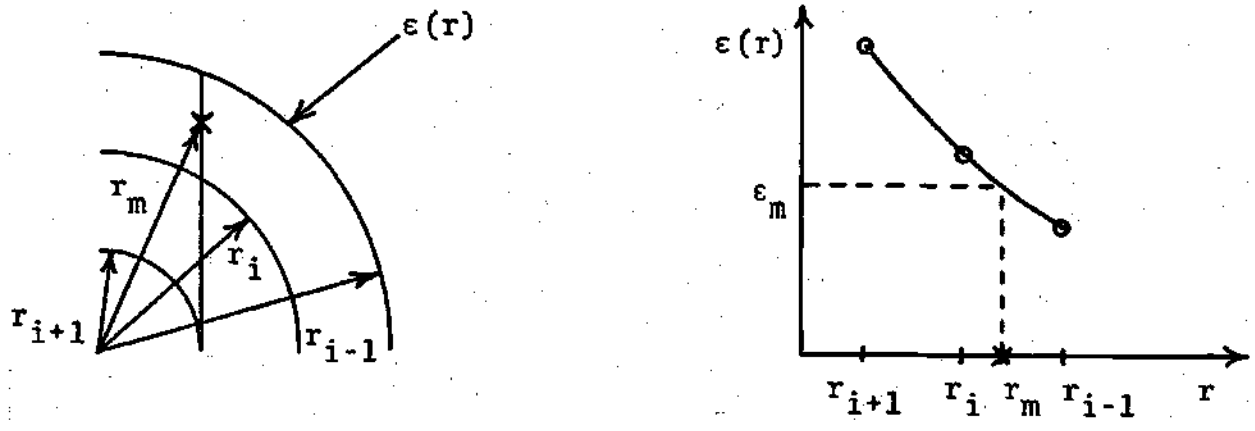

Figure 5-5. Parabolic Interpolation Method Used for Determination of Emission Coefficients at Chordal Midpoints for Use in Gill's Method Solution to Equation (5-3)

spatial position of the detector, the predicted intensities from the solution to equation (2-20) and the predicted intensities from the solution to equation (2-6) with κ_λ set equal to zero. The user has the option of obtaining monochromatic intensity comparisons between the two assumptions for the line intensity detected from arc center.

This program can also start with a given temperature profile and iterate the emission coefficients until a specified spatial intensity profile is matched. The author prefers to use the optically thin intensities internally generated using the temperature profile output from TPAD, since LOCAD may be using more data points than the original data; however, the user is not limited to that choice. The method used starts with the outside chord and corrects its central emission base point. The two outside base points are always equal to zero. After the outside chord has been iterated to match its specified intensity the program progresses inward to each succeeding chord. The average run for each base point consists of first solving equation (5-3), integrating across the bandpass and subtracting the result (S1) from the specified value (S2). The second guess for the middle base point emission along that chord is

$$\varepsilon_2 = \varepsilon_1 \left(\frac{S2}{S1}\right) \qquad (5\text{-}4)$$

which now replaces the old value, and changes all linked parameters associated with the emission coefficient. Equation (5-3) is solved again and the result is again subtracted from the specified value. If this difference (D_i) is not within one percent of zero, the third guess and each succeeding guess is determined by

$$\varepsilon_{i+1} = \frac{\varepsilon_{i-1} D_i - \varepsilon_i D_{i-1}}{D_i - D_{i-1}} \qquad (5\text{-}5)$$

which is geometrically depicted in Figure 5-6. The third guess has nearly always yielded line intensities within one percent of the specified intensities. The user has the option to store these absorption corrected emission coefficients within a data file for future use.

These corrected emission coefficient and temperature profiles now account for the spectral line absorption within an arc which is in LTE. Although the user is able to account for self-absorption this method does have its limitations. The spectral line shapes are only as accurate as the line width and shift data used in the program and are subject to the same restrictions used in acquiring this information. The accuracy of the method increases with the number of base points used in the analysis. The most important factor is that at lower temperatures or pressure, Doppler broadening becomes significant and the spectral profiles would no longer be Lorentz in character. An example is shown in Table 5-1

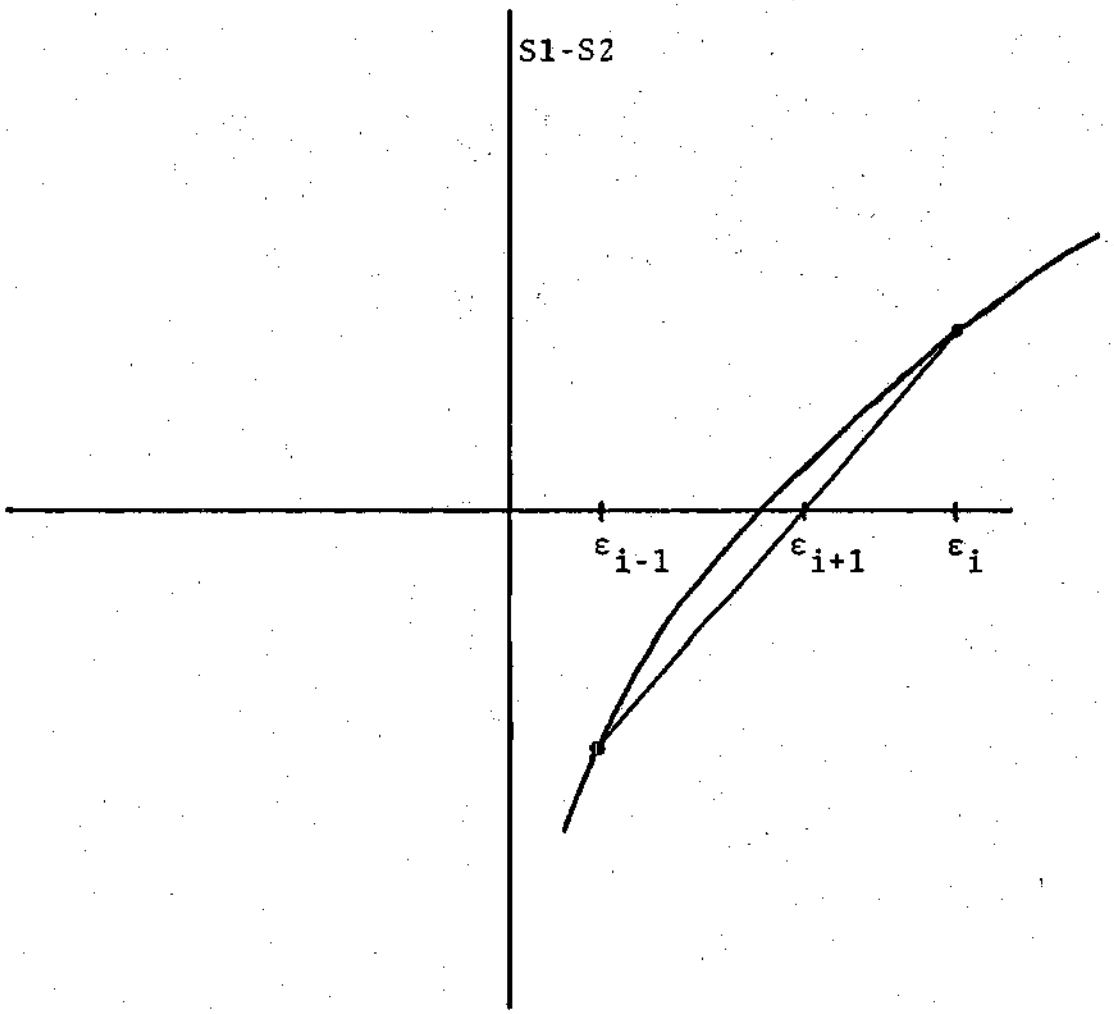

Figure 5-6. Method for Finding the Central Emission Coefficient Base Point which Matches the Predicted Chordal Intensity with a Specified Chordal Intensity

Table 5-1. (Half) Half-Widths for Oxygen 844.65 nm Line at 30 Atmospheres Using Equations (2-14) and (2-16)

T (°K)	w_D (nm)	w_S (nm)
6000	.0070	.0012
8000	.0081	.0094
10000	.0091	.0546
12000	.0099	.2330

for the oxygen line at a wavelength of 844.65 nm and a pressure of 30 atmospheres. One can see that at lower temperatures Doppler broadening is quite significant. This comparison forces one to investigate how the assumed spectral line shape affects the radial temperature distribution.

To examine this effect several different profiles were considered as seen in Figure 5-7. The first one checked was the Lorentz profile fitting the established parameters for (half) half-widths and shifts. The second profile was rectangular with the widths corresponding to the same half-width information and the heights making the total area equal to the total line emission coefficient. The third profile was triangular and fit the same requirements for the second profile. The Voigt profile, a convolution of the Lorentz- and Doppler profiles was the fourth one checked. This profile was determined by using Hermite quadrature [13,15] to solve equation (2-18). The intensity comparisons, integrated across the spectrometer bandpass are plotted in Figure 5-8, with plots of the intensity profiles from the same temperature profile when the arc was assumed optically thin. Differences in the plots for a transparent arc were caused by loss of some of the intensity in the Lorentz and Voigt profiles due to the finite spectrometer bandpass. One can see from the figure that while the shape of the profile is important, at high pressures it is not necessary to account for Doppler

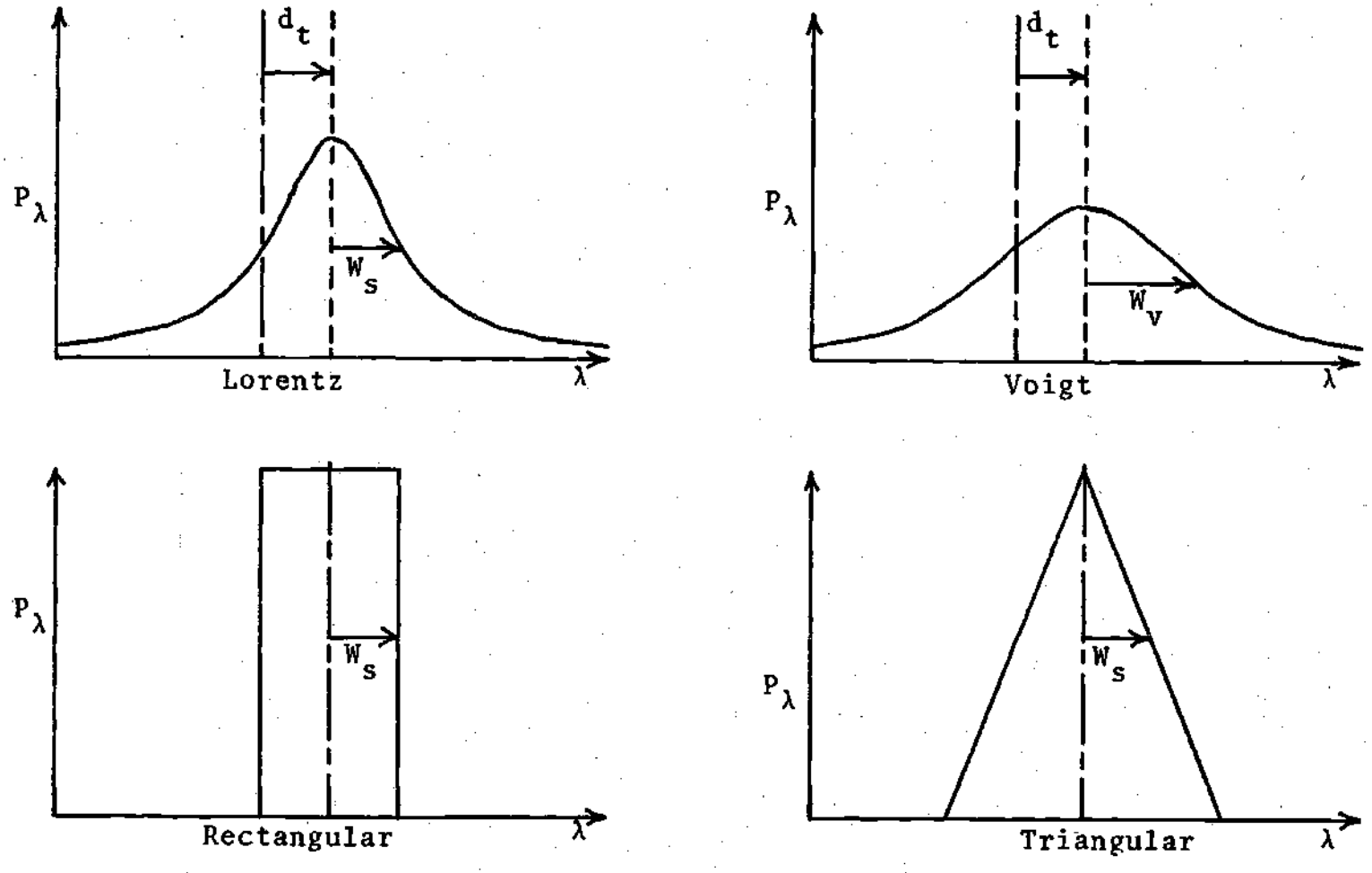

Figure 5-7. Profiles Used to Determine the Dependence of Absorption Upon the Assumed Emission Coefficient Profile

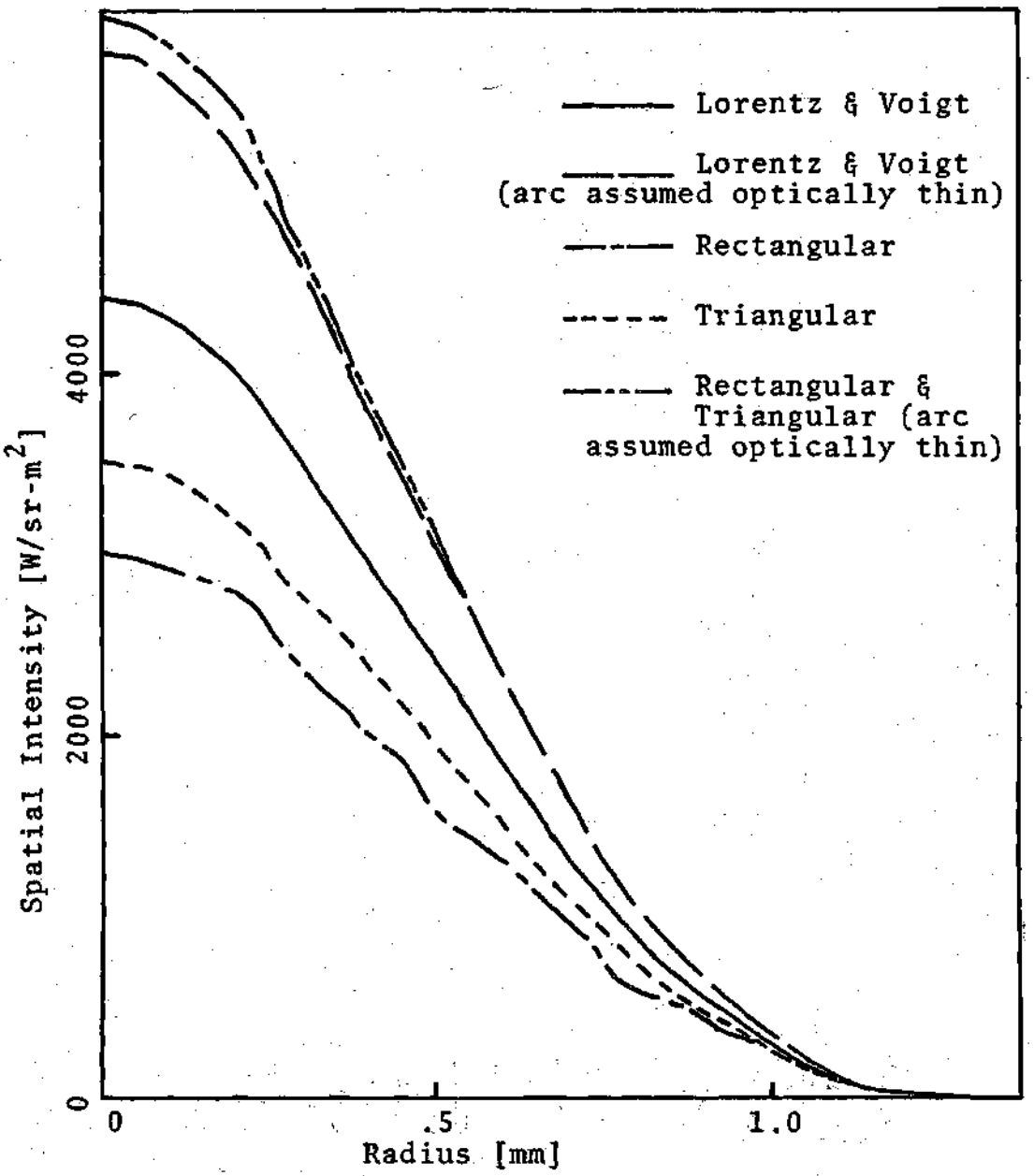

Figure 5-8. Effect of Different Profile Shapes, Shown in Figure 5-7, Upon the Predicted Intensity Distribution for Identical Radial Temperature Profiles

broadening when determining the temperature distribution within the arc.

CHAPTER VI

ANALYSIS

The analyses in this paper are made with the assumption that there were two different mechanisms which attenuated radiation from the arc. These mechanisms were the self absorption of radiation within the arc following Kirchoff's Law and attenuation of radiation outside the arc by the surrounding medium. The radiant absorption within the arc was analyzed by the newly developed computer programs, and the attenuation outside the arc was treated as an absorption process which was independent of wavelength over the spectral line. This attenuation in the surrounding medium was determined from analysis of backlight transmission through this medium for two cases: through the arc and far to the side of the arc, as shown in Figure 4-1. Since the apparent color of the backlight radiation appeared to be white, visual observations of the color of the transmitted backlight also provided useful qualitative information.

When air was injected into the test section, the color of the arc turned from blue-white to yellow-white. The color of the backlighted medium to the side of the arc appeared to be yellow, which gradually diminished in intensity and slowly became increasingly orange as the experiment progressed.

The transmission spectrum taken to the side of the air arc over the water channel, when compared to the baseline spectrum taken at the same place, showed a slow decrease in transmission as one moved higher in wavelength. This effect can be seen in Table 6-1.

Table 6-1. Relative Mean Spectral Transmission Through Outside Medium Across 1.3 nm Wavelength Intervals

Wavelength (nm)	Backlight Transmittance
844.65	1.000
850.00	.762
862.92	.571

This spectral scan took less than one minute and scanned downward with respect to wavelength.

Lateral measurements of the transmission of the backlight radiation across the entire window section showed an almost constant plateau in the arc region bounded by troughs with another plateau in the outside region, as shown in Figure 6-1. Since the transmittance was almost constant across the arc, the measured transmittance through arc center was used for all subsequent transmission calculations. Table 6-2 shows these transmittance values for all wavelengths used in temperature determinations. These measurements were taken in the same order shown in the table. Since this absorption had a small wavelength dependency, it was assumed

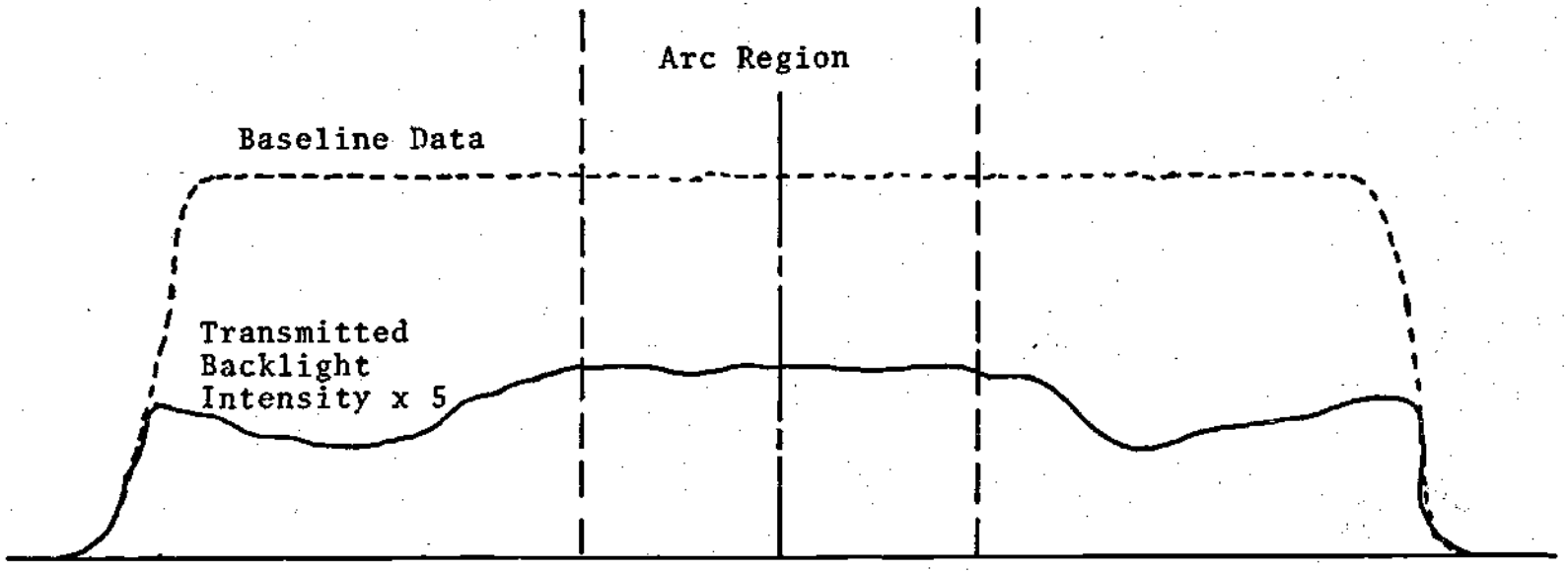

Figure 6-1. Comparison of Spatial Distribution of Transmitted Backlight Intensity with Baseline Data Across Entire Window Area Shown in Figure 4-2

Table 6-2. Mean Transmission Through Arc Center and Surrounding Medium Used in Temperature Determination (Arc was Assumed Optically Thin in the Determination of Arc Radiation Transmittance)

Scan Number	Wavelength (nm)	Measured Backlight Transmittance	Deduced Arc Radiation Transmittance
13	844.65	.115	.339
14	850.00	.065	.255
17	862.92	.028	.166
19	844.65	.034	.185

to be constant across the small wavelength bandpass of the spectrometer. This assumption enabled the use of an exponential decay of the backlight radiation through the medium in question. Arc radiation transmission through half this medium, hence, was found by taking the square root of the backlight transmission.

Comparison between the two oxygen line measurements in Table 6-2 indicated that either the transmission of the medium itself had dropped or the system optics had shifted. Visual observations mentioned above favor the first conclusion. It should be noted that in this series, approximately 30 minutes elapsed between scan numbers 13 and 19 with roughly an equal amount of time spent at each wavelength. A transmission comparison between scan numbers 17 and 19 confirmed an increase in medium absorption corresponding to an increase in wavelength. The data from the spectral line

at a wavelength of 856.77 nm were not usable for temperature determination due to problems with continuum measurements for that wavelength.

Once the transmission data were reduced, absolute intensity spatial profiles (shutter closed) for each wavelength were analyzed. This procedure consisted of finding the single or two most symmetric spatial profiles for each wavelength and folding them upon themselves as seen in Figure 6-2. The reduced intensity profile was a smooth half curve drawn manually which was the best fit of the two superimposed half curves. Absolute intensities were then recorded for equally spaced base points, starting from the central peak and working to but not including the point called the arc boundary. This boundary was defined to be the point where the measured intensity was undetectable. Since the measured transmittance across the arc was almost constant, these discrete intensity profiles were corrected for medium absorption by dividing them by "arc radiation transmittance" values found in Table 6-2 corresponding to their respective scan numbers. These corrected intensities were used as the actual intensities leaving the arc before passing through the surrounding medium. The corrected intensities for 850 nm were used as continuum measurements for the other wavelengths, and the other intensities were for the emission lines plus the continuum. Since equation (2-5) could only be used for line emission, the continuum measurements were subtracted

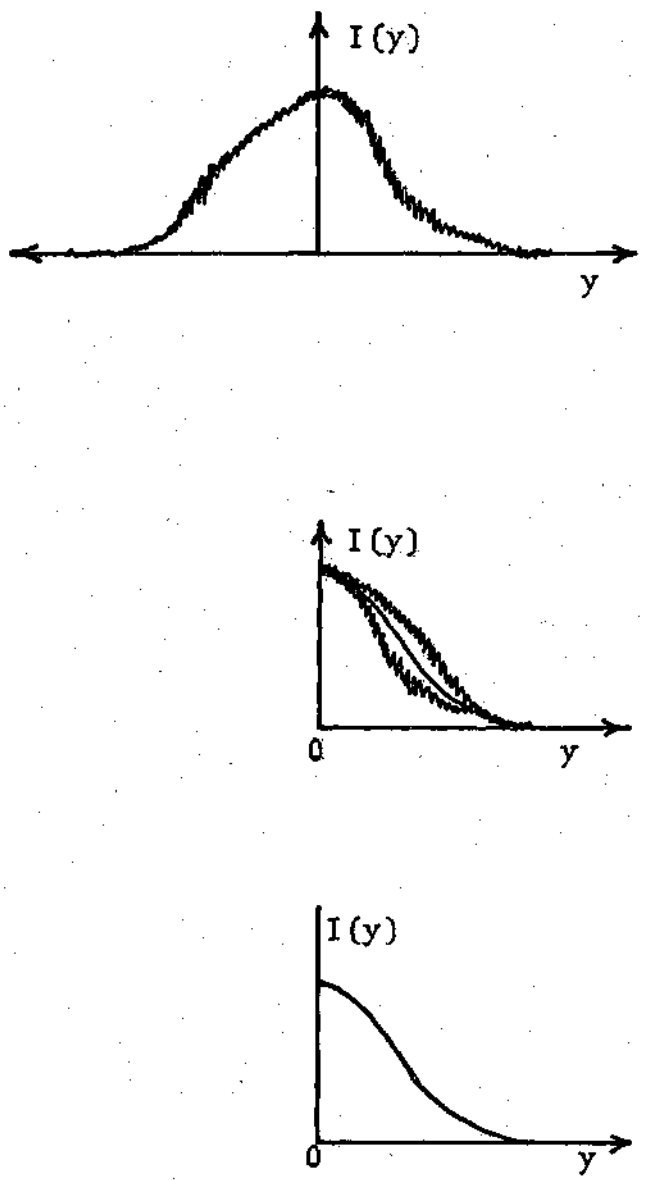

Figure 6-2. Method Used to Determine Experimental Intensity Profiles (Asymmetry Exaggerated for Clarity)

from the other intensity measurements for each respective base point. The resultant line intensities, along with other information, were input to TPAD which yielded the initial radial temperature distributions of an "optically thin" arc, shown in Figure 6-3.

The respective outputs from TPAD were input to LOCAD to regenerate the spatial intensity profiles from an "optically thin" arc for comparison with the actual intensity data. These "regenerated actual data" agreed with the actual data to within one percent and were used in subsequent comparisons since these intensities were smoother than the actual data. This use of the regenerated actual data also enabled the user to use more base points than there were original data points.

This execution of LOCAD also generated a predicted spatial intensity profile which would be observed if the arc were not assumed to be "optically thin." The differences between these "predicted intensities" and the regenerated actual data, shown in Figure 6-4, indicated that self absorption had a significant effect upon the intensity leaving the arc.

Once this absorption effect was noted the regenerated actual intensities were entered into LOCAD along with the output from TPAD. These executions generated final temperature profiles whose "predicted intensities" matched the "regenerated actual data" within one percent and accounted for this absorption effect. The comparison of these final

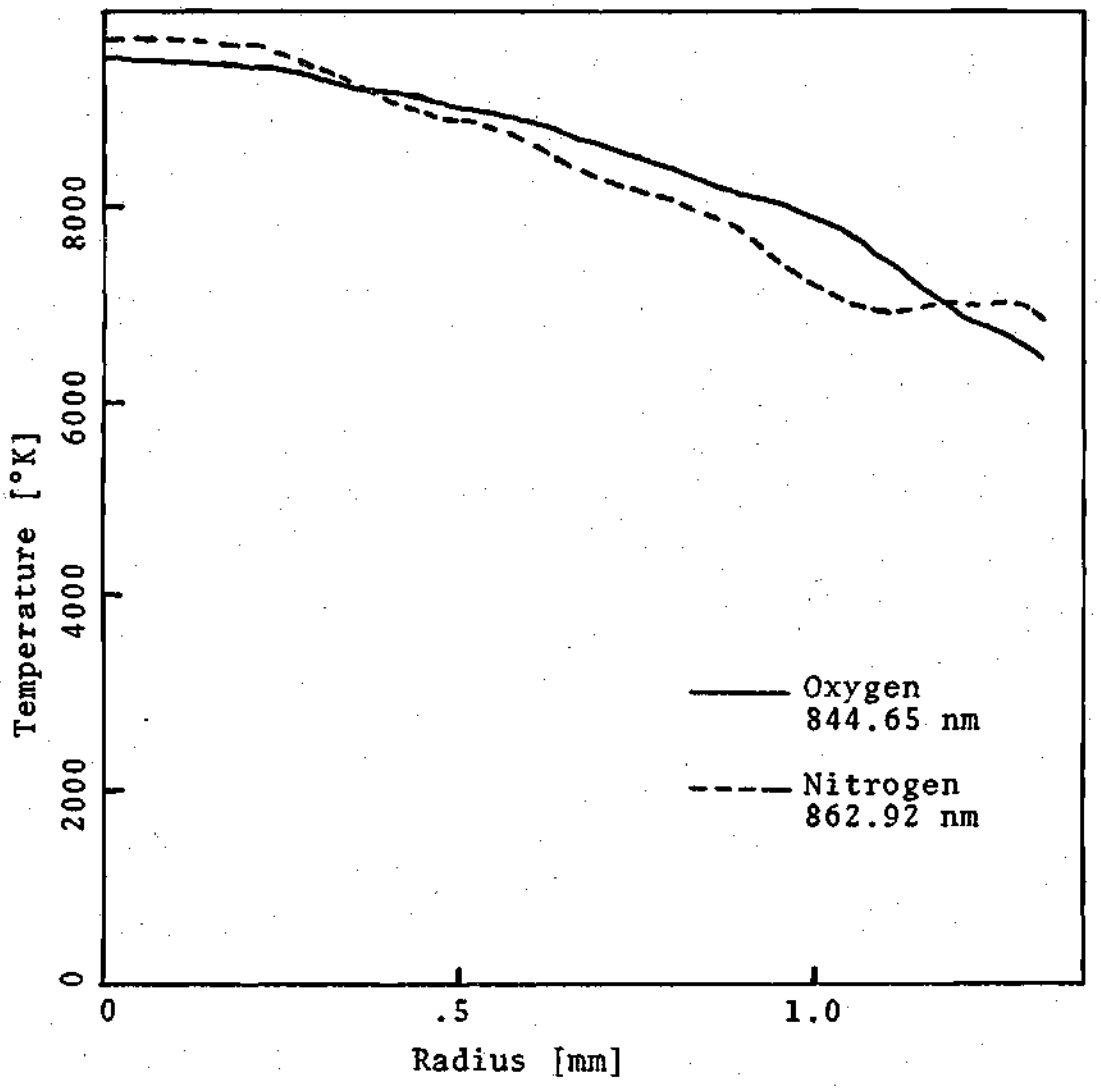

Figure 6-3. First Approximations for Radial Temperature Profiles Arc Assumed Optically Thin.

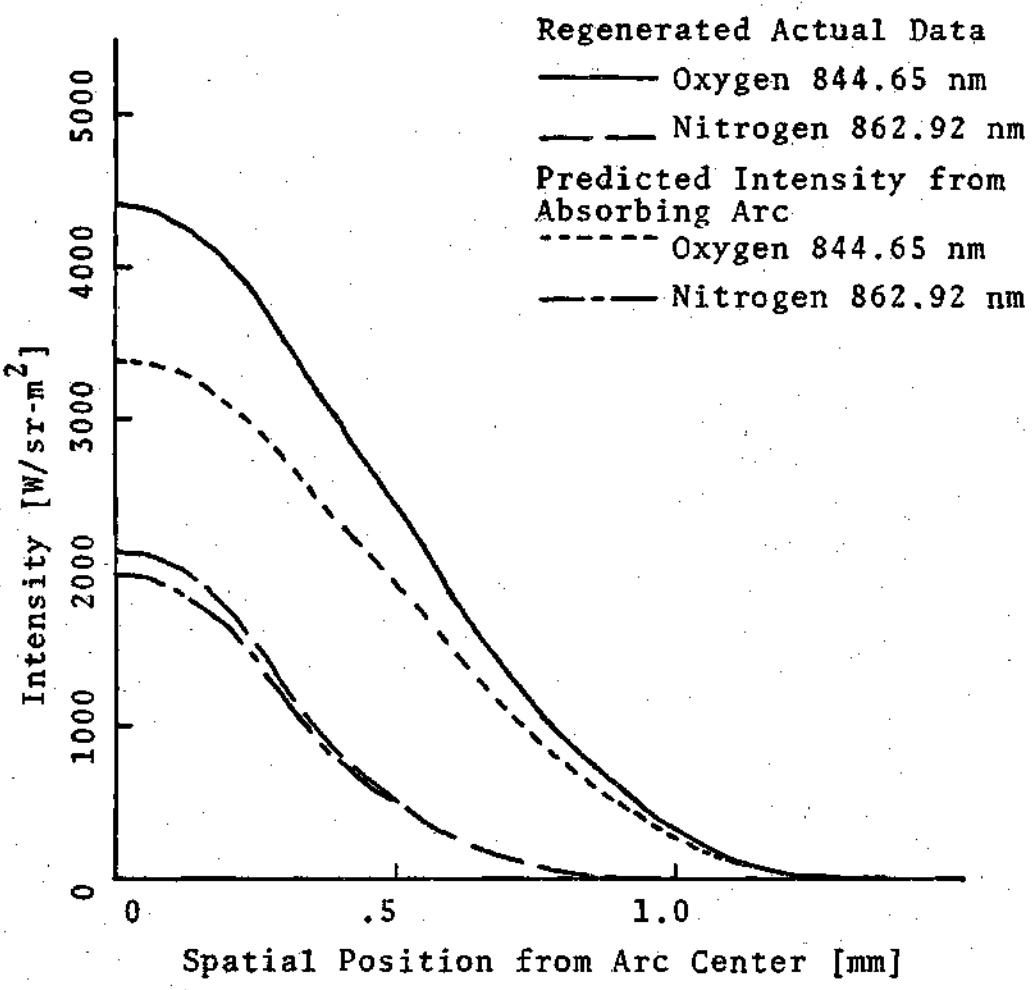

Figure 6-4. Effect of Absorption Upon Predicted Intensity Profiles Using Initial Radial Temperature Profiles from TPAD

temperature profiles with their first approximations can be seen in Figures 6-5 and 6-6, and a comparison of the final temperature profiles for the two spectral lines is shown in Figure 6-7. Absorption effects upon the predicted spectral line intensity from an arc with the final temperature profiles can be seen in Figure 6-8.

Once the final temperature profiles were obtained, they were used to find the transmission of the backlight radiation across the central chord of the arc itself (a worst case). For these calculations LOCAD was executed twice for each wavelength. In the first calculation the initial monochromatic intensity entering from the rear of the arc was set to zero, and a predicted spectral intensity distribution about line center was obtained for the central chord along with its integrated line intensity. The output included the optically thick and optically thin assumptions. The monochromatic backlight intensity was then set at 1000 ($W/sr\text{-}nm\text{-}m^2$) for each discrete wavelength used in LOCAD and the execution was repeated. The peak of the "optically thick" monochromatic intensity predicted in the first execution ($I_{\lambda m1}$), as well as its spectral position, was found by maximizing a parabolic interpolating polynomial using the three base points immediately surrounding that peak. This spectral position was used to find the optically thick monochromatic intensity in the second execution ($I_{\lambda m2}$). The spectral transmittance of the backlight radiation at this peak was found by

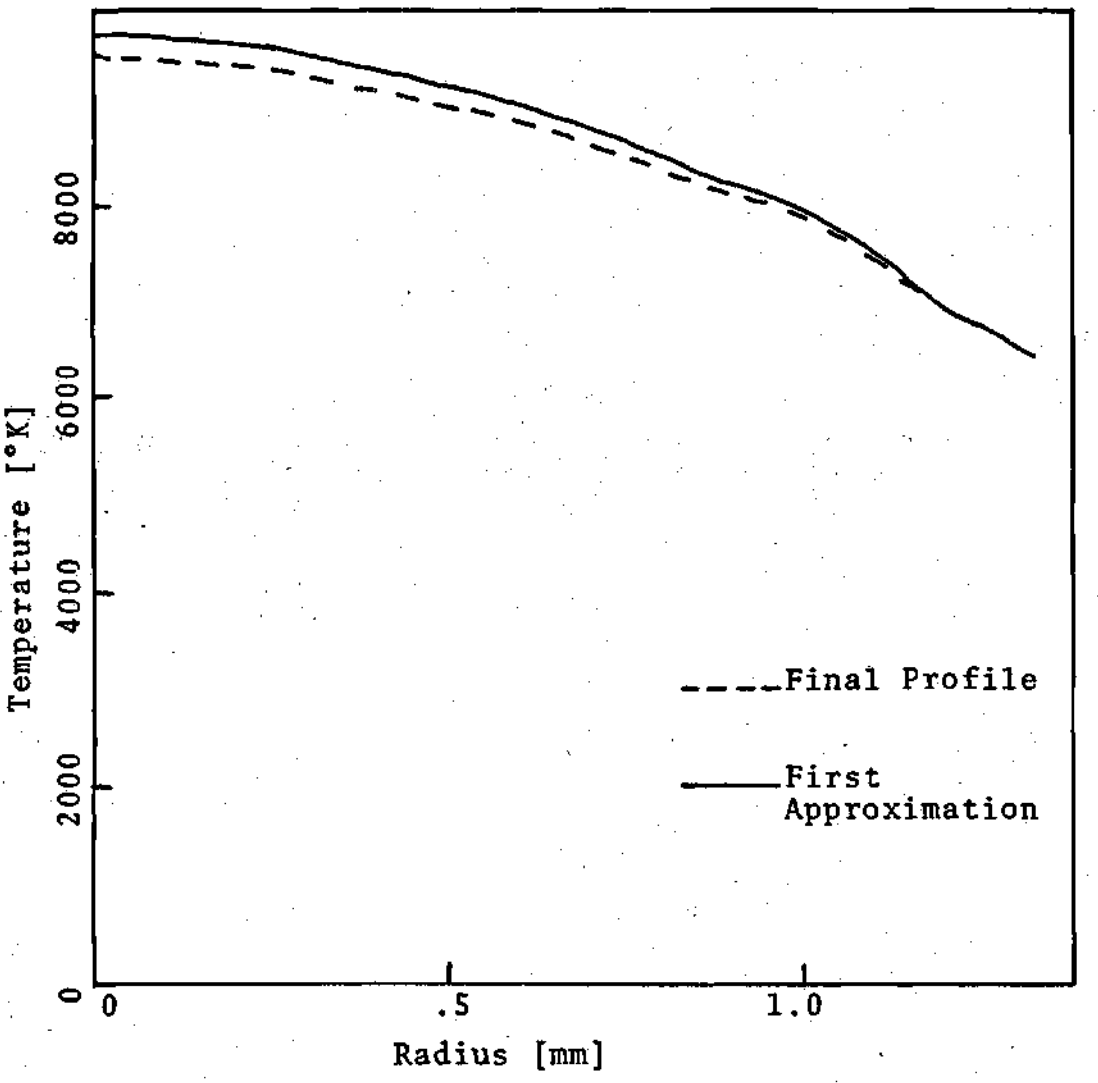

Figure 6-5. Comparison of First Temperature Approximation from TPAD with Final Temperature Profile Using the Oxygen 844.65 nm Spectral Line Data from an Air Arc.

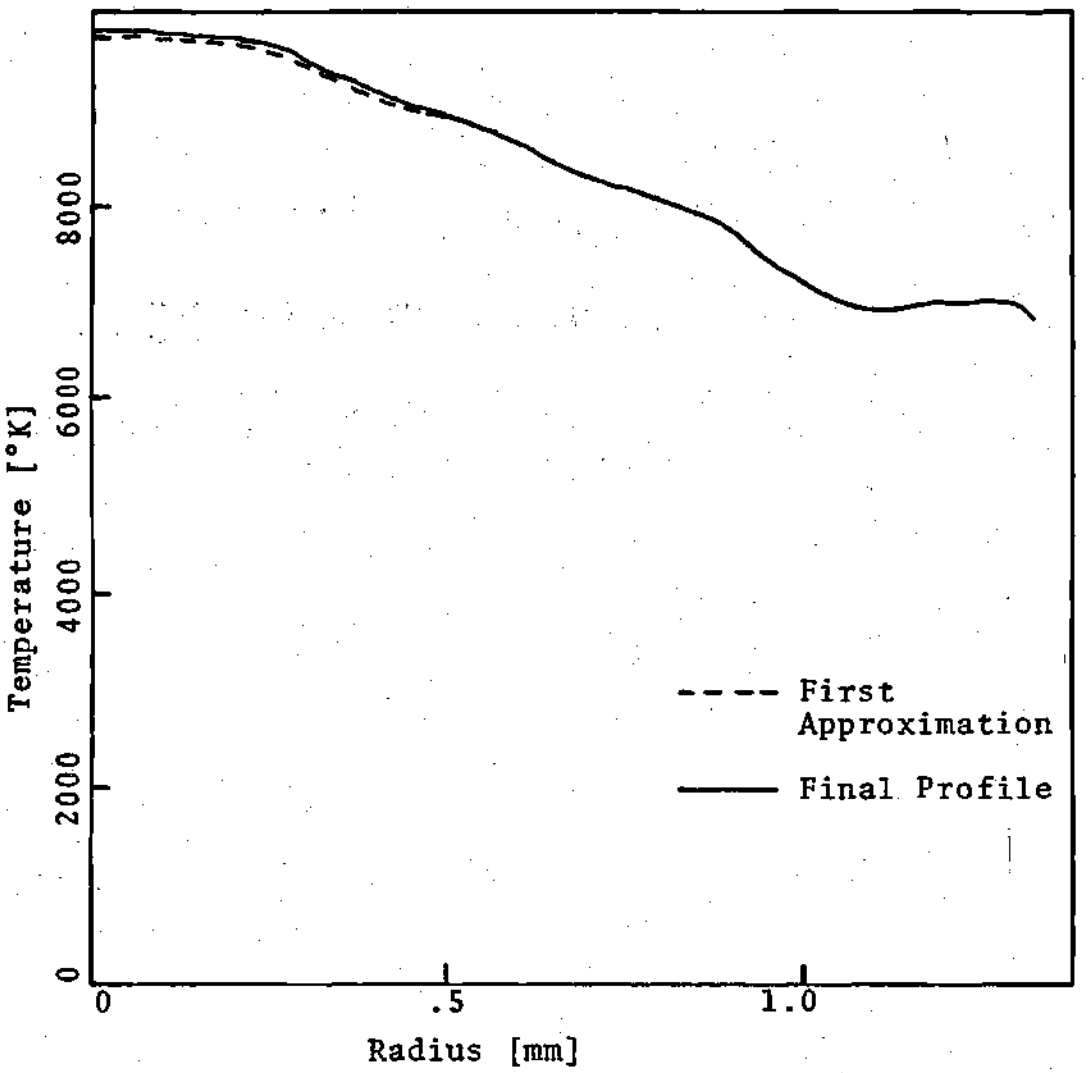

Figure 6-6. Comparison of First Temperature Approximation from TPAD with Final Temperature Profile Using the Nitrogen 862.92 nm Spectral Line Data from an Air Arc

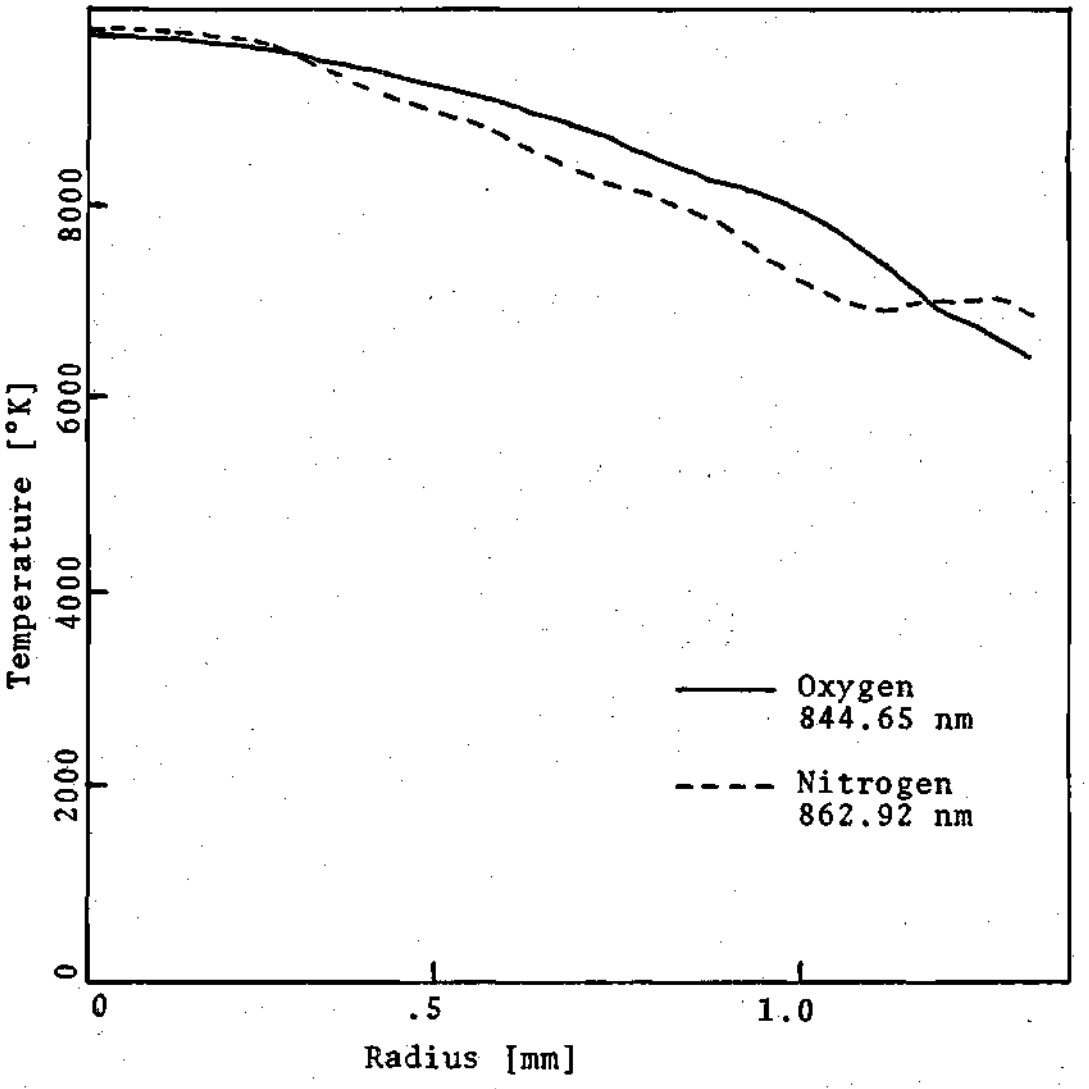

Figure 6-7. Final Temperature Profiles from Data for the Two Spectral Lines

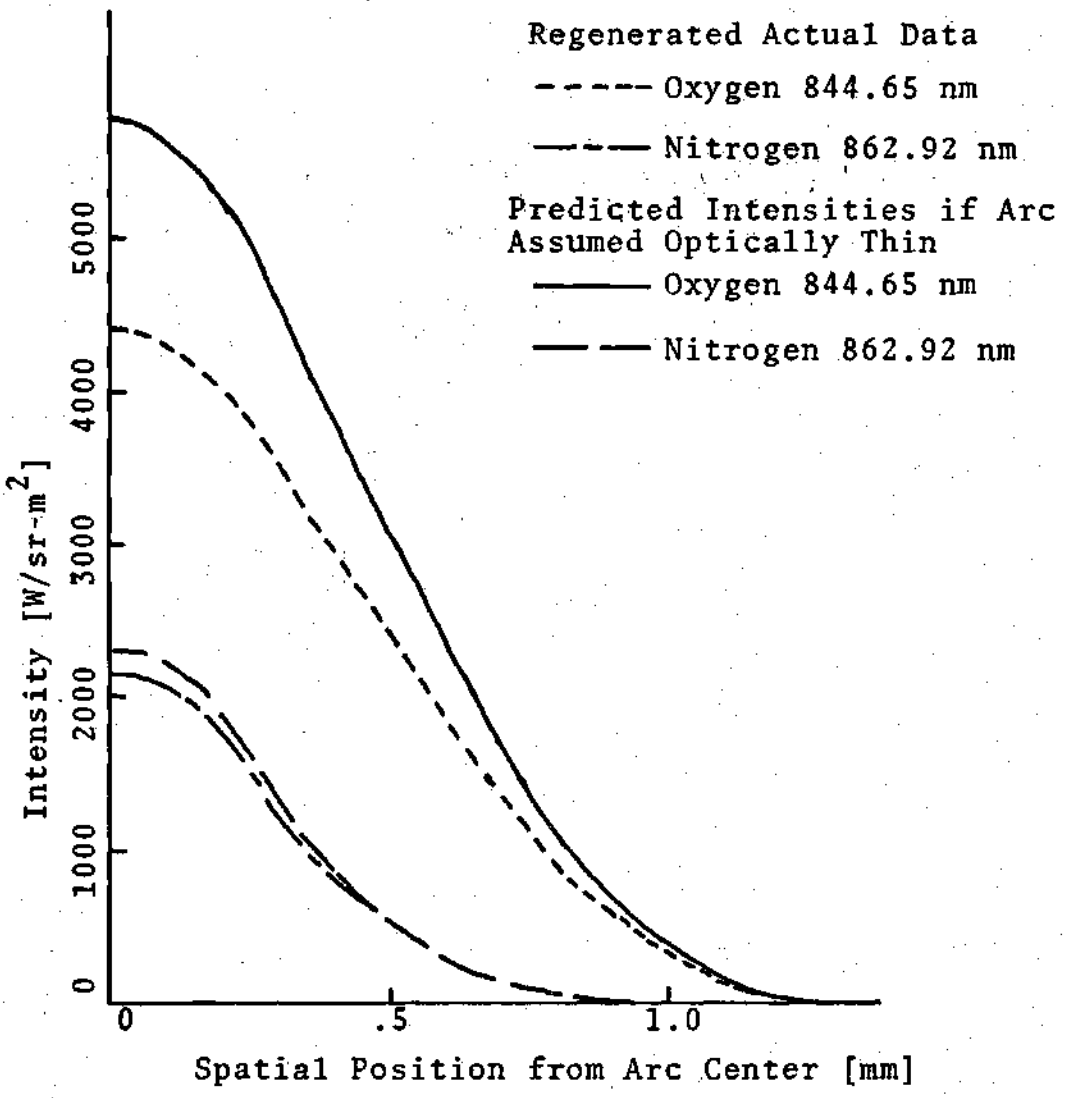

Figure 6-8. Effect of Arc Absorption Upon the Predicted Intensity Profiles Using the Final Radial Temperature Profiles for the Two Used Spectral Lines

$$T_{\lambda m} = \frac{I_{\lambda m2} - I_{\lambda m1}}{1000} \qquad (6\text{-}1)$$

where λm is the spectral position mentioned above and the numeric subscripts represent the execution number of the output used. The backlight transmission across the portion of the emission line falling upon the photomultiplier tube was found by

$$T_L = \frac{I_2 - I_1}{(Bp)x1000}$$

where the intensities for the central chord were used and Bp is the spectrometer's spectral bandpass in nanometers. The results, shown in Table 6-3, indicate that while there was

Table 6-3. Backlight Transmission Through Arc Center

Wavelength (nm)	$T_{\lambda m}$	T_L
844.65	.31	.94
862.92	.74	.97

significant absorption of the backlight radiation at the peak of the spectral intensity distribution for the two spectral lines, the total absorption of the backlight radiation across the spectral bandpass of the spectrometer was six percent or less. This six percent figure was insignificant compared to the respective measured attenuations of the

backlight radiation by the medium and arc of 88.5% and 97.2% for the oxygen and nitrogen spectral lines and justified the "optically thin" assumption used in Table 6-2. Further tests showed that these transmission values in Table 6-3 were independent of the magnitude of the set backlight intensity used in the "second" executions of LOCAD using the final temperature profiles.

CHAPTER VII

CONCLUSION AND RECOMMENDATIONS

When attempting to determine optically the temperature distribution within a plasma at pressures significantly higher than one atmosphere, it must be determined if there is an appreciable amount of reabsorption of the radiation emitted within that plasma. If there is significant reabsorption the experimenter must account for this absorption to accurately describe the environment within the plasma.

If the absorption phenomena is negligible the computer program TPAD can be used to accurately determine the radial temperature distribution for an axisymmetric arc observed from the side. If absorption is not negligible the computer program LOCAD may be used in conjunction with TPAD to account for this absorption and subsequently deduce such temperature profiles.

Radiant intensities were generated by LOCAD, assuming an optically thin arc from temperature profiles generated by TPAD. These intensities, compared with original observed intensities on a point by point basis, were within one percent of these observed intensities. Thus the two programs were mutually consistent.

Absorption of radiation by air byproducts immediately

surrounding the arc was accounted for by finding the transmittance of that medium.

An experiment was performed on an air arc at a pressure of 30 atmospheres and with a current of 11.9 amperes. Absolute radiant intensity data was collected for two different spectral emission lines--the oxygen line and the nitrogen line at respective wavelengths of 844.65 nm and 862.92 nm. Using these absolute intensities temperature profiles determined from these two lines agreed within three percent at points well within the arc radius. The arc was found to absorb a significant amount of radiation at these two spectral lines and necessitated the use of LOCAD in the analysis. With an arc centerline temperature of 9800°K, arc absorption along the central chord of its own emitted spectral line intensity was determined to be approximately 24% for the entire oxygen line and 7% for the entire nitrogen line.

The accuracy of the temperatures generated by LOCAD is dependent upon the ratio of the spectral line intensity height to the height of the continuum intensity over the whole line. Since LOCAD does not account for absorption by the continuum a small ratio will give a greater temperature error than a large ratio. Such an accounting in LOCAD could reduce this error if one works with such small ratios.

Subsequent research has determined that the radiation emitted by an axisymmetric arc could be significantly

affected by refraction caused by local temperature gradients immediately outside the arc. Since LOCAD calculates radiant intensities along a chordal path, it may be adapted to follow a bending ray and account for any refractive effects.

APPENDIX A

KIRCHOFF'S LAW FOR RADIATING GAS

For spontaneous emission, the emission coefficient

$$\epsilon_\nu = \frac{h\nu}{4\pi} A_{u\ell} N_u$$

where N_u is the number density of atoms with an electron in the upper energy level. The effective absorption coefficient is equal to the spontaneous absorption coefficient reduced by the induced emission coefficient or

$$k_\nu = \frac{h\nu}{C} (B_{\ell u} N_\ell - B_{u\ell} N_u)$$

where N_ℓ is the corresponding lower energy state number density, $B_{\ell u}$ and Bu_ℓ are transition probabilities [2]. From quantum mechanics

$$A_{u\ell} = 8\pi \frac{h\nu^3}{C^3} B_{u\ell}$$

and

$$g_\ell B_{\ell u} = g_u B_{u\ell}$$

where g_ℓ and g_u are the corresponding statistical weights of the two energy states. From these one can obtain

$$\frac{\varepsilon_\nu}{k_\nu} = \frac{2h\nu^3}{c^2} \left[\exp\left(\frac{h\nu}{kT}\right) - 1\right]^{-1}$$

or

$$\frac{\varepsilon_\nu}{k_\nu} = B_\nu$$

which is Kirchoff's Law for a radiating gas.

APPENDIX B

ERROR ANALYSIS

From an alternate form of equation (2-5)

$$\varepsilon_L = \frac{h\nu}{4\pi} A_{u\ell} g_u \frac{N(T)}{U(T)} \exp\left(-\frac{E_u}{kT}\right)$$

one can differentiate and divide by ε_L to obtain

$$\frac{d\varepsilon}{\varepsilon} = \frac{d\nu}{\nu} + \frac{dA_{u\ell}}{A_{u\ell}} + \frac{dN}{N} - \frac{dU}{U} - \frac{dE_u}{kT} + \left(\frac{E_u}{kT}\right)\frac{dT}{T}$$

for small changes, Upon rearranging and adjusting for use in error determination

$$\frac{\Delta T}{T} = \frac{kT}{E_u}\left(\frac{\Delta\varepsilon_L}{\varepsilon_L} + \frac{\Delta A_{u\ell}}{A_{u\ell}} + \frac{\Delta\nu}{\nu} + \frac{\Delta N}{N} + \frac{\Delta u}{u}\right) + \frac{\Delta E_u}{E_u}$$

which yields the relative error in temperature for relative errors in other parameters. Compared to the first two terms the other error terms are insignificant [2], and the equation effectively becomes

$$\frac{\Delta T}{T} = \frac{kT}{E_u}\left(\frac{\Delta\varepsilon_L}{\varepsilon_L} + \frac{\Delta A_{u\ell}}{A_{u\ell}}\right)$$

for the use of absolute emission coefficients in temperature determination. For the oxygen spectral line and the nitrogen line the respective uncertainties in the values used for $A_{u\ell}$ (4) were 10% and 25%. If there is an uncertainty in ε_L of 10% [2] the respective temperature errors would be 1.41% and 2.24% at 9000°K. At 9000°K this error is 127°K for the oxygen line and 202°K for the nitrogen line. At this temperature the two lines are 300°K apart and converge at higher temperatures.

APPENDIX C

TPAD AND LOCAD COMPUTER PROGRAMS

TPAD

```
      PROGRAM TPAD(INPUT,OUT,OUTPUT,TAPE5=INPUT,
     *     TAPE6=OUTPUT,TAPE7=OUT)
      DIMENSION X(100),Y(100),A1(100),A2(100),A3(100),A4(100),EC(100)
      DIMENSION YP(100),R(100),ECL(51),TL(51),T(100),XX(7),YY(7)
      DIMENSION ECLA(51),XR(100)
      PI=ATAN2(0.,-1.)
      READ(5,*) (ECL(I),I=1,51)
      DO 10 I=1,51
   10 TL(I)=6000.+200.*(I-1)
      READ(5,*) ICODE,NP,RAD,RES,ALAM,CURR,PRESS
      READ(5,1007) ILAM
      READ(5,*) ND,(Y(I),I=1,ND)
      READ(5,*) AT1,AT2,AT3
      READ(5,*) WB1,WB2,WB3
      READ(5,*) DWB1,DWB2,DWB3
      READ(5,*) ALB1,ALB2,ALB3
      READ(5,*) ATE1,ATE2,AXE1,AXE2
      WRITE(6,1004) ILAM,ALAM,PRESS
      WRITE(6,1002) (TL(I),ECL(I),I=1,51)
      RADM=RAD
      RAD=RAD/1000.
      AL1=RES/2.
      ND=ND+1
      NP=NP+1
      N1=ND-1
      N2=ND-2
      Y(ND)=0.
C     CALCULATE STARK BROADENING PARAMETER COEFFICIENTS
      AT1=ALOG(AT1)
      AT2=ALOG(AT2)
      AT3=ALOG(AT3)
      WA1=AT2-AT1
      WA2=AT2*AT2-AT1*AT1
      WA3=AT3-AT1
      WA4=AT3*AT3-AT1*AT1
      AW2=WA1*(WB3-WB1)-WA3*(WB2-WB1)
      AW2=AW2/(WA1*WA4-WA2*WA3)
      AW1=(WB2-WB1-AW2*WA2)/WA1
      AW0=WB1-AW1*AT1-AW2*AT1*AT1
      AD2=WA1*(DWB3-DWB1)-WA3*(DWB2-DWB1)
      AD2=AD2/(WA1*WA4-WA2*WA3)
      AD1=(DWB2-DWB1-AD2*WA2)/WA1
      AD0=DWB1-AD1*AT1-AD2*AT1*AT1
      AA2=WA1*(ALB3-ALB1)-WA3*(ALB2-ALB1)
      AA2=AA2/(WA1*WA4-WA2*WA3)
      AA1=(ALB2-ALB1-AA2*WA2)/WA1
      AA0=ALB1-AA1*AT1-AA2*AT1*AT1
      BOLTZ=1.38054E-23
      ANE1=PRESS*AXE1*.101348/BOLTZ/ATE1
      ANE2=PRESS*AXE2*.101348/BOLTZ/ATE2
      AME1=ALOG(ANE1)
      AME2=ALOG(ANE2)
      AME=(AME2-AME1)/(ATE2-ATE1)
      ABE=ANE1*EXP(-AME*ATE1)
C     COMPENSATE FOR FINITE EXIT SLIT WIDTH
      DO 50 I=1,51
      AT=ALOG(TL(I))
      ANE=ABE*EXP(AME*TL(I))
      W=(AW0+AW1*AT+AW2*AT*AT)*ANE*1.0E-16
      ALPHA=(AA0+AA1*AT+AA2*AT*AT)*SQRT(SQRT(ANE*1.0E-16))
      RR=.08985/SQRT(TL(I))*ANE**(1./6.)
```

```
      W12=(1.+1.75*ALPHA*(1.-.75*RR))*W
      DW=AD0+AD1*AT+AD2*AT*AT
      DT=(DW+2.*ALPHA*(1.-.75*RR))*W
   50 ECLA(I)=ECL(I)/PI*(ATAN((AL1-DT)/W12)-ATAN((-AL1-DT)/W12))
      DO 100 I=1,ND
      X(I)=RAD*(I-1)/(ND-1)
  100 XR(I)=X(I)*1000.
      DO 150 I=1,NP
  150 R(I)=RAD*(I-1)/(NP-1)
      AH=X(2)
      DH=1./AH
      DH2=DH*DH
      DH3=DH2*DH
      DH4=DH3*DH
      D12=1./12.
      D6=1./6.
C     CALCULATE SPATIAL INTENSITY DERIVATIVES
      DO 170 I=1,3
      X(ND+I)=X(ND)+X(I+1)
  170 Y(ND+I)=Y(ND-I)
      YP(1)=0.
      YP(ND)=0.
      IM=7
      XX(1)=X(3)
      XX(2)=X(2)
      XX(3)=X(1)
      XX(4)=X(2)
      XX(5)=X(3)
      XX(6)=X(4)
      XX(7)=X(5)
      YY(1)=Y(3)
      YY(2)=Y(2)
      YY(3)=Y(1)
      YY(4)=Y(2)
      YY(5)=Y(3)
      YY(6)=Y(4)
      YY(7)=Y(5)
      YP(2)=YCAL(XX,YY,IM,1)
      IM1=IM-1
      IM2=IM/2
      DO 200 I=3,N1
      DO 180 J=1,IM1
      XX(J)=XX(J+1)
  180 YY(J)=YY(J+1)
      XX(7)=X(I+IM2)
      YY(7)=Y(I+IM2)
  200 YP(I)=YCAL(XX,YY,IM,1)
      WRITE(6,1005) ICODE,RADM,N1,CURR,PRESS,ILAM,ALAM,RES
      WRITE(6,1000) (I,XR(I),Y(I),YP(I),I=1,N1)
C     CALCULATE THIRD DEGREE POLYNOMIAL COEFFICIENTS
C     FITTING THE SPATIAL DERIVATIVES
      A1(1)=0.
      A2(1)=(YP(2)*8-YP(3))*DH*D6
      A3(1)=0.
      A4(1)=-(YP(2)*2-YP(3))*DH3*D6
      DO 275 I=2,N2
      I2=I*I
      I3=I2*I
      TMP=YP(I-1)*(I3-I)-YP(I)*(3*I3-3*I2-6*I)
      TMP=TMP+YP(I+1)*(3*I3-6*I2-3*I+6)
      A1(I)=(TMP-YP(I+2)*(I3-3*I2+2*I))*D6
      TMP=YP(I-1)*(3*I2-1)-YP(I)*(9*I2-6*I-6)
      TMP=TMP+YP(I+1)*(9*I2-12*I-3)
      A2(I)=-(TMP-YP(I+2)*(3*I2-6*I+2))*DH*D6
      TMP=YP(I-1)*I-YP(I)*(3*I-1)+YP(I+1)*(3*I-2)
      A3(I)=(TMP-YP(I+2)*(I-1))*DH2*.5
```

```
  275 A4(I)=-(YP(I-1)-YP(I)*3+YP(I+1)*3-YP(I+2))*DH3*D6
      I=N1
      A1(I)=A1(I-1)
      A2(I)=A2(I-1)
      A3(I)=A3(I-1)
      A4(I)=A4(I-1)
      DO 285 I=1,ND
      XP=X(I)
      XP2=XP*XP
      XP3=XP2*XP
  285 YP(I)=A1(I)+A2(I)*XP+A3(I)*XP2+A4(I)*XP3
C     CALCULATE EMISSION COEFFICIENTS
      SUM=A2(1)*X(2)+A4(1)*X(2)*X(2)*X(2)/3.
      DO 300 J=2,N1
      J1=J+1
      SUMA=A4(J)*(X(J1)*X(J1)*X(J1)-X(J)*X(J)*X(J))/3.
      SUMB=A3(J)*(X(J1)*X(J1)-X(J)*X(J))/2.
      SUMC=A2(J)*(X(J1)-X(J))+A1(J)*ALOG(X(J1)/X(J))
  300 SUM=SUM+SUMA+SUMB+SUMC
      EC(1)=-SUM/PI
      NP1=NP-1
      DO 500 I=2,NP1
      SUM=0.
      RO=R(I)
      XL=R(I)
      IL=(I-1)*(ND-1)/(NP-1)+1
      DO 400 J=IL,N1
      J1=J+1
      IF (J.GT.IL) XL=X(J)
      SQ1=SQRT(X(J1)*X(J1)-RO*RO)
      SQ=SQRT(XL*XL-RO*RO)
      ALN=ALOG((X(J1)+SQ1)/(XL+SQ))
      SUMA=A4(J)*((X(J1)*X(J1)+RO*RO*2)*SQ1-(XL*XL+
     *     RO*RO*2)*SQ)/3.
      SUMB=A3(J)*(X(J1)*SQ1-XL*SQ+RO*RO*ALN)/2.
      SUMC=A2(J)*(SQ1-SQ)+A1(J)*ALN
  400 SUM=SUM+SUMA+SUMB+SUMC
  500 EC(I)=-SUM/PI
      RAD=RAD*1000.
      DO 550 I=1,N1
  550 X(I)=X(I)*1000.
C     CALCULATE TEMPERATURE AND ADJUST EMISSION COEFFICIENTS
C     COMPENSATING FOR FINITE EXIT SLIT WIDTH
      DO 600 I=1,NP1
      R(I)=R(I)*1000.
      T(I)=TCAL(EC(I),ECLA)
      AT=ALOG(T(I))
      ANE=ABE*EXP(AME*T(I))
      W=(AW0+AW1*AT+AW2*AT*AT)*ANE*1.0E-16
      ALPHA=(AA0+AA1*AT+AA2*AT*AT)*SQRT(SQRT(ANE*1.0E-16))
      RR=.08985/SQRT(T(I))*ANE**(1./6.)
      W12=(1.+1.75*ALPHA*(1.-.75*RR))*W
      DW=AD0+AD1*AT+AD2*AT*AT
      DT=(DW+2.*ALPHA*(1.-.75*RR))*W
  600 EC(I)=EC(I)*PI/(ATAN((AL1-DT)/W12)-ATAN((-AL1-DT)/W12))
      AT1=EXP(AT1)
      AT2=EXP(AT2)
      AT3=EXP(AT3)
      WRITE(6,1006)
      WRITE(6,1003) (R(I),EC(I),T(I),I=1,NP1)
      WRITE(7,*) (ECL(I),I=1,51)
      WRITE(7,*) ICODE,RAD,RES,ALAM,CURR,PRESS,NP1,(EC(I),I=1,NP1)
      WRITE(7,1007) ILAM
      WRITE(7,*) AT1,AT2,AT3,WB1,WB2,WB3,DWB1,DWB2,DWB3,ALB1,ALB2,ALB3
      WRITE(7,*) ATE1,ATE2,AXE1,AXE2
 1000 FORMAT(1X,I3,5X,F13.4,5X,F14.2,6X,E14.4)
```

```
1001 FORMAT(1X,I3,5X,1PE14.3,5X,1PE14.3)
1002 FORMAT(1X,F12.0,5X,E17.4)
1003 FORMAT(1X,F13.3,6X,E14.4,5X,F12.1)
1004 FORMAT(////,1H1,4X,'EMISSION COEFFICIENT LIBRARY FOR THE ',
     *      A8,' LINE AT ',/,5X,F7.2,' NM AND A PRESSURE OF ',
     *      F4.0,' ATMOSPHERES.',//,4X,'TEMPERATURE',11X,'EMISSION',
     *      /,3X,'(DEG. KELVIN)',8X,'(W/SR-M**3)',/)
1005 FORMAT(////,1H1,4X,'ANALYSIS OF AN OPTICALLY THIN AIR '
     *      'ARC',//,10X,'RUN CODE IS ',I4,/,10X,'ARC RADIUS IS ',
     *      F6.4,' MM.',/,10X,I2,' POINTS WERE USED FOR DATA AND',
     *      ' ANALYSIS.',/,10X,'THE CURRENT WAS ',F7.1,' AMPS.',
     *      /,10X,'THE PRESSURE WAS ',F6.1,' ATM.',/10X,
     *      'THE ',A8,1X,F9.2,' NM LINE WAS USED.',/,10X,
     *      'THE SPECTROMETER RESOLUTION WAS ',F6.2,' NM.',////,20X,
     *      'OBSERVED INTENSITY',//,15X,'SPATIAL',11X,
     *      'OBSERVED',6X,'SPATIAL DERIVATIVE',/,' ZONE',
     *      10X,'POSITION',10X,'INTENSITY',8X,'OF INTENSITY',
     *      /,17X,'(MM)',11X,'(W/SR-M**2)',8X,'(W/SR-M**3)',/)
1006 FORMAT(////,1H1,7X,'RADIUS',7X,'LINE EMISSION',
     *      8X,'TEMPERATURE',/,9X,'(MM)',10X,'(W/SR-M**3)',
     *      7X,'(DEG. KELVIN)',/)
1007 FORMAT(A8)
2000 FORMAT(4(F12.4))
     END
```

```
      FUNCTION TCAL(EC,ECL)
      DIMENSION ECL(1)
    5 DO 10 I=3,51,2
      IF (EC.LT.ECL(I)) GO TO 15
   10 CONTINUE
   15 IS=I-2
      N=30+IS
      ACL1=ALOG(ECL(IS))
      ACL2=ALOG(ECL(IS+1))
      ACL3=ALOG(ECL(IS+2))
      T1=200.*(N-1)
      T2=200.*N
      T3=200.*(N+1)
      EX=(ALOG(EC)-ACL1)/(ACL3-ACL1)
      AX=(ACL2-ACL1)/(ACL3-ACL1)
      AA=T1
      BB=(AX*AX*(T1-T3)+T2-T1)/AX/(1.-AX)
      CC=(AX*(T3-T1)-T2+T1)/AX/(1.-AX)
      TCAL=AA+EX*BB+EX*EX*CC
      RETURN
      END
```

```
      FUNCTION YCAL(X,Y,M,IFLAG)
      DIMENSION X(1),Y(1)
      S1=S2=S3=S4=S5=S6=S7=S8=S9=S10=0.
      DO 10 I=1,M
      X1=X(I)
      X2=X1*X1
      X3=X2*X1
      X4=X3*X1
      X5=X4*X1
      X6=X5*X1
      X7=X1*Y(I)
      X8=X2*Y(I)
      X9=X3*Y(I)
      X10=Y(I)
      S1=S1+X1
      S2=S2+X2
      S3=S3+X3
      S4=S4+X4
      S5=S5+X5
      S6=S6+X6
      S7=S7+X7
      S8=S8+X8
      S9=S9+X9
   10 S10=S10+X10
      A1=S2-S1*S1/M
      A2=S3-S1*S2/M
      A3=S4-S1*S3/M
      A4=S4-S2*S2/M
      A5=S5-S2*S3/M
      A6=S6-S3*S3/M
      B1=S7-S1*S10/M
      B2=S8-S2*S10/M
      B3=S9-S3*S10/M
      C1=A2*A2-A1*A4
      C2=A2*A3-A1*A5
      C3=A3*A3-A1*A6
      D1=B1*A2-B2*A1
      D2=B1*A3-B3*A1
      D=(D1*C2-D2*C1)/(C2*C2-C1*C3)
      C=(D1-D*C2)/C1
      B=(B1-D*A3-C*A2)/A1
      A=(S10-D*S3-C*S2-B*S1)/M
      IF (IFLAG.NE.1) GO TO 20
      A=B
      B=C*2
      C=D*3
      D=0.
   20 N=M/2+1
      XP=X(N)
      XP2=XP*XP
      XP3=XP2*XP
      YCAL=A+B*XP+C*XP2+D*XP3
      RETURN
      END
```

LOCAD

```
      PROGRAM LOCAD(INPUT,IN,OUT,OUTPUT,TAPE4=IN,TAPE5=INPUT,
     *      TAPE6=OUTPUT,TAPE7=OUT)
      DIMENSION EC(200),BL(200),Y(250),F(250),DL(200),W12(200)
      DIMENSION T(200),DT(200),AEC(200),XX(200),YY(200),RR(200)
      DIMENSION ADT(200),AW(200),ABL(200)
      DIMENSION S1(100),S2(100),ECL(51),REC(100),RT(100)
      READ(4,*) (ECL(I),I=1,51)
      READ(4,*) ICODE,XO,RES,ALAM,CURR,PRESS,N1,(EC(I),I=1,N1)
      READ(4,1007) ILAM
      READ(4,*) AT1,AT2,AT3,WB1,WB2,WB3,DWB1,DWB2,DWB3,ALB1,ALB2,ALB3
      READ(4,*) ATE1,ATE2,AXE1,AXE2
      READ(5,*) IY,YO,JFLAG,IFLAG,KFLAG
      IF (IY.LT.0) READ(5,*) (S2(I),I=1,N1)
      WRITE(6,1009)
      WRITE(6,1010) AT1,WB1,DWB1,ALB1,AT2,WB2,DWB2,ALB2,AT3,WB3,
     *     DWB3,ALB3
      BLAM=ALAM
      ALAM=ALAM*1E-9
      RADM=XO
      ARES=RES/2.
      NP=N1
      NXD=N1+1
      EC(NXD)=0.
      DO 20 I=1,N1
   20 T(I)=TCAL(EC(I),ECL)
      T(NXD)=6000.
      WRITE(6,1003) ICODE,RADM,NP,CURR,PRESS,ILAM,BLAM,RES
      PI=ATAN2(0.,-1.)
      NX=NXD*2-1
      NX1=NX-1
C     CALCULATE STARK BROADENING PARAMETER COEFFICIENTS
      AT1=ALOG(AT1)
      AT2=ALOG(AT2)
      AT3=ALOG(AT3)
      WA1=AT2-AT1
      WA2=AT2*AT2-AT1*AT1
      WA3=AT3-AT1
      WA4=AT3*AT3-AT1*AT1
      AW2=WA1*(WB3-WB1)-WA3*(WB2-WB1)
      AW2=AW2/(WA1*WA4-WA2*WA3)
      AW1=(WB2-WB1-AW2*WA2)/WA1
      AW0=WB1-AW1*AT1-AW2*AT1*AT1
      AD2=WA1*(DWB3-DWB1)-WA3*(DWB2-DWB1)
      AD2=AD2/(WA1*WA4-WA2*WA3)
      AD1=(DWB2-DWB1-AD2*WA2)/WA1
      AD0=DWB1-AD1*AT1-AD2*AT1*AT1
      AA2=WA1*(ALB3-ALB1)-WA3*(ALB2-ALB1)
      AA2=AA2/(WA1*WA4-WA2*WA3)
      AA1=(ALB2-ALB1-AA2*WA2)/WA1
      AA0=ALB1-AA1*AT1-AA2*AT1*AT1
      BOLTZ=1.38054E-23
      ANE1=PRESS*AXE1*.10134B/BOLTZ/ATE1
      ANE2=PRESS*AXE2*.10134B/BOLTZ/ATE2
      AME1=ALOG(ANE1)
      AME2=ALOG(ANE2)
      AME=(AME2-AME1)/(ATE2-ATE1)
      ABE=ANE1*EXP(-AME*ATE1)
      DO 100 I=1,NXD
      AT=ALOG(T(I))
      ANE=ABE*EXP(AME*T(I))
      W=(AW0+AW1*AT+AW2*AT*AT)*ANE*1.0E-16
```

```
      ALPHA=(AA0+AA1*AT+AA2*AT*AT)*SQRT(SQRT(ANE*1.0E-16))
      R=.08985/SQRT(T(I))*ANE**(1./6.)
      W12(I)=(1.+1.75*ALPHA*(1.-.75*R))*W
      DW=AD0+AD1*AT+AD2*AT*AT
      RR(I)=X0*(I-1)/(NXD-1)
      DT(I)=(DW+2.*ALPHA*(1.-.75*R))*W
      BL(I)=.59544E-16*2/(EXP(.014388/(ALAM*T(I)))-1.)
  100 BL(I)=BL(I)/ALAM**5*1E-9
      WRITE(6,1011) (RR(I),EC(I),T(I),I=1,NP)
      X0=X0/1000.
      DO 150 I=1,NXD
  150 RR(I)=RR(I)*.001
      NX2=NXD-1
      DO 200 I=1,NXD
      IXD=2*NXD-I
      JXD=NXD-I+1
      EC(IXD)=EC(JXD)
      RR(IXD)=RR(JXD)
      BL(IXD)=BL(JXD)
      DT(IXD)=DT(JXD)
  200 W12(IXD)=W12(JXD)
      DO 300 I=1,N1
      IXD=NXD*2-I
      EC(I)=EC(IXD)
      RR(I)=RR(IXD)
      BL(I)=BL(IXD)
      DT(I)=DT(IXD)
  300 W12(I)=W12(IXD)
      HL=.05
      N=158
      N2=N/2
      N21=N2-1
      N22=N21-1
      NN1=N
      IF(IFLAG.EQ.1) NN1=N/2
      DL(1)=-ARES
      DL(2)=-.65
      DO 340 I=2,N22
      DL(I+1)=DL(I)+HL
      IF (I.EQ.9) HL=.01
      IF (I.EQ.29) HL=.005
      IF(I.EQ.49) HL=.01
      IF(I.EQ.69) HL=.05
  340 CONTINUE
      DL(N2)=ARES
      IY1=1
      IY2=NP
      IYC=0
      IF (IY.EQ.0) GO TO 345
      IY1=IY
      IY2=IY
      IF (IY.GT.0) GO TO 345
      IY1=1
      IY2=NP
      IYC=-1
      IFLAG=1
      NN1=N/2
C     CALCULATE SPECTRAL RADIATION TRANSPORT ACROSS ARC
  345 DO 600 IY=IY1,IY2
      IYT=IY*(1+IYC)-IYC*(NP+1-IY)
      ISTAT=0
      NJ=(NXD-IYT)*2
      NJD=NJ/2
      NJD1=NJD+1
      NJ1=NJ+1
      YY(IYT)=X0*(IYT-1)/N1
```

```
      YYI=YY(IYT)
      NJ2=2*NJ+1
      CALL ECAL(EC,AEC,XX,RR,XO,YYI,NJ,NXD)
  350 CALL ACAL(W12,AW,XX,RR,YYI,NJ)
      CALL ACAL(DT,ADT,XX,RR,YYI,NJ)
      CALL ACAL(BL,ABL,XX,RR,YYI,NJ)
      DO 355 I=1,N2
      Y(I)=YO
      Y(N2+I)=YO
  355 CONTINUE
      II=1
      M=0
      DO 400 I=1,NJ
      IH=2*I-1
      H=XX(IH+2)-XX(IH)
  360 CALL RUNGE(NN1,Y,F,II,H,M,K)
      IF (K-1) 370,370,390
  370 DO 380 J=1,N2
      DX=DL(J)-ADT(II)
      AFAC=1./(PI*AW(II)*(1.+(DX/AW(II))**2))
      EL=AEC(II)*AFAC
      F(J)=EL*(1.-Y(J)/ABL(II))
      F(N2+J)=EL
  380 CONTINUE
      F(N+1)=AEC(II)
      GO TO 360
  390 CONTINUE
  400 CONTINUE
      IF (IY.NE.1.OR.JFLAG.NE.0) GO TO 405
      IF (IFLAG.EQ.0) GO TO 403
      WRITE(6,1008)
      WRITE(6,1002) (I,DL(I),Y(I),I=1,N2)
      GO TO 405
  403 WRITE(6,1004)
      WRITE(6,1000) (I,DL(I),Y(I),Y(N2+I),I=1,N2)
C     INTEGRATE SPECTRAL INTENSITIES ACROSS SPECTROMETER
C     RESOLUTION TO GET PREDICTED LINE INTENSITIES
  405 H=.05
      SUMA=Y(2)
      DO 410 I=3,9,2
  410 SUMA=SUMA+Y(I)*4+Y(I+1)*2
      SUMA=(SUMA-Y(10))*H/3
      SUMB=Y(10)
      H=.01
      DO 420 I=11,29,2
  420 SUMB=SUMB+Y(I)*4+Y(I+1)*2
      SUMB=(SUMB-Y(30))*H/3
      SUMC=Y(30)
      H=.005
      DO 430 I=31,49,2
  430 SUMC=SUMC+Y(I)*4+Y(I+1)*2
      SUMC=(SUMC-Y(50))*H/3
      H=.01
      SUMD=Y(50)
      DO 440 I=51,69,2
  440 SUMD=SUMD+Y(I)*4+Y(I+1)*2
      SUMD=(SUMD-Y(70))*H/3
      SUME=Y(70)
      H=.05
      DO 450 I=71,N22,2
  450 SUME=SUME+Y(I)*4+Y(I+1)*2
      SUME=(SUME-Y(N21))*H/3
      H=(DL(2)-DL(1))
      SUME=SUME+H*(Y(1)+Y(2)+Y(N21)+Y(N2))/2.
      S1(IYT)=SUMA+SUMB+SUMC+SUMD+SUME
      IF (IFLAG.EQ.1) GO TO 550
```

```
      H=.05
      SUMF=Y(N2+2)
      DO 460 I=3,9,2
  460 SUMF=SUMF+Y(N2+I)*4+Y(N2+1+I)*2
      SUMF=(SUMF-Y(N2+10))*H/3
      SUMG=Y(N2+10)
      H=.01
      DO 470 I=11,29,2
  470 SUMG=SUMG+Y(I+N2)*4+Y(I+N2+1)*2
      SUMG=(SUMG-Y(N2+30))*H/3
      SUMH=Y(N2+30)
      H=.005
      DO 480 I=31,49,2
  480 SUMH=SUMH+Y(N2+I)*4+Y(N2+1+I)*2
      SUMH=(SUMH-Y(N2+50))*H/3
      H=.01
      SUMI=Y(N2+50)
      DO 490 I=51,69,2
  490 SUMI=SUMI+Y(N2+I)*4+Y(N2+1+I)*2
      SUMI=(SUMI-Y(N2+70))*H/3
      SUMJ=Y(N2+70)
      H=.05
      DO 500 I=71,N22,2
  500 SUMJ=SUMJ+Y(I+N2)*4+Y(I+N2+1)*2
      SUMJ=(SUMJ-Y(N-1))*H/3
      H=(DL(2)-DL(1))
      SUMJ=SUMJ+H*(Y(1+N2)+Y(N2+2)+Y(N-1)+Y(N))/2.
      S2(IYT)=SUMF+SUMG+SUMH+SUMI+SUMJ
  550 IF (IYC.EQ.0) GO TO 600
      IF (ISTAT.EQ.1) GO TO 560
C     EMISSION ADJUSTMENTS TO ACCOUNT FOR LINE OPACITY
      ISTAT=1
      FS=S1(IYT)-S2(IYT)
      ETEMP=AEC(NJ1)
      FTEMP=FS
      EC(NJD1)=AEC(NJ1)*S2(IYT)/S1(IYT)
      GO TO 570
  560 FS=S1(IYT)-S2(IYT)
      PCT=FS/S2(IYT)
      IF (ABS(PCT).LT..005) GO TO 590
      AETEMP=AEC(NJ1)
      EC(NJD1)=(ETEMP*FS-AETEMP*FTEMP)/(FS-FTEMP)
      ETEMP=AETEMP
      FTEMP=FS
  570 TT=TCAL(EC(NJD1),ECL)
      AT=ALOG(TT)
      ANE=ABE*EXP(AME*TT)
      W=(AW0+AW1*AT+AW2*AT*AT)*ANE*1.0E-16
      ALPHA=(AA0+AA1*AT+AA2*AT*AT)*SQRT(SQRT(ANE*1.0E-16))
      DW=AD0+AD1*AT+AD2*AT*AT
      R=.08985/SQRT(TT)*ANE**(1./6.)
      W12(NJD1)=(1.+1.75*ALPHA*(1.-.75*R))*W
      DT(NJD1)=(DW+2.*ALPHA*(1.-.75*R))*W
      BL(NJD1)=.59544E-16*2/(EXP(.014388/(ALAM*TT))-1.)
      BL(NJD1)=BL(NJD1)/ALAM**5*1E-9
      II=2*(NP+1)-NJD1
      EC(II)=EC(NJD1)
      W12(II)=W12(NJD1)
      DT(II)=DT(NJD1)
      BL(II)=BL(NJD1)
      CALL ACAL(EC,AEC,XX,RR,YYI,NJ)
      GO TO 350
  590 EC(NJD1)=AEC(NJ1)
      II=2*(NP+1)-NJD1
      EC(II)=AEC(NJ1)
      T(NJD1)=TCAL(EC(NJD1),ECL)
```

```
      T(II)=T(NJD1)
      AT=ALOG(T(NJD1))
      ANE=ABE*EXP(AME*T(NJD1))
      W=(AW0+AW1*AT+AW2*AT*AT)*ANE*1.0E-16
      ALPHA=(AA0+AA1*AT+AA2*AT*AT)*SQRT(SQRT(ANE*1.0E-16))
      DW=AD0+AD1*AT+AD2*AT*AT
      R=.08985/SQRT(T(NJD1))*ANE**(1./6.)
      W12(NJD1)=(1.+1.75*ALPHA*(1.-.75*R))*W
      DT(NJD1)=(DW+2.*ALPHA*(1.-.75*R))*W
      BL(NJD1)=.59544E-16*2/(EXP(.014388/(ALAM*T(NJD1)))-1.)
      BL(NJD1)=BL(NJD1)/ALAM**5*1E-9
      W12(II)=W12(NJD1)
      DT(II)=DT(NJD1)
      BL(II)=BL(NJD1)
      REC(IYT)=EC(NJD1)
      RT(IYT)=T(NJD1)
  600 CONTINUE
      DO 700 I=IY1,IY2
  700 YY(I)=YY(I)*1000.
      IF (IFLAG.NE.0) GO TO 710
      WRITE(6,1001)
      WRITE(6,1000)(I,YY(I),S1(I),S2(I),I=IY1,IY2)
  710 IF (IFLAG.NE.1) GO TO 720
      WRITE(6,1005)
      WRITE(6,1002)(I,YY(I),S1(I),I=IY1,IY2)
  720 IF (IYC.NE.-1) GO TO 730
      WRITE(6,1006)
      WRITE(6,1011) (YY(I),REC(I),RT(I),I=1,NP)
  730 IF (KFLAG.NE.1) GO TO 999
      X0=X0*1000.
      ALAM=ALAM*1E9
      AT1=EXP(AT1)
      AT2=EXP(AT2)
      AT3=EXP(AT3)
      WRITE(7,*) (ECL(I),I=1,51)
      WRITE(7,*) ICODE,X0,RES,ALAM,CURR,PRESS,N1,(REC(I),I=1,N1)
      WRITE(7,1007) ILAM
      WRITE(7,*) AT1,AT2,AT3,WB1,WB2,WB3,DWB1,DWB2,DWB3,ALB1,ALB2,ALB3
      WRITE(7,*) ATE1,ATE2,AXE1,AXE2
 1000 FORMAT(1X,I3,9X,F7.4,14X,F8.2,10X,F8.2)
 1001 FORMAT('1',1H1,10X,'COMPARISON OF THE PREDICTED INTENSITY ACC',
     *     'OUNTING FOR OPACITY',/,11X,'WITH THE PREDICTED INTENSITY ',
     *     'ASSUMING OPTICALLY THIN LINE FOR A ',/,11X,'GIVEN EMISSION ',
     *     'PROFILE.',//,13X,'SPATIAL',13X,'OPTICALLY',10X,'OPTICALLY',/,
     *     ' ZONE',7X,'POSITION',15X,'THICK',14X,'THIN',/,14X,'(MM)',
     *     14X,'(W/SR-M**2)',8X,'(W/SR-M**2)',/)
 1002 FORMAT(1X,I3,9X,F7.4,14X,F8.2)
 1003 FORMAT('1',1H1,4X,'ANALYSIS OF AN OPTICALLY THICK AIR '
     *     'ARC',//,10X,'RUN CODE IS ',I4,/,10X,'ARC RADIUS IS ',
     *     F6.4,' MM.',/,10X,I2,' POINTS WERE USED FOR DATA AND',
     *     ' ANALYSIS.',/,10X,'THE CURRENT WAS ',F7.1,' AMPS.',
     *     /,10X,'THE PRESSURE WAS ',F6.1,' ATM.',/10X,
     *     'THE ',A8,1X,F9.2,' NM LINE WAS USED.',/,10X,
     *     'THE SPECTROMETER RESOLUTION WAS ',F6.2,' NM.','////,20X,
     *     'PLASMA PROPERTIES',//,7X,'RADIUS',7X,'LINE EMISSION',8X,
     *     'TEMPERATURE',/,9X,'(MM)',10X,'(W/SR-M**3)',7X,
     *     '(DEG. KELVIN)',/)
 1004 FORMAT('1',1H1,10X,'SPECTRAL DISTRIBUTION ABOUT LINE ',
     *     'CENTER OF THE PREDICTED LINE',/,11X,'INTENSITY ALONG ',
     *     'CENTRAL CORD FOR OPTICALLY THICK AND',/,11X,
     *     'OPTICALLY THIN CASES.',//,10X,'DISTANCE FROM',10X,
     *     'OPTICALLY',10X,'OPTICALLY',/,11X,'LINE CENTER',13X,
     *     'THICK',14X,'THIN',/,14X,
     *     '(NM)',12X,'(W/SR-NM-M**2)',5X,'(W/SR-NM-M**2)',/)
 1005 FORMAT('1',1H1,10X,'SPATIAL DISTRIBUTION OF THE PREDICTED ',
     *     'LINE INTENSITY FOR AN OPTICALLY',/,11X,'THICK LINE.',
```

```
     *     //,13X,'SPATIAL',13X,'PREDICTED',/,' ZONE',7X,
     *     'POSITION',13X,'INTENSITY',/,14X,'(MM)',11X,
     *     '(W/SR-M**2)',/)
 1006 FORMAT(////,1H1,10X,'EMISSION AND TEMPERATURE DISTRIBUTION ',
     *     'USING AN OPTICALLY THICK LINE.',//,7X,'RADIUS',7X,
     *     'LINE EMISSION',8X,'TEMPERATURE',/,9X,'(MM)',10X,
     *     '(W/SR-M**3)',7X,'(DEG. KELVIN)',/)
 1007 FORMAT(A8)
 1008 FORMAT(////,1H1,10X,'SPECTRAL DISTRIBUTION ABOUT LINE ',
     *     'CENTER OF THE PREDICTED LINE',/,11X,'INTENSITY ALONG ',
     *     'THE CENTRAL CORD FOR AN OPTICALLY',/,11X,'THICK ',
     *     'LINE.',//,10X,'DISTANCE FROM',11X,'SPECTRAL',/,11X,
     *     'LINE CENTER',12X,'INTENSITY',/,15X,'(NM)',
     *     12X,'(W/SR-NM-M**2)',/)
 1009 FORMAT(////,10X,'STARK BROADENING PARAMETERS',//,
     *     9X,'TEMPERATURE',11X,1HW,15X,3HD/W,13X,5HALPHA,/)
 1010 FORMAT(4(5X,F12.4))
 1011 FORMAT(1X,F13.3,6X,E14.5,5X,F12.1)
  999 CONTINUE
      END
```

```
      SUBROUTINE ACAL(EC,AEC,X,R,Y,NJ)
      DIMENSION EC(1),AEC(1),X(1),R(1)
      NJD=NJ/2
      DO 10 I=1,NJD
      INJ=2*I-1
      AEC(INJ)=EC(I)
      II=2*NJ+2-INJ
   10 AEC(II)=EC(I)
      AEC(NJ+1)=EC(NJD+1)
      DO 20 I=2,NJ,2
      ID=I/2+1
      RX=SQRT(X(I)*X(I)+Y*Y)
      IF (ABS(R(ID+1)-R(ID-1)).GT.1E-10) GO TO 15
      RX=.5*(RX-R(ID-1))/R(ID-1)
      GO TO 18
   15 RX=(RX-R(ID-1))/(R(ID+1)-R(ID-1))
   18 AX=.5
      AA=EC(ID-1)
      BB=AX*AX*(EC(ID-1)-EC(ID+1))+EC(ID)-EC(ID-1)
      BB=BB/AX/(1.-AX)
      CC=AX*(EC(ID+1)-EC(ID-1))-EC(ID)+EC(ID-1)
      CC=CC/AX/(1.-AX)
      AEC(I)=AA+RX*BB+RX*RX*CC
      II=2*NJ+2-I
   20 AEC(II)=AEC(I)
      RETURN
      END
```

```
      SUBROUTINE ECAL(EC,AEC,X,R,XO,YY,NJ,NXD)
      DIMENSION EC(1),AEC(1),X(1),R(1)
      NJD=NJ/2
      DO 10 I=1,NJD
      INJ=2*I-1
      X(INJ)=-SQRT(R(I)*R(I)-YY*YY)
      AEC(INJ)=EC(I)
      II=2*NJ+2-INJ
      X(II)=-X(INJ)
   10 AEC(II)=EC(I)
      NJ1=NJ+1
      X(NJ1)=0.
      AEC(NJ1)=EC(NJD+1)
      DO 20 I=2,NJ,2
      ID=I/2+1
      X(I)=.5*(X(I-1)+X(I+1))
      RX=SQRT(X(I)*X(I)+YY*YY)
      IF (ABS(R(ID+1)-R(ID-1)).GT.1E-10) GO TO 15
      RX=.5*(RX-R(ID-1))/R(ID-1)
      GO TO 18
   15 RX=(RX-R(ID-1))/(R(ID+1)-R(ID-1))
   18 AX=.5
      AA=EC(ID-1)
      BB=AX*AX*(EC(ID-1)-EC(ID+1))+EC(ID)-EC(ID-1)
      BB=BB/AX/(1.-AX)
      CC=AX*(EC(ID+1)-EC(ID-1))-EC(ID)+EC(ID-1)
      CC=CC/AX/(1.-AX)
      AEC(I)=AA+RX*BB+RX*RX*CC
      II=2*NJ+2-I
      X(II)=-X(I)
   20 AEC(II)=AEC(I)
      RETURN
      END
```

```
      SUBROUTINE RUNGE(N,Y,F,II,H,M,K)
      DIMENSION Y(1),F(1),Q(200)
      M=M+1
      GO TO (1,4,5,3,7),M
    1 DO 2 I=1,N
    2 Q(I)=0.
      A=.5
      GO TO 9
    3 A=1.7071067811865475244
    4 II=II+1
    5 DO 6 I=1,N
      Y(I)=Y(I)+A*(F(I)*H-Q(I))
    6 Q(I)=2.*A*H*F(I)+(1.-3.*A)*Q(I)
      A=.29283188134524756
      GO TO 9
    7 DO 8 I=1,N
    8 Y(I)=Y(I)+H*F(I)/6-Q(I)/3
      M=0
      K=2
      GO TO 10
    9 K=1
   10 RETURN
      END
```

```
      FUNCTION TCAL(EC,ECL)
      DIMENSION ECL(1)
    5 DO 10 I=3,51,2
      IF (EC.LT.ECL(I)) GO TO 15
   10 CONTINUE
   15 IS=I-2
      N=30+IS
      ACL1=ALOG(ECL(IS))
      ACL2=ALOG(ECL(IS+1))
      ACL3=ALOG(ECL(IS+2))
      T1=200.*(N-1)
      T2=200.*N
      T3=200.*(N+1)
      EX=(ALOG(EC)-ACL1)/(ACL3-ACL1)
      AX=(ACL2-ACL1)/(ACL3-ACL1)
      AA=T1
      BB=(AX*AX*(T1-T3)+T2-T1)/AX/(1.-AX)
      CC=(AX*(T3-T1)-T2+T1)/AX/(1.-AX)
      TCAL=AA+EX*BB+EX*EX*CC
      RETURN
      END
```

APPENDIX D

TPAD AND LOCAD EXECUTIONS USED IN ANALYSIS OF EXPERIMENTAL DATA

LGO,D301,DATA

1 EMISSION COEFFICIENT LIBRARY FOR THE OXYGEN LINE AT
844.65 NM AND A PRESSURE OF 30. ATMOSPHERES.

TEMPERATURE (DEG. KELVIN)	EMISSION (W/SR-M**3)
6000.	.3329E+04
6200.	.6478E+04
6400.	.1201E+05
6600.	.2134E+05
6800.	.3646E+05
7000.	.6013E+05
7200.	.9597E+05
7400.	.1484E+06
7600.	.2234E+06
7800.	.3278E+06
8000.	.4692E+06
8200.	.6582E+06
8400.	.9054E+06
8600.	.1223E+07
8800.	.1627E+07
9000.	.2134E+07
9200.	.2769E+07
9400.	.3550E+07
9600.	.4508E+07
9800.	.5680E+07
10000.	.7093E+07
10200.	.8793E+07
10400.	.1081E+08
10600.	.1321E+08
10800.	.1603E+08
11000.	.1929E+08
11200.	.2307E+08
11400.	.2745E+08
11600.	.3240E+08
11800.	.3806E+08
12000.	.4435E+08
12200.	.5133E+08
12400.	.5924E+08
12600.	.6791E+08
12800.	.7744E+08
13000.	.8789E+08
13200.	.9920E+08
13400.	.1114E+09
13600.	.1247E+09
13800.	.1387E+09
14000.	.1536E+09
14200.	.1695E+09
14400.	.1861E+09
14600.	.2038E+09
14800.	.2238E+09
15000.	.2405E+09
15200.	.2601E+09
15400.	.2798E+09
15600.	.3001E+09
15800.	.3206E+09
16000.	.3410E+09

1 ANALYSIS OF AN OPTICALLY THIN AIR ARC

RUN CODE IS 301
ARC RADIUS IS 1.3740 MM.
25 POINTS WERE USED FOR DATA AND ANALYSIS.
THE CURRENT WAS 11.9 AMPS.
THE PRESSURE WAS 30.0 ATM.
THE OXYGEN 844.65 NM LINE WAS USED.
THE SPECTROMETER RESOLUTION WAS 1.34 NM.

OBSERVED INTENSITY

ZONE	SPATIAL POSITION (MM)	OBSERVED INTENSITY (W/SR-M**2)	SPATIAL DERIVATIVE OF INTENSITY (W/SR-M**3)
1	0.0000	4450.00	0.
2	.0550	4421.00	-.1471E+07
3	.1099	4303.00	-.2119E+07
4	.1649	4149.00	-.3144E+07
5	.2198	3997.00	-.4319E+07
6	.2748	3681.00	-.5439E+07
7	.3298	3369.00	-.5908E+07
8	.3847	3062.00	-.5501E+07
9	.4397	2761.00	-.5311E+07
10	.4946	2472.00	-.5537E+07
11	.5496	2175.00	-.5650E+07
12	.6046	1833.00	-.5463E+07
13	.6595	1567.00	-.5154E+07
14	.7145	1298.00	-.4887E+07
15	.7694	1022.00	-.4426E+07
16	.8244	794.70	-.3452E+07
17	.8794	652.90	-.2665E+07
18	.9343	508.40	-.2641E+07
19	.9893	362.40	-.2556E+07
20	1.0442	212.20	-.2045E+07
21	1.0992	144.90	-.1338E+07
22	1.1542	76.13	-.7005E+06
23	1.2091	50.30	-.3424E+06
24	1.2641	41.58	-.2594E+06
25	1.3190	34.36	-.1964E+06

1

RADIUS (MM)	LINE EMISSION (W/SR-M**3)	TEMPERATURE (DEG. KELVIN)
0.000	.4174E+07	9534.8
.055	.4061E+07	9511.6
.110	.3869E+07	9471.2
.165	.3781E+07	9452.0
.220	.3649E+07	9422.7
.275	.3418E+07	9369.1
.330	.3067E+07	9281.4
.385	.2696E+07	9179.2
.440	.2423E+07	9096.5
.495	.2196E+07	9021.6
.550	.1950E+07	8932.5
.605	.1690E+07	8827.4
.660	.1443E+07	8714.7
.714	.1210E+07	8592.8
.769	.9714E+06	8445.8
.824	.7469E+06	8278.0
.879	.5976E+06	8141.7
.934	.5043E+06	8041.5
.989	.3921E+06	7898.3
1.044	.2628E+06	7682.9
1.099	.1511E+06	7408.5
1.154	.7710E+05	7104.8
1.209	.4195E+05	6854.6
1.264	.2735E+05	6691.0
1.319	.1329E+05	6434.1

.497 CP SECONDS EXECUTION TIME

```
LGO,,DATA
7 0,0.,1,0,0
```

STARK BROADENING PARAMETERS

TEMPERATURE	W	D/W	ALPHA
5000.0000	.0039	.9086	.0260
10000.0000	.0051	.7257	.0210
20000.0000	.0069	.5137	.0170

1 ANALYSIS OF AN OPTICALLY THICK AIR ARC

RUN CODE IS 301
ARC RADIUS IS 1.3740 MM.
25 POINTS WERE USED FOR DATA AND ANALYSIS.
THE CURRENT WAS 11.9 AMPS.
THE PRESSURE WAS 30.0 ATM.
THE OXYGEN 844.65 NM LINE WAS USED.
THE SPECTROMETER RESOLUTION WAS 1.34 NM.

PLASMA PROPERTIES

RADIUS (MM)	LINE EMISSION (W/SR-M**3)	TEMPERATURE (DEG. KELVIN)
0.000	.41743E+07	9534.8
.055	.40605E+07	9511.6
.110	.38691E+07	9471.2
.165	.37807E+07	9452.0
.220	.36493E+07	9422.7
.275	.34185E+07	9369.1
.330	.30675E+07	9281.4
.385	.26964E+07	9179.2
.440	.24227E+07	9096.5
.495	.21959E+07	9021.6
.550	.19498E+07	8932.5
.605	.16899E+07	8827.4
.660	.14429E+07	8714.7
.714	.12101E+07	8592.8
.769	.97143E+06	8445.8
.824	.74695E+06	8278.0
.879	.59764E+06	8141.7
.934	.50427E+06	8041.5
.989	.39209E+06	7898.3
1.044	.26276E+06	7682.9
1.099	.15107E+06	7408.5
1.154	.77102E+05	7104.8
1.209	.41952E+05	6854.6
1.264	.27350E+05	6691.0
1.319	.13289E+05	6434.1

1 COMPARISON OF THE PREDICTED INTENSITY ACCOUNTING FOR OPACITY WITH THE PREDICTED INTENSITY ASSUMING OPTICALLY THIN LINE FOR A GIVEN EMISSION PROFILE.

ZONE	SPATIAL POSITION (MM)	OPTICALLY THICK (W/SR-M**2)	OPTICALLY THIN (W/SR-M**2)
1	0.0000	3393.25	4419.81
2	.0550	3374.84	4394.05
3	.1099	3298.37	4290.85
4	.1649	3195.10	4148.92
5	.2198	3044.89	3944.40
6	.2748	2845.61	3675.80
7	.3298	2610.73	3360.95
8	.3847	2374.74	3043.23
9	.4397	2156.87	2747.33
10	.4946	1938.40	2451.27
11	.5496	1708.84	2143.31
12	.6046	1477.95	1836.53
13	.6595	1255.91	1544.17
14	.7145	1043.95	1268.39
15	.7694	843.75	1011.78
16	.8244	671.01	793.15
17	.8794	537.89	626.09
18	.9343	423.03	484.27
19	.9893	303.99	341.63
20	1.0442	193.90	213.51
21	1.0992	110.49	118.91
22	1.1542	58.34	61.30
23	1.2091	31.76	32.77
24	1.2641	17.17	17.49
25	1.3190	5.68	5.72

19.955 CP SECONDS EXECUTION TIME

LGO,RDT301,DATA,RDATA

STARK BROADENING PARAMETERS

TEMPERATURE	W	D/W	ALPHA
5000.0000	.0039	.9086	.0260
10000.0000	.0051	.7257	.0210
20000.0000	.0069	.5137	.0170

1 ANALYSIS OF AN OPTICALLY THICK AIR ARC

RUN CODE IS 301
ARC RADIUS IS 1.3740 MM.
25 POINTS WERE USED FOR DATA AND ANALYSIS.
THE CURRENT WAS 11.9 AMPS.
THE PRESSURE WAS 30.0 ATM.
THE OXYGEN 844.65 NM LINE WAS USED.
THE SPECTROMETER RESOLUTION WAS 1.34 NM.

PLASMA PROPERTIES

RADIUS (MM)	LINE EMISSION (W/SR-M**3)	TEMPERATURE (DEG. KELVIN)
0.000	.41743E+07	9534.8
.055	.40605E+07	9511.6
.110	.38691E+07	9471.2
.165	.37807E+07	9452.0
.220	.36493E+07	9422.7
.275	.34185E+07	9369.1
.330	.30675E+07	9281.4
.385	.26964E+07	9179.2
.440	.24227E+07	9096.5
.495	.21959E+07	9021.6
.550	.19498E+07	8932.5
.605	.16899E+07	8827.4
.660	.14429E+07	8714.7
.714	.12101E+07	8592.8
.769	.97143E+06	8445.8
.824	.74695E+06	8278.0
.879	.59764E+06	8141.7
.934	.50427E+06	8041.5
.989	.39209E+06	7898.3
1.044	.26276E+06	7682.9
1.099	.15107E+06	7408.5
1.154	.77102E+05	7104.8
1.209	.41952E+05	6854.6
1.264	.27350E+05	6691.0
1.319	.13289E+05	6434.1

1 SPATIAL DISTRIBUTION OF THE PREDICTED LINE INTENSITY FOR AN OPTICALLY THICK LINE.

ZONE	SPATIAL POSITION (MM)	PREDICTED INTENSITY (W/SR-M**2)
1	0.0000	4422.74
2	.0550	4396.94
3	.1099	4294.47
4	.1649	4152.63
5	.2198	3947.56
6	.2748	3679.49
7	.3298	3364.29
8	.3847	3046.05
9	.4397	2749.64
10	.4946	2453.07
11	.5496	2144.60
12	.6046	1838.23
13	.6595	1544.94
14	.7145	1268.59
15	.7694	1012.38
16	.8244	793.42
17	.8794	626.23
18	.9343	484.37
19	.9893	341.63
20	1.0442	213.50
21	1.0992	118.89
22	1.1542	61.30
23	1.2091	32.77
24	1.2641	17.46
25	1.3190	5.73

1 EMISSION AND TEMPERATURE DISTRIBUTION USING AN OPTICALLY THICK LINE.

RADIUS (MM)	LINE EMISSION (W/SR-M**3)	TEMPERATURE (DEG. KELVIN)
0.000	.53793E+07	9752.2
.055	.54785E+07	9768.2
.110	.52153E+07	9725.2
.165	.50781E+07	9702.0
.220	.48722E+07	9666.3
.275	.45479E+07	9607.5
.330	.40706E+07	9513.6
.385	.35697E+07	9404.5
.440	.31907E+07	9313.1
.495	.28687E+07	9228.0
.550	.25212E+07	9127.1
.605	.21664E+07	9011.3
.660	.18276E+07	8884.7
.714	.15107E+07	8747.1
.769	.11973E+07	8585.5
.824	.90678E+06	8401.0
.879	.71368E+06	8249.7
.934	.59026E+06	8134.2
.989	.44834E+06	7973.9
1.044	.29364E+06	7741.1
1.099	.16441E+06	7449.0
1.154	.81383E+05	7128.0
1.209	.43394E+05	6868.0
1.264	.27800E+05	6697.1
1.319	.13395E+05	6436.8

56.012 CP SECONDS EXECUTION TIME

```
LGO;,RDATA
? 0,0.,0,0,0
```

STARK BROADENING PARAMETERS

TEMPERATURE	W	D/W	ALPHA
5000.0000	.0039	.9086	.0260
10000.0000	.0051	.7257	.0210
20000.0000	.0069	.5137	.0170

1 ANALYSIS OF AN OPTICALLY THICK AIR ARC

RUN CODE IS 301
ARC RADIUS IS 1.3740 MM.
25 POINTS WERE USED FOR DATA AND ANALYSIS.
THE CURRENT WAS 11.9 AMPS.
THE PRESSURE WAS 30.0 ATM.
THE OXYGEN 844.65 NM LINE WAS USED.
THE SPECTROMETER RESOLUTION WAS 1.34 NM.

PLASMA PROPERTIES

RADIUS (MM)	LINE EMISSION (W/SR-M**3)	TEMPERATURE (DEG. KELVIN)
0.000	.53793E+07	9752.2
.055	.54785E+07	9768.2
.110	.52153E+07	9725.2
.165	.50781E+07	9702.0
.220	.48722E+07	9666.3
.275	.45479E+07	9607.5
.330	.40706E+07	9513.6
.385	.35697E+07	9404.5
.440	.31907E+07	9313.1
.495	.28687E+07	9228.0
.550	.25212E+07	9127.1
.605	.21664E+07	9011.3
.660	.18276E+07	8884.7
.714	.15107E+07	8747.1
.769	.11973E+07	8585.5
.824	.90678E+06	8401.0
.879	.71368E+06	8249.7
.934	.59026E+06	8134.2
.989	.44834E+06	7973.9
1.044	.29364E+06	7741.1
1.099	.16441E+06	7449.0
1.154	.81383E+05	7128.0
1.209	.43394E+05	6868.0
1.264	.27800E+05	6697.1
1.319	.13395E+05	6436.8

1 SPECTRAL DISTRIBUTION ABOUT LINE CENTER OF THE PREDICTED LINE INTENSITY ALONG CENTRAL CORD FOR OPTICALLY THICK AND OPTICALLY THIN CASES.

	DISTANCE FROM LINE CENTER (NM)	OPTICALLY THICK (W/SR-NM-M**2)	OPTICALLY THIN (W/SR-NM-M**2)
1	-.6700	121.12	121.25
2	-.6500	128.38	128.53
3	-.6000	149.64	149.85
4	-.5500	176.66	176.94
5	-.5000	211.69	212.09
6	-.4500	258.24	258.85
7	-.4000	321.98	322.92
8	-.3500	412.47	414.02
9	-.3000	547.02	549.75
10	-.2500	759.37	764.66
11	-.2400	816.43	822.55
12	-.2300	880.12	887.23
13	-.2200	951.49	959.81
14	-.2100	1031.82	1041.62
15	-.2000	1122.67	1134.29
16	-.1900	1225.92	1239.79
17	-.1800	1343.92	1360.62
18	-.1700	1479.56	1499.85
19	-.1600	1636.51	1661.38
20	-.1500	1819.38	1850.20
21	-.1400	2034.09	2072.75
22	-.1300	2288.34	2337.46
23	-.1200	2592.21	2655.52
24	-.1100	2959.11	3042.06
25	-.1000	3407.15	3517.88
26	-.0900	3961.20	4112.12
27	-.0800	4655.87	4866.61
28	-.0700	5540.33	5842.88
29	-.0600	6685.51	7134.14
30	-.0500	8195.46	8886.48
31	-.0450	9132.93	10004.72
32	-.0400	10224.78	11338.26
33	-.0350	11502.39	12943.97
34	-.0300	13003.89	14898.42
35	-.0250	14775.17	17306.99
36	-.0200	16870.45	20318.64
37	-.0150	19351.47	24152.37
38	-.0100	22282.86	29149.30
39	-.0050	25713.41	35895.58
40	.0000	29567.29	45593.09
41	.0050	32980.62	56188.94
42	.0100	34985.08	61371.24
43	.0150	35772.15	62374.20
44	.0200	35704.86	60780.68
45	.0250	34940.05	57470.03
46	.0300	33571.71	52995.80
47	.0350	31705.68	47859.30
48	.0400	29471.92	42504.94
49	.0450	27017.24	37284.96
50	.0500	24487.03	32439.98
51	.0600	19662.32	24314.11
52	.0700	15579.18	18297.41
53	.0800	12359.34	13984.42
54	.0900	9895.60	10899.80
55	.1000	8023.80	8666.72
56	.1100	6594.88	7020.80
57	.1200	5492.62	5783.77

58	.1300	4631.45	4836.16
59	.1400	3949.65	4097.23
60	.1500	3402.78	3511.58
61	.1600	2958.74	3040.54
62	.1700	2594.03	2656.63
63	.1800	2291.31	2339.98
64	.1900	2037.61	2075.97
65	.2000	1823.08	1853.71
66	.2100	1640.19	1664.94
67	.2200	1483.12	1503.31
68	.2300	1347.29	1363.93
69	.2400	1229.08	1242.91
70	.2500	1125.61	1137.19
71	.3000	761.34	766.62
72	.3500	548.34	551.07
73	.4000	413.38	414.93
74	.4500	322.63	323.57
75	.5000	258.72	259.33
76	.5500	212.05	212.46
77	.6000	176.94	177.22
78	.6500	149.86	150.07
79	.6700	140.75	140.92

1 COMPARISON OF THE PREDICTED INTENSITY ACCOUNTING FOR OPACITY WITH THE PREDICTED INTENSITY ASSUMING OPTICALLY THIN LINE FOR A GIVEN EMISSION PROFILE.

ZONE	SPATIAL POSITION (MM)	OPTICALLY THICK (W/SR-M**2)	OPTICALLY THIN (W/SR-M**2)
1	0.0000	4422.74	5783.87
2	.0550	4383.98	5732.10
3	.1099	4275.95	5587.00
4	.1649	4132.28	5390.12
5	.2198	3925.61	5109.25
6	.2748	3656.80	4747.08
7	.3298	3341.71	4324.79
8	.3847	3024.64	3897.90
9	.4397	2729.78	3497.47
10	.4946	2434.55	3097.24
11	.5496	2127.50	2684.82
12	.6046	1822.99	2279.39
13	.6595	1531.61	1895.01
14	.7145	1257.34	1537.25
15	.7694	1003.23	1210.33
16	.8244	786.28	934.62
17	.8794	620.94	726.20
18	.9343	480.34	551.94
19	.9893	338.52	381.51
20	1.0442	211.38	233.30
21	1.0992	117.66	126.86
22	1.1542	60.72	63.87
23	1.2091	32.58	33.63
24	1.2641	17.40	17.73
25	1.3190	5.71	5.76

24.575 CP SECONDS EXECUTION TIME

/

```
 LGO,,RDATA
? 0,1000.,0,0,0
```

STARK BROADENING PARAMETERS

TEMPERATURE	W	D/W	ALPHA
5000.0000	.0039	.9086	.0260
10000.0000	.0051	.7257	.0210
20000.0000	.0069	.5137	.0170

1 ANALYSIS OF AN OPTICALLY THICK AIR ARC

RUN CODE IS 301
ARC RADIUS IS 1.3740 MM.
25 POINTS WERE USED FOR DATA AND ANALYSIS.
THE CURRENT WAS 11.9 AMPS.
THE PRESSURE WAS 30.0 ATM.
THE OXYGEN 844.65 NM LINE WAS USED.
THE SPECTROMETER RESOLUTION WAS 1.34 NM.

PLASMA PROPERTIES

RADIUS (MM)	LINE EMISSION (W/SR-M**3)	TEMPERATURE (DEG. KELVIN)
0.000	.53793E+07	9752.2
.055	.54785E+07	9768.2
.110	.52153E+07	9725.2
.165	.50781E+07	9702.0
.220	.48722E+07	9666.3
.275	.45479E+07	9607.5
.330	.40706E+07	9513.6
.385	.35697E+07	9404.5
.440	.31907E+07	9313.1
.495	.28687E+07	9228.0
.550	.25212E+07	9127.1
.605	.21664E+07	9011.3
.660	.18276E+07	8884.7
.714	.15107E+07	8747.1
.769	.11973E+07	8585.5
.824	.90678E+06	8401.0
.879	.71368E+06	8249.7
.934	.59026E+06	8134.2
.989	.44834E+06	7973.9
1.044	.29364E+06	7741.1
1.099	.16441E+06	7449.0
1.154	.81383E+05	7128.0
1.209	.43394E+05	6868.0
1.264	.27800E+05	6697.1
1.319	.13395E+05	6436.8

1 SPECTRAL DISTRIBUTION ABOUT LINE CENTER OF THE PREDICTED LINE INTENSITY ALONG CENTRAL CORD FOR OPTICALLY THICK AND OPTICALLY THIN CASES.

	DISTANCE FROM LINE CENTER (NM)	OPTICALLY THICK (W/SR-NM-M**2)	OPTICALLY THIN (W/SR-NM-M**2)
1	-.6700	1118.93	1121.25
2	-.6500	1126.05	1128.53
3	-.6000	1146.93	1149.85
4	-.5500	1173.45	1176.94
5	-.5000	1207.85	1212.09
6	-.4500	1253.56	1258.85
7	-.4000	1316.14	1322.92
8	-.3500	1404.99	1414.02
9	-.3000	1537.09	1549.75
10	-.2500	1745.58	1764.66
11	-.2400	1801.60	1822.55
12	-.2300	1864.13	1887.23
13	-.2200	1934.20	1959.81
14	-.2100	2013.07	2041.62
15	-.2000	2102.26	2134.29
16	-.1900	2203.63	2239.79
17	-.1800	2319.47	2360.62
18	-.1700	2452.64	2499.85
19	-.1600	2606.72	2661.38
20	-.1500	2786.24	2850.20
21	-.1400	2997.03	3072.75
22	-.1300	3246.63	3337.46
23	-.1200	3544.92	3655.52
24	-.1100	3905.09	4042.06
25	-.1000	4344.90	4517.88
26	-.0900	4888.73	5112.12
27	-.0800	5570.58	5866.61
28	-.0700	6438.66	6842.88
29	-.0600	7562.53	8134.14
30	-.0500	9044.24	9886.48
31	-.0450	9964.08	11004.72
32	-.0400	11035.28	12338.26
33	-.0350	12288.58	13943.97
34	-.0300	13761.29	15898.42
35	-.0250	15498.24	18306.99
36	-.0200	17552.30	21318.64
37	-.0150	19983.45	25152.37
38	-.0100	22853.88	30149.30
39	-.0050	26208.56	36895.58
40	.0000	29963.54	46593.09
41	.0050	33294.68	57188.94
42	.0100	35276.75	62371.24
43	.0150	36067.26	63374.20
44	.0200	36016.96	61780.68
45	.0250	35278.50	58470.03
46	.0300	33944.43	53995.80
47	.0350	32119.15	48859.30
48	.0400	29930.77	43504.94
49	.0450	27523.88	38284.96
50	.0500	25041.67	33439.98
51	.0600	20306.50	25314.11
52	.0700	16297.99	19297.41
53	.0800	13136.56	14984.42
54	.0900	10717.35	11899.80
55	.1000	8879.30	9666.72
56	.1100	7476.13	8020.80
57	.1200	6393.72	6783.77

58	.1300	5548.05	5836.16
59	.1400	4878.51	5097.23
60	.1500	4341.49	4511.58
61	.1600	3905.43	4040.54
62	.1700	3547.29	3656.63
63	.1800	3250.02	3339.98
64	.1900	3000.88	3075.97
65	.2000	2790.21	2853.71
66	.2100	2610.62	2664.94
67	.2200	2456.38	2503.31
68	.2300	2322.99	2363.93
69	.2400	2206.91	2242.91
70	.2500	2105.30	2137.19
71	.3000	1747.60	1766.62
72	.3500	1538.44	1551.07
73	.4000	1405.92	1414.93
74	.4500	1316.80	1323.57
75	.5000	1254.05	1259.33
76	.5500	1208.22	1212.46
77	.6000	1173.74	1177.22
78	.6500	1147.15	1150.07
79	.6700	1138.20	1140.92

1 COMPARISON OF THE PREDICTED INTENSITY ACCOUNTING FOR OPACITY WITH THE PREDICTED INTENSITY ASSUMING OPTICALLY THIN LINE FOR A GIVEN EMISSION PROFILE.

ZONE	SPATIAL POSITION (MM)	OPTICALLY THICK (W/SR-M**2)	OPTICALLY THIN (W/SR-M**2)
1	0.0000	5679.98	7123.87
2	.0550	5641.80	7072.10
3	.1099	5535.40	6927.00
4	.1649	5393.94	6730.12
5	.2198	5190.45	6449.25
6	.2748	4925.82	6087.08
7	.3298	4615.68	5664.79
8	.3847	4303.71	5237.90
9	.4397	4013.75	4837.47
10	.4946	3723.55	4437.24
11	.5496	3421.84	4024.82
12	.6046	3122.76	3619.39
13	.6595	2836.74	3235.01
14	.7145	2567.70	2877.25
15	.7694	2318.61	2550.33
16	.8244	2106.16	2274.62
17	.8794	1944.46	2066.20
18	.9343	1807.10	1891.94
19	.9893	1668.67	1721.51
20	1.0442	1544.75	1573.30
21	1.0992	1453.59	1466.86
22	1.1542	1398.39	1403.87
23	1.2091	1371.22	1373.63
24	1.2641	1356.63	1357.73
25	1.3190	1345.43	1345.76

19.860 CP SECONDS EXECUTION TIME

/

LGO,D302,DATAN

1 EMISSION COEFFICIENT LIBRARY FOR THE NITROGEN LINE AT
862.92 NM AND A PRESSURE OF 30. ATMOSPHERES.

TEMPERATURE (DEG. KELVIN)	EMISSION (W/SR-M**3)
6000.	.3395E+02
6200.	.9537E+02
6400.	.2504E+03
6600.	.6179E+03
6800.	.1435E+04
7000.	.3171E+04
7200.	.6653E+04
7400.	.1329E+05
7600.	.2541E+05
7800.	.4663E+05
8000.	.8232E+05
8200.	.1400E+06
8400.	.2300E+06
8600.	.3647E+06
8800.	.5605E+06
9000.	.8386E+06
9200.	.1218E+07
9400.	.1727E+07
9600.	.2392E+07
9800.	.3246E+07
10000.	.4323E+07
10200.	.5649E+07
10400.	.7288E+07
10600.	.9252E+07
10800.	.1163E+08
11000.	.1442E+08
11200.	.1769E+08
11400.	.2154E+08
11600.	.2594E+08
11800.	.3098E+08
12000.	.3667E+08
12200.	.4307E+08
12400.	.5021E+08
12600.	.5821E+08
12800.	.6705E+08
13000.	.7677E+08
13200.	.8735E+08
13400.	.9866E+08
13600.	.1110E+09
13800.	.1242E+09
14000.	.1380E+09
14200.	.1529E+09
14400.	.1685E+09
14600.	.1845E+09
14800.	.2013E+09
15000.	.2187E+09
15200.	.2362E+09
15400.	.2543E+09
15600.	.2722E+09
15800.	.2906E+09
16000.	.3085E+09

1 ANALYSIS OF AN OPTICALLY THIN AIR ARC

RUN CODE IS 302
ARC RADIUS IS 1.3740 MM.
25 POINTS WERE USED FOR DATA AND ANALYSIS.
THE CURRENT WAS 11.9 AMPS.
THE PRESSURE WAS 30.0 ATM.
THE NITROGEN 862.92 NM LINE WAS USED.
THE SPECTROMETER RESOLUTION WAS 1.33 NM.

OBSERVED INTENSITY

ZONE	SPATIAL POSITION (MM)	OBSERVED INTENSITY (W/SR-M**2)	SPATIAL DERIVATIVE OF INTENSITY (W/SR-M**3)
1	0.0000	2190.00	0.
2	.0550	2116.00	-.1216E+07
3	.1099	2027.00	-.1994E+07
4	.1649	1926.00	-.3179E+07
5	.2198	1662.00	-.4843E+07
6	.2748	1405.00	-.5533E+07
7	.3298	1064.00	-.4821E+07
8	.3847	858.70	-.3757E+07
9	.4397	683.20	-.2778E+07
10	.4946	540.00	-.2739E+07
11	.5496	389.00	-.2437E+07
12	.6046	258.00	-.1943E+07
13	.6595	183.00	-.1181E+07
14	.7145	126.00	-.7160E+06
15	.7694	102.30	-.6234E+06
16	.8244	62.19	-.5442E+06
17	.8794	30.68	-.4485E+06
18	.9343	18.33	-.2022E+06
19	.9893	8.85	-.6700E+05
20	1.0442	8.14	-.2287E+05
21	1.0992	7.44	.1077E+04
22	1.1542	6.73	-.1286E+05
23	1.2091	6.02	-.6658E+04
24	1.2641	5.32	-.3398E+05
25	1.3190	4.61	-.2686E+05

1

RADIUS (MM)	LINE EMISSION (W/SR-M**3)	TEMPERATURE (DEG. KELVIN)
0.000	.3003E+07	9747.7
.055	.2931E+07	9731.6
.110	.2809E+07	9703.5
.165	.2743E+07	9687.9
.220	.2556E+07	9642.3
.275	.2113E+07	9522.3
.330	.1580E+07	9347.5
.385	.1153E+07	9169.9
.440	.8771E+06	9023.3
.495	.7136E+06	8917.9
.550	.5331E+06	8776.0
.605	.3611E+06	8595.5
.660	.2221E+06	8385.5
.714	.1507E+06	8228.8
.769	.1164E+06	8128.7
.824	.8412E+05	8007.9
.879	.5100E+05	7830.7
.934	.2037E+05	7530.4
.989	.7427E+04	7230.9
1.044	.3438E+04	7021.2
1.099	.2481E+04	6936.6
1.154	.3188E+04	7001.4
1.209	.3244E+04	7005.9
1.264	.3732E+04	7042.9
1.319	.1727E+04	6845.5

.658 CP SECONDS EXECUTION TIME

```
 LGO,,DATAN
? 0,0.,1,0,0
```

STARK BROADENING PARAMETERS

TEMPERATURE	W	D/W	ALPHA
5000.0000	.0060	1.0956	.0340
10000.0000	.0073	.9739	.0300
20000.0000	.0092	.7638	.0250

1 ANALYSIS OF AN OPTICALLY THICK AIR ARC

RUN CODE IS 302
ARC RADIUS IS 1.3740 MM.
25 POINTS WERE USED FOR DATA AND ANALYSIS.
THE CURRENT WAS 11.9 AMPS.
THE PRESSURE WAS 30.0 ATM.
THE NITROGEN 862.92 NM LINE WAS USED.
THE SPECTROMETER RESOLUTION WAS 1.33 NM.

PLASMA PROPERTIES

RADIUS (MM)	LINE EMISSION (W/SR-M**3)	TEMPERATURE (DEG. KELVIN)
0.000	.30029E+07	9747.7
.055	.29311E+07	9731.6
.110	.28088E+07	9703.5
.165	.27429E+07	9688.0
.220	.25562E+07	9642.3
.275	.21127E+07	9522.2
.330	.15796E+07	9347.5
.385	.11534E+07	9169.9
.440	.87714E+06	9023.3
.495	.71360E+06	8917.9
.550	.53305E+06	8776.0
.605	.36110E+06	8595.5
.660	.22207E+06	8385.5
.714	.15066E+06	8228.8
.769	.11636E+06	8128.7
.824	.84117E+05	8007.9
.879	.50997E+05	7830.7
.934	.20370E+05	7530.4
.989	.74268E+04	7230.9
1.044	.34376E+04	7021.2
1.099	.24813E+04	6936.6
1.154	.31884E+04	7001.4
1.209	.32438E+04	7005.9
1.264	.37318E+04	7042.9
1.319	.17274E+04	6845.5

1 COMPARISON OF THE PREDICTED INTENSITY ACCOUNTING FOR OPACITY WITH THE PREDICTED INTENSITY ASSUMING OPTICALLY THIN LINE FOR A GIVEN EMISSION PROFILE.

ZONE	SPATIAL POSITION (MM)	OPTICALLY THICK (W/SR-M**2)	OPTICALLY THIN (W/SR-M**2)
1	0.0000	1990.48	2147.06
2	.0550	1968.83	2122.73
3	.1099	1887.55	2032.20
4	.1649	1761.78	1892.29
5	.2198	1563.79	1674.04
6	.2748	1298.03	1383.76
7	.3298	1029.63	1092.31
8	.3847	810.71	855.50
9	.4397	644.33	676.22
10	.4946	507.37	529.47
11	.5496	371.95	385.78
12	.6046	256.79	264.72
13	.6595	173.28	177.64
14	.7145	124.37	126.93
15	.7694	90.41	91.91
16	.8244	59.04	59.79
17	.8794	32.23	32.51
18	.9343	13.83	13.90
19	.9893	7.07	7.09
20	1.0442	5.05	5.07
21	1.0992	4.51	4.52
22	1.1542	4.38	4.39
23	1.2091	3.71	3.72
24	1.2641	2.75	2.76
25	1.3190	.91	.91

23.507 CP SECONDS EXECUTION TIME

```
LGO,RDT302,DATAN,RDATAN
```

STARK BROADENING PARAMETERS

TEMPERATURE	W	D/W	ALPHA
5000.0000	.0060	1.0956	.0340
10000.0000	.0073	.9739	.0300
20000.0000	.0092	.7638	.0250

1 ANALYSIS OF AN OPTICALLY THICK AIR ARC

RUN CODE IS 302
ARC RADIUS IS 1.3740 MM.
25 POINTS WERE USED FOR DATA AND ANALYSIS.
THE CURRENT WAS 11.9 AMPS.
THE PRESSURE WAS 30.0 ATM.
THE NITROGEN 862.92 NM LINE WAS USED.
THE SPECTROMETER RESOLUTION WAS 1.33 NM.

PLASMA PROPERTIES

RADIUS (MM)	LINE EMISSION (W/SR-M**3)	TEMPERATURE (DEG. KELVIN)
0.000	.30029E+07	9747.7
.055	.29311E+07	9731.6
.110	.28088E+07	9703.5
.165	.27429E+07	9688.0
.220	.25562E+07	9642.3
.275	.21127E+07	9522.2
.330	.15796E+07	9347.5
.385	.11534E+07	9169.9
.440	.87714E+06	9023.3
.495	.71360E+06	8917.9
.550	.53305E+06	8776.0
.605	.36110E+06	8595.5
.660	.22207E+06	8385.5
.714	.15066E+06	8228.8
.769	.11636E+06	8128.7
.824	.84117E+05	8007.9
.879	.50997E+05	7830.7
.934	.20370E+05	7530.4
.989	.74268E+04	7230.9
1.044	.34376E+04	7021.2
1.099	.24813E+04	6936.6
1.154	.31884E+04	7001.4
1.209	.32438E+04	7005.9
1.264	.37318E+04	7042.9
1.319	.17274E+04	6845.5

1 SPATIAL DISTRIBUTION OF THE PREDICTED LINE INTENSITY FOR AN OPTICALLY THICK LINE.

ZONE	SPATIAL POSITION (MM)	PREDICTED INTENSITY (W/SR-M**2)
1	0.0000	2147.01
2	.0550	2122.99
3	.1099	2031.98
4	.1649	1891.97
5	.2198	1673.98
6	.2748	1383.98
7	.3298	1091.99
8	.3847	855.50
9	.4397	676.20
10	.4946	529.50
11	.5496	385.80
12	.6046	264.70
13	.6595	177.60
14	.7145	126.90
15	.7694	91.91
16	.8244	59.57
17	.8794	32.45
18	.9343	13.88
19	.9893	7.08
20	1.0442	5.06
21	1.0992	4.52
22	1.1542	4.38
23	1.2091	3.71
24	1.2641	2.76
25	1.3190	.91

1 EMISSION AND TEMPERATURE DISTRIBUTION USING AN OPTICALLY THICK LINE.

RADIUS (MM)	LINE EMISSION (W/SR-M**3)	TEMPERATURE (DEG. KELVIN)
0.000	.32596E+07	9802.8
.055	.32249E+07	9795.6
.110	.30770E+07	9764.0
.165	.29908E+07	9745.0
.220	.27717E+07	9694.8
.275	.22795E+07	9569.6
.330	.16916E+07	9387.7
.385	.12290E+07	9205.0
.440	.92892E+06	9053.4
.495	.75081E+06	8943.5
.550	.55651E+06	8796.6
.605	.37410E+06	8611.5
.660	.22856E+06	8397.4
.714	.15425E+06	8238.1
.769	.11901E+06	8137.3
.824	.84964E+05	8011.5
.879	.51374E+05	7833.2
.934	.20455E+05	7531.7
.989	.74482E+04	7231.7
1.044	.34447E+04	7021.7
1.099	.24854E+04	6937.0
1.154	.31946E+04	7001.9
1.209	.32491E+04	7006.4
1.264	.37371E+04	7043.2
1.319	.17287E+04	6845.7

48.700 CP SECONDS EXECUTION TIME

```
LGO,,RDATAN
? 0,0.,,0,0,0
```

STARK BROADENING PARAMETERS

TEMPERATURE	W	D/W	ALPHA
5000.0000	.0060	1.0956	.0340
10000.0000	.0073	.9739	.0300
20000.0000	.0092	.7638	.0250

1 ANALYSIS OF AN OPTICALLY THICK AIR ARC

RUN CODE IS 302
ARC RADIUS IS 1.3740 MM.
25 POINTS WERE USED FOR DATA AND ANALYSIS.
THE CURRENT WAS 11.9 AMPS.
THE PRESSURE WAS 30.0 ATM.
THE NITROGEN 862.92 NM LINE WAS USED.
THE SPECTROMETER RESOLUTION WAS 1.33 NM.

PLASMA PROPERTIES

RADIUS (MM)	LINE EMISSION (W/SR-M**3)	TEMPERATURE (DEG. KELVIN)
0.000	.32596E+07	9802.8
.055	.32249E+07	9795.6
.110	.30770E+07	9764.0
.165	.29908E+07	9745.0
.220	.27717E+07	9694.8
.275	.22795E+07	9569.6
.330	.16916E+07	9387.7
.385	.12290E+07	9205.0
.440	.92892E+06	9053.4
.495	.75081E+06	8943.5
.550	.55651E+06	8796.6
.605	.37410E+06	8611.5
.660	.22856E+06	8397.4
.714	.15425E+06	8238.1
.769	.11901E+06	8137.3
.824	.84964E+05	8011.5
.879	.51374E+05	7833.2
.934	.20455E+05	7531.7
.989	.74482E+04	7231.7
1.044	.34447E+04	7021.7
1.099	.24854E+04	6937.0
1.154	.31946E+04	7001.9
1.209	.32491E+04	7006.4
1.264	.37371E+04	7043.2
1.319	.17287E+04	6845.7

1 SPECTRAL DISTRIBUTION ABOUT LINE CENTER OF THE PREDICTED LINE INTENSITY ALONG CENTRAL CORD FOR OPTICALLY THICK AND OPTICALLY THIN CASES.

	DISTANCE FROM LINE CENTER (NM)	OPTICALLY THICK (W/SR-NM-M**2)	OPTICALLY THIN (W/SR-NM-M**2)
1	-.6665	73.63	73.68
2	-.6500	77.12	77.17
3	-.6000	89.32	89.40
4	-.5500	104.66	104.77
5	-.5000	124.31	124.46
6	-.4500	150.04	150.25
7	-.4000	184.62	184.94
8	-.3500	232.61	233.12
9	-.3000	301.90	302.77
10	-.2500	407.10	408.67
11	-.2400	434.61	436.40
12	-.2300	464.98	467.03
13	-.2200	498.60	500.97
14	-.2100	535.97	538.70
15	-.2000	577.64	580.81
16	-.1900	624.29	628.00
17	-.1800	676.74	681.11
18	-.1700	735.97	741.15
19	-.1600	803.20	809.37
20	-.1500	879.88	887.30
21	-.1400	967.85	976.84
22	-.1300	1069.38	1080.38
23	-.1200	1187.33	1200.93
24	-.1100	1325.36	1342.35
25	-.1000	1488.15	1509.63
26	-.0900	1681.79	1709.34
27	-.0800	1914.32	1950.17
28	-.0700	2196.45	2243.91
29	-.0600	2542.74	2606.80
30	-.0500	2973.31	3061.68
31	-.0450	3228.65	3333.42
32	-.0400	3516.59	3641.64
33	-.0350	3842.71	3993.09
34	-.0300	4213.87	4396.20
35	-.0250	4638.58	4861.66
36	-.0200	5127.56	5403.32
37	-.0150	5694.62	6039.52
38	-.0100	6358.03	6795.46
39	-.0050	7142.98	7707.45
40	.0000	8085.48	8830.75
41	.0050	9196.27	10197.20
42	.0100	10277.60	11554.79
43	.0150	11218.04	12755.09
44	.0200	11946.11	13692.07
45	.0250	12465.38	14358.33
46	.0300	12805.39	14788.38
47	.0350	12981.77	15001.04
48	.0400	13006.56	15012.17
49	.0450	12893.42	14841.52
50	.0500	12655.75	14509.70
51	.0600	11856.47	13442.01
52	.0700	10722.66	11985.59
53	.0800	9406.84	10354.36
54	.0900	8069.47	8750.80
55	.1000	6829.70	7308.18
56	.1100	5747.89	6081.30
57	.1200	4837.92	5071.02

58	.1300	4087.55	4252.21
59	.1400	3474.16	3592.11
60	.1500	2973.57	3059.41
61	.1600	2563.97	2627.45
62	.1700	2227.12	2274.80
63	.1800	1948.30	1984.66
64	.1900	1715.88	1744.01
65	.2000	1520.74	1542.78
66	.2100	1355.71	1373.19
67	.2200	1215.19	1229.21
68	.2300	1094.72	1106.08
69	.2400	990.80	1000.10
70	.2500	900.62	908.30
71	.3000	590.19	593.48
72	.3500	415.02	416.64
73	.4000	307.15	308.04
74	.4500	236.25	236.77
75	.5000	187.23	187.56
76	.5500	151.97	152.19
77	.6000	125.78	125.93
78	.6500	105.81	105.91
79	.6665	100.25	100.34

1 COMPARISON OF THE PREDICTED INTENSITY ACCOUNTING FOR OPACITY WITH THE PREDICTED INTENSITY ASSUMING OPTICALLY THIN LINE FOR A GIVEN EMISSION PROFILE.

ZONE	SPATIAL POSITION (MM)	OPTICALLY THICK (W/SR-M**2)	OPTICALLY THIN (W/SR-M**2)
1	0.0000	2147.01	2319.23
2	.0550	2119.98	2288.92
3	.1099	2027.77	2186.17
4	.1649	1887.52	2030.00
5	.2198	1669.34	1789.24
6	.2748	1379.52	1472.35
7	.3298	1088.22	1155.72
8	.3847	852.75	900.74
9	.4397	674.21	708.16
10	.4946	528.05	551.42
11	.5496	384.69	399.20
12	.6046	263.96	272.21
13	.6595	177.17	181.67
14	.7145	126.68	129.31
15	.7694	91.78	93.32
16	.8244	59.47	60.23
17	.8794	32.41	32.70
18	.9343	13.87	13.94
19	.9893	7.08	7.11
20	1.0442	5.06	5.07
21	1.0992	4.52	4.53
22	1.1542	4.38	4.40
23	1.2091	3.71	3.72
24	1.2641	2.76	2.76
25	1.3190	.91	.91

22.819 CP SECONDS EXECUTION TIME

```
 LGO;,RDATAN
? 0,1000.,0,0,0
```

STARK BROADENING PARAMETERS

TEMPERATURE	W	D/W	ALPHA
5000.0000	.0060	1.0956	.0340
10000.0000	.0073	.9739	.0300
20000.0000	.0092	.7638	.0250

1 ANALYSIS OF AN OPTICALLY THICK AIR ARC

RUN CODE IS 302
ARC RADIUS IS 1.3740 MM.
25 POINTS WERE USED FOR DATA AND ANALYSIS.
THE CURRENT WAS 11.9 AMPS.
THE PRESSURE WAS 30.0 ATM.
THE NITROGEN 862.92 NM LINE WAS USED.
THE SPECTROMETER RESOLUTION WAS 1.33 NM.

PLASMA PROPERTIES

RADIUS (MM)	LINE EMISSION (W/SR-M**3)	TEMPERATURE (DEG. KELVIN)
0.000	.32596E+07	9802.8
.055	.32249E+07	9795.6
.110	.30770E+07	9764.0
.165	.29908E+07	9745.0
.220	.27717E+07	9694.8
.275	.22795E+07	9569.6
.330	.16916E+07	9387.7
.385	.12290E+07	9205.0
.440	.92892E+06	9053.4
.495	.75081E+06	8943.5
.550	.55651E+06	8796.6
.605	.37410E+06	8611.5
.660	.22856E+06	8397.4
.714	.15425E+06	8238.1
.769	.11901E+06	8137.3
.824	.84964E+05	8011.5
.879	.51374E+05	7833.2
.934	.20455E+05	7531.7
.989	.74482E+04	7231.7
1.044	.34447E+04	7021.7
1.099	.24854E+04	6937.0
1.154	.31946E+04	7001.9
1.209	.32491E+04	7006.4
1.264	.37371E+04	7043.2
1.319	.17287E+04	6845.7

1 SPECTRAL DISTRIBUTION ABOUT LINE CENTER OF THE PREDICTED LINE INTENSITY ALONG CENTRAL CORD FOR OPTICALLY THICK AND OPTICALLY THIN CASES.

	DISTANCE FROM LINE CENTER (NM)	OPTICALLY THICK (W/SR-NM-M**2)	OPTICALLY THIN (W/SR-NM-M**2)
1	-.6665	1072.25	1073.68
2	-.6500	1075.66	1077.17
3	-.6000	1087.64	1089.40
4	-.5500	1102.69	1104.77
5	-.5000	1121.97	1124.46
6	-.4500	1147.21	1150.25
7	-.4000	1181.14	1184.94
8	-.3500	1228.22	1233.12
9	-.3000	1296.21	1302.77
10	-.2500	1399.41	1408.67
11	-.2400	1426.40	1436.40
12	-.2300	1456.19	1467.03
13	-.2200	1489.18	1500.97
14	-.2100	1525.83	1538.70
15	-.2000	1566.71	1580.81
16	-.1900	1612.48	1628.00
17	-.1800	1663.93	1681.11
18	-.1700	1722.04	1741.15
19	-.1600	1787.98	1809.37
20	-.1500	1863.20	1887.30
21	-.1400	1949.49	1976.84
22	-.1300	2049.08	2080.38
23	-.1200	2164.78	2200.93
24	-.1100	2300.17	2342.35
25	-.1000	2459.83	2509.63
26	-.0900	2649.75	2709.34
27	-.0800	2877.79	2950.17
28	-.0700	3154.45	3243.91
29	-.0600	3494.01	3606.80
30	-.0500	3916.16	4061.68
31	-.0450	4166.49	4333.42
32	-.0400	4448.74	4641.64
33	-.0350	4768.39	4993.09
34	-.0300	5132.13	5396.20
35	-.0250	5548.30	5861.66
36	-.0200	6027.34	6403.32
37	-.0150	6582.73	7039.52
38	-.0100	7232.25	7795.46
39	-.0050	8000.36	8707.45
40	.0000	8921.86	9830.75
41	.0050	10007.02	11197.20
42	.0100	11065.51	12554.79
43	.0150	11987.70	13755.09
44	.0200	12703.00	14692.07
45	.0250	13214.41	15358.33
46	.0300	13550.31	15788.38
47	.0350	13725.72	16001.04
48	.0400	13752.29	16012.17
49	.0450	13643.33	15841.52
50	.0500	13411.94	15509.70
51	.0600	12630.50	14442.01
52	.0700	11519.79	12985.59
53	.0800	10229.72	11354.36
54	.0900	8918.00	9750.80
55	.1000	7701.74	8308.18
56	.1100	6640.33	7081.30
57	.1200	5747.45	6071.02

58	.1300	5011.14	5252.21
59	.1400	4409.23	4592.11
60	.1500	3918.00	4059.41
61	.1600	3516.06	3627.45
62	.1700	3185.49	3274.80
63	.1800	2911.88	2984.66
64	.1900	2683.80	2744.01
65	.2000	2492.31	2542.78
66	.2100	2330.36	2373.19
67	.2200	2192.46	2229.21
68	.2300	2074.25	2106.08
69	.2400	1972.27	2000.10
70	.2500	1883.77	1908.30
71	.3000	1579.14	1593.48
72	.3500	1407.25	1416.64
73	.4000	1301.40	1308.04
74	.4500	1231.82	1236.77
75	.5000	1183.72	1187.56
76	.5500	1149.12	1152.19
77	.6000	1123.42	1125.93
78	.6500	1103.82	1105.91
79	.6665	1098.37	1100.34

1 COMPARISON OF THE PREDICTED INTENSITY ACCOUNTING FOR OPACITY WITH THE PREDICTED INTENSITY ASSUMING OPTICALLY THIN LINE FOR A GIVEN EMISSION PROFILE.

ZONE	SPATIAL POSITION (MM)	OPTICALLY THICK (W/SR-M**2)	OPTICALLY THIN (W/SR-M**2)
1	0.0000	3438.66	3652.23
2	.0550	3412.09	3621.92
3	.1099	3321.42	3519.17
4	.1649	3183.56	3363.00
5	.2198	2969.08	3122.24
6	.2748	2684.23	2805.35
7	.3298	2398.09	2488.72
8	.3847	2167.00	2233.74
9	.4397	1991.93	2041.16
10	.4946	1848.73	1884.42
11	.5496	1708.36	1732.20
12	.6046	1590.25	1605.21
13	.6595	1505.44	1514.67
14	.7145	1456.17	1462.31
15	.7694	1422.16	1426.32
16	.8244	1390.70	1393.23
17	.8794	1364.38	1365.70
18	.9343	1346.38	1346.94
19	.9893	1339.81	1340.11
20	1.0442	1337.86	1338.07
21	1.0992	1337.34	1337.53
22	1.1542	1337.21	1337.40
23	1.2091	1336.56	1336.72
24	1.2641	1335.65	1335.76
25	1.3190	1333.87	1333.91

21.104 CP SECONDS EXECUTION TIME

/

BIBLIOGRAPHY

1. Daniel P. Dodson, "Preliminary Investigation of Radiation Phenomena in High Pressure Air and Argon Arcs," M.S. Thesis, Georgia Institute of Technology, December 1977.

2. F. Cabannes and J. Chappelle, "Spectroscopic Plasma Diagnostics," Reactions Under Plasma Conditions, ed. M. Venugopalan, Vol. 1, Wiley-Interscience, New York, 1971.

3. H. W. Drawin and P. Felenbok, Data for Plasmas in Local Thermodynamic Equilibrium, Gauthier-Villars, ed. Paris, 1965.

4. National Standards Reference Data Series, NBS, No. 22, Vol. 2.

5. A. S. Predvoditelev, et al., Tables of Thermodynamic Functions of Air for the Temperature Range 6000-12000°K and Pressure Range 0.001-1000 Atm., Infosearch Limited, London, 1958.

6. A. S. Predvoditelev, et al., Tables of Thermodynamic Functions of Air For Temperatures of 12,000 to 20000°K and Pressures of 0.001 to 1000 Atm., translated by Associated Technical Services, Inc., 1962.

7. W. L. Wiese, "Line Broadening," Plasma Diagnostic Techniques, ed. Richard H. Huddlestone and Stanley L. Leonard, Academic Press, New York, 1965.

8. Hans R. Griem, Plasma Spectroscopy, McGraw-Hill, New York, 1964.

9. Griem, Spectral Line Broadening by Plasmas, Academic Press, New York, 1974.

10. V. Helbig, D. E. Kelleher, and W. L. Wiese, "Stark Broadening Study of Neutral Nitrogen Lines," Physical Review A, Vol. 14, No. 3, September 1976, p. 1082.

11. Baxter H. Armstrong and Ralph W. Nicholls, Emission, Absorption, and Transfer of Radiation in Heated Atmospheres, Pergamon Press, New York, 1972.

12. Robert T. Murray, private communications, Georgia Institute of Technology, 1976-78.

13. Carnahan, Luther, and Wilkes, Applied Numerical Methods, John Wiley & Sons, Inc., New York, 1969.

14. Frank M. White, Viscous Fluid Flow, McGraw Hill, New York, 1974, p. 675.

15. H. Salzer, R. Zucker and R. Capuano, "Table of the Zeroes and Weight Factors of the First Twenty Hermite Polynomials," Journal of Research of the National Bureau of Standards, Research Paper 2294, Vol. 48, No. 2, February 1952, p. 111.